

GEOLOGY AND PETROGENESIS
OF THE
TUSCARORA INTRUSION OF THE DULUTH COMPLEX,
GILLIS LAKE 7.5' QUADRANGLE,
NORTHEASTERN MINNESOTA

A THESIS
SUBMITTED TO THE FACULTY OF THE GRADUATE SCHOOL
OF THE UNIVERSITY OF MINNESOTA
BY

Daniel Edward Costello

IN PARTIAL FULFILLMENT OF THE REQUIREMENTS
FOR THE DEGREE OF
MASTER OF ARTS SCIENCE

Advisor: James Miller

September 2010

© Daniel Costello 2010

Acknowledgements

This project would not have been possible without the guidance of my advisor, Dr. James Miller, whose passion for the geology of Northeastern Minnesota serves as an inspiration to all his students. Thank you for the numerous suggestions, edits, and encouragement which helped bring this project to completion. Thanks also to Drs. John Goodge and Paul Siders for serving on my committee and providing critical feedback on the final drafts. During work on this thesis, I was fortunate to receive fellowships from the University of Minnesota and the National Science Foundation GK-12 Program; it would have been difficult to earn my masters' without this financial support.

I would also like to thank those that helped me during field work- Mark Jirsa, for leading the initial trip which led to the development of my thesis project, and Steve Hoaglund and Steve Flood for accompanying me on mapping trips in the Boundary Waters. Thanks also to the faculty and other graduate students at the University of Minnesota Duluth, for your support during this work.

A special thanks is due to the geology department at Saint Norbert College – Elizabeth Gordon, Nelson Ham, and Tim Flood- for introducing me to geology and challenging me to pursue my masters. The classes and field trips were a great experience, and I learned many lessons that will stay with me for life.

Finally, I would like to thank my parents, Ed and Colleen Costello, for supporting me in all my decisions, even when I am unsure about what I am doing. You both serve as a great example of how to work hard, treat others, and enjoy life.

Abstract

The Tuscarora Intrusion is a layered mafic intrusion located at the base of the 1.1 Ga Duluth Complex in northeastern Minnesota. Detailed field mapping (1:12,000) and follow-up petrographic and geochemical analyses were conducted to evaluate the troctolitic igneous stratigraphy of the Tuscarora Intrusion, as well as to understand the petrologic relationship between the troctolitic cumulates and the plagioclase-rich gabbros of the overlying Anorthositic Series. Previous studies have interpreted the two lithologies as being interlayered, a relationship that would be unique within the Duluth Complex.

Field mapping has identified two lithologically distinct stratigraphic zones within the Tuscarora Intrusion. The lower zone is composed of olivine gabbro to augite troctolite that is typically heterogeneous in mode and texture and locally displays modal layering and foliation. Most notably, it contains abundant, large (>100m) basaltic hornfels inclusions. The upper zone is composed of homogenous, foliated troctolite to leucotroctolite, which grades upward from melatroctolite at the base of the zone. Inclusions in the upper zone are mostly large, often elongate blocks of anorthositic rocks and are especially abundant near the contact with the Anorthositic Series. No field evidence was found for an interlayered relationship between the two lithologies and geochemical studies imply distinct parent magma compositions.

This study concludes that the Tuscarora Intrusion and Anorthositic Series are two separate intrusive suites, as found in other areas of the Duluth Complex. Furthermore, the lower and upper zones of the Tuscarora are interpreted to have formed successively from major emplacement episodes of moderately evolved tholeiitic mafic magma. The emplacement model proposed has plagioclase porphyritic magmas intruding at some level above the base of the North Shore Volcanic Group to create the Anorthositic Series. This was followed by emplacement of lower zone magmas closer to base of the volcanic pile. This resulted in the incorporation of abundant volcanic inclusions and in strong contamination of the magma by interaction with pre-rift rocks of the footwall. Emplacement of upper zone magmas occurred above the newly crystallized Lower Zone and below the Anorthositic Series cap, which contributed anorthositic inclusions.

TABLE OF CONTENTS

Acknowledgements.....	i
Abstract	ii
Table of Contents	iv
List of Figures.....	vi
List of Tables	vii
I. Introduction	1
1) Geologic Setting of the Tuscarora Intrusion	4
2) Previous Studies of the Tuscarora Intrusion	13
3) Terminology and Nomenclature.....	20
II. Statement of Problem.....	23
III. Methods of Investigation.....	27
1) Geologic Mapping	27
2) Sample Selection	29
3) Petrographic Observations.....	30
4) Mineral Chemistry	31
5) Whole Rock Geochemistry	32
IV. Results	33
1) Field Data Compilation.....	33
2) Petrographic Descriptions	34
3) Mineral Chemistry	38
4) Whole Rock Geochemistry	41

V. Discussion	46
1) Geology of the Tuscarora Intrusion and Related Rocks.....	46
a. Footwall.....	49
b. Lower Zone of the Tuscarora Intrusion.....	51
i. Basal Heterogeneous Unit	
ii. Augite Troctolite Unit	
iii. Inclusions of the Lower Zone	
c. Upper Zone of the Tuscarora Intrusion.....	62
i. Melatroctolite Unit	
ii. Troctolite Unit	
iii. Troctolitic Dike	
iv. Anorthositic Inclusions of the Upper Zone	
d. Anorthositic Series.....	74
e. Structural Elements of the Tuscarora Intrusion.....	78
2) Comparison to Previous Work.....	80
a. Comparison with Previous Mapping Studies of the Tuscarora.....	80
b. Comparison with other Layered Intrusions of the Duluth Complex....	84
3) Parental Magma of the Tuscarora Intrusion.....	86
a. Evidence from Mineral Chemical Data.....	87
b. Evidence from Whole Rock Geochemistry.....	92
c. Estimation of the Tuscarora Parental Magma Composition.....	98
4) Emplacement Model for the Tuscarora Intrusion.....	109
VI. Conclusions	116
VII. References	118

LIST OF FIGURES

Figure 1: Generalized Geology of the Duluth Complex	2
Figure 2: Regional Extent of the Midcontinent Rift	5
Figure 3: Tecto-magmatic evolution of the Midcontinent Rift System.....	6
Figure 4: Tecto-magmatic evolution of the MRS, illustrating rocks of the Lake Superior Region.....	10
Figure 5: Generalized geologic map of the northern Duluth Complex	15
Figure 6: Bedrock geologic map of the Long Island Lake quadrangle	17
Figure 7: Distribution of map units identified by Beitsch.....	19
Figure 8: Modal Rock Classification Scheme for mafic intrusive rocks	21
Figure 9: Map showing extent of recent wildfires and prescribed burns	28
Figure 10: Modal mineralogy of select samples collected during field work	36
Figure 11: Anorthite-Diopside-Fosterite phase diagram,.....	37
Figure 12: Box and whisker diagram illustrating Fo content of olivines.....	39
Figure 13: Box and whisker diagram illustrating En' content of augite	40
Figure 14: Ternary diagram of En-Wo-Fs components in augite	41
Figure 15: REE variation diagram(normalized to Chondrites).....	43
Figure 16: Spider diagram (normalized to E-MORB abundances)	44
Figure 17: Spider diagram (normalized to Chondrites).....	45
Figure 18: Generalized geology of the Tuscarora Intrusion	48
Figure 19: Modal mineralogy of samples from Lower Zone	55
Figure 20: Texture of basal heterogeneous unit	56
Figure 21: Texture of augite troctolite unit	56
Figure 22: Photomicrograph from augite troctolite unit.....	57
Figure 23: Field photograph of mafic horfels inclusions in augite troctolite.....	61
Figure 24: Field photograph of cherty inclusion in augite troctolie.....	62
Figure 25: Photomicrograph of melatroctolite	64

Figure 26: Modal mineralogy of the Upper Zone	67
Figure 27: Field photograph of leucotroctolite	68
Figure 28: Photomicrograph of troctolite.....	69
Figure 29: Field photograph of anorthositic inclusion	74
Figure 30: Modal mineralogy of Anorthositic Series	76
Figure 31: Photomicrograph of Anorthositic Series	77
Figure 32: Texture of poikilitic troctolitic anorthosite	78
Figure 33: Cryptic variation of Fo and En' in Tuscarora Intrusion.....	89
Figure 34: Fo content of olivines as a function of pyroxene abundance	91
Figure 35: REE concentrations of Upper and Lower Zones	93
Figure 36: Partition coefficients of REE between minerals and mafic magmas....	96
Figure 37: Trace element concentrations of Upper and Lower Zones	97
Figure 38: Trace element concentrations of NSVG analogues for parental melt.	108
Figure 39: Emplacement model for the Tuscarora Intrusion.... ..	113

LIST OF TABLES

Table 1: Cumulate code for mafic rocks used during field work	22
Table 1: Whole rock geochemical results	45
Table 3: Compositions of NSVG samples serving as analogues for the Tuscarora parental magma	104
Table 4: Liquidus temperatures and early saturated phases of NSVG samples ..	106

I. Introduction

The Duluth Complex of northeastern Minnesota is the largest intrusive component of the Midcontinent Rift (MCR), which was magmatically active between 1110 and 1086 Ma. The Duluth Complex was emplaced as multiple intrusions into the basal sections of the comagmatic North Shore Volcanic Group. Previous workers have divided the Duluth Complex into four informal series based on magnetic polarity, dominant lithologies, internal structure, and, more recently, by their emplacement ages - the felsic, early gabbro, anorthositic, and layered series (Miller et al., 2002; Figure 1). Based on their reversed magnetic polarity and a U-Pb ages of 1109 – 1107 Ma, the felsic and early gabbro series are associated with the early magmatic stage of the MCR. Following a time of reduced magmatic activity, the anorthositic and layered series formed during the main magmatic stage from 1102-1094 Ma to form the majority of the complex.

The petrogenetic relationship between the layered series and the anorthositic series of the Duluth Complex is incompletely understood. The layered series occurs as a number of discrete mafic layered intrusions at the lower and mid-levels of the complex, all of which are overlain by a structurally complex cap of plagioclase-rich gabbros of the Anorthositic Series and granophyric rocks of the felsic series (Figure 1). Field relationships observed over many decades of study throughout the Duluth Complex typically show Anorthositic Series rock types as inclusions within layered

series rocks or show layered series rock intrusive into anorthositic rocks. These observations, along with the very distinctive lithologies and internal structures of the two series, had long been interpreted to suggest that the Anorthositic Series was significantly older than the layered series (Miller and Weiblen, 1990). However, U-Pb zircon ages show that the two units are essentially the same age (1099 Ma +/-0.5 Ma; Paces and Miller 1993).

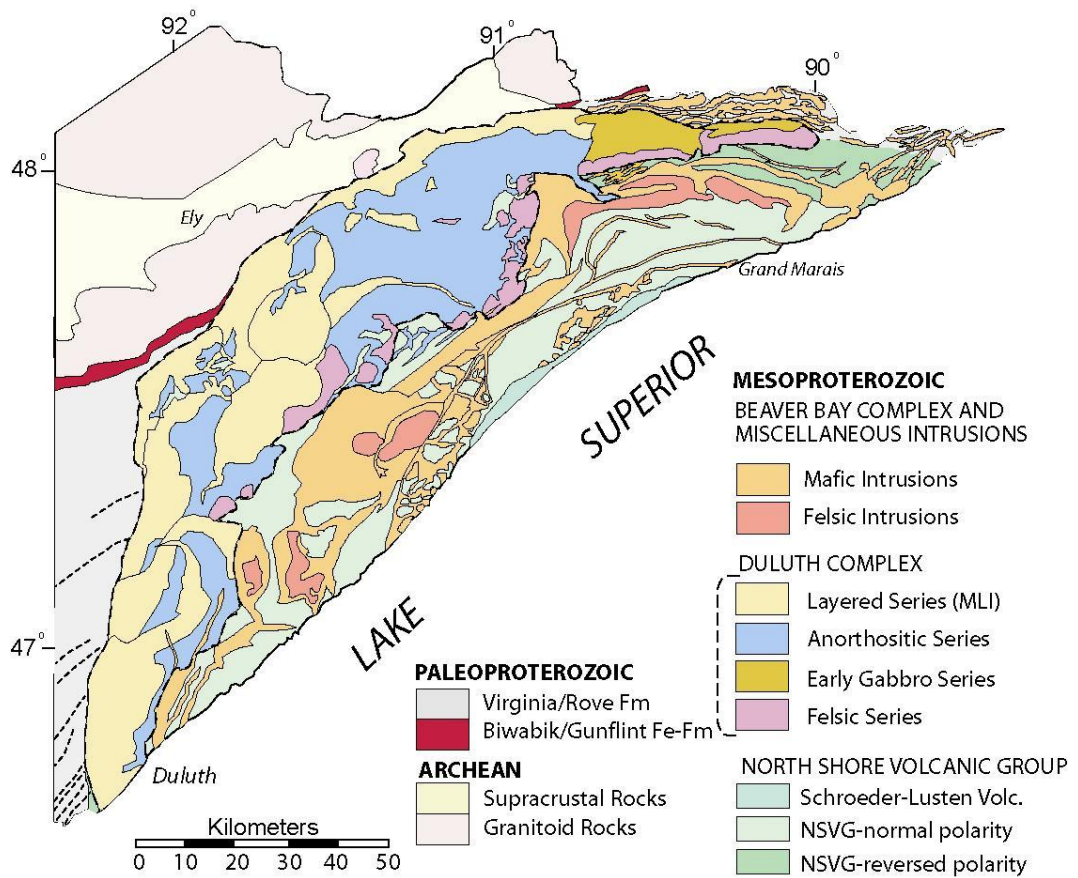


Figure 1: Generalized geology of the Duluth Complex and related rocks in northeastern Minnesota. The outline of the Duluth Complex is delineated by the dashed line and the distribution of the four main series are show. (After Miller et al., 2002)

These age data imply not only that the two main stage rock series of the Duluth Complex are approximately the same age, but also that they may be comagmatic or at least part of the same magmatic event. This possibility of a closer genetic relationship between the two series is actually supported by many gradational to ambiguous relationships between the two series, which in the past had been largely ignored as inconsequential anomalies (Miller, 1992). The Tuscarora Intrusion (Morey et al., 1981), located near the base of the complex along its northern margin, has been cited as possibly one of the best examples of this ambiguous relationship.

Previous reconnaissance work in the Tuscarora has separated the intrusion into three basic packages (Morey and Nathan, 1977; Morey et al., 1981, Beitsch, 1991). In general, the lowermost unit is a sequence of troctolitic cumulates which grades upwards into a transitional unit of interlayered troctolite and anorthosite. The interlayered package then grades upward into a unit of gabbroic to troctolitic anorthosite, typical of the Anorthositic Series. It is not clear from these previous studies whether the interlayering of anorthositic and troctolitic rock types is gradational or sharp. The nature of these contacts would have strong implications for how these rock types are related.

Due to its remote location within the Boundary Waters Canoe Area Wilderness (BWCAW) and thick brush cover, the Tuscarora Intrusion has been mapped only at a reconnaissance scale (Grout et al., 1950, Morey et al., 1981, Beitsch, 1981). However, major forest fires in 2006 and 2007 resulted in great improvements in the exposure of

local bedrock. This project seeks to take advantage of this excellent exposure to conduct detailed mapping and petrologic studies of the Tuscarora Intrusion in order to delineate the petrogenetic relationship between the Anorthositic Series and layered series. Field work concentrated on mapping the Tuscarora Intrusion in the Gillis Lake 7.5' quadrangle at a 1:12,000 scale, focusing on the igneous stratigraphy of the intrusion and the contact relationship between the layered and Anorthositic Series. Following field work, petrographic and geochemical (both mineral and whole rock) studies were conducted to better understand the petrologic relationships of these lithologic units.

I.1 Geologic Setting of the Tuscarora Intrusion

As mentioned above, the Tuscarora Intrusion and the Duluth Complex are intrusive components of the Mesoproterozoic Midcontinent Rift (MCR; Figure 1). The MCR formed through a failed attempt at rifting of the North American continent at 1.1 Ga. Geologic, geophysical and geochemical evidence point to the 2000 km-long arcuate rift as having been initiated by the tensional effects of a starting mantle plume, which is thought to have impacted the lithosphere beneath the area now occupied by the Lake Superior basin (Cannon et al., 1990; Cannon and Hinze, 1992; Nicholson et al., 1997). While the rift is only exposed in the Lake Superior region, magnetic and gravity surveys trace buried remnants of the rift from NE Kansas, through Lake Superior to Michigan (Figure 2). Geochronologic data show that magmatism associated with the rift began at 1109 Ma and continued through

1086 Ma, though recent dating by Heaman et al. (2007) implies that MCR-related magmatism may have begun as early as 1120 Ma. Various lines of evidence suggests that the MCR failed due to the waning effects of the plume, in addition to the compressional forces resulting from the Grenville Orogeny on the eastern margin of the North American craton around this time (Cannon and Hinze, 1992).

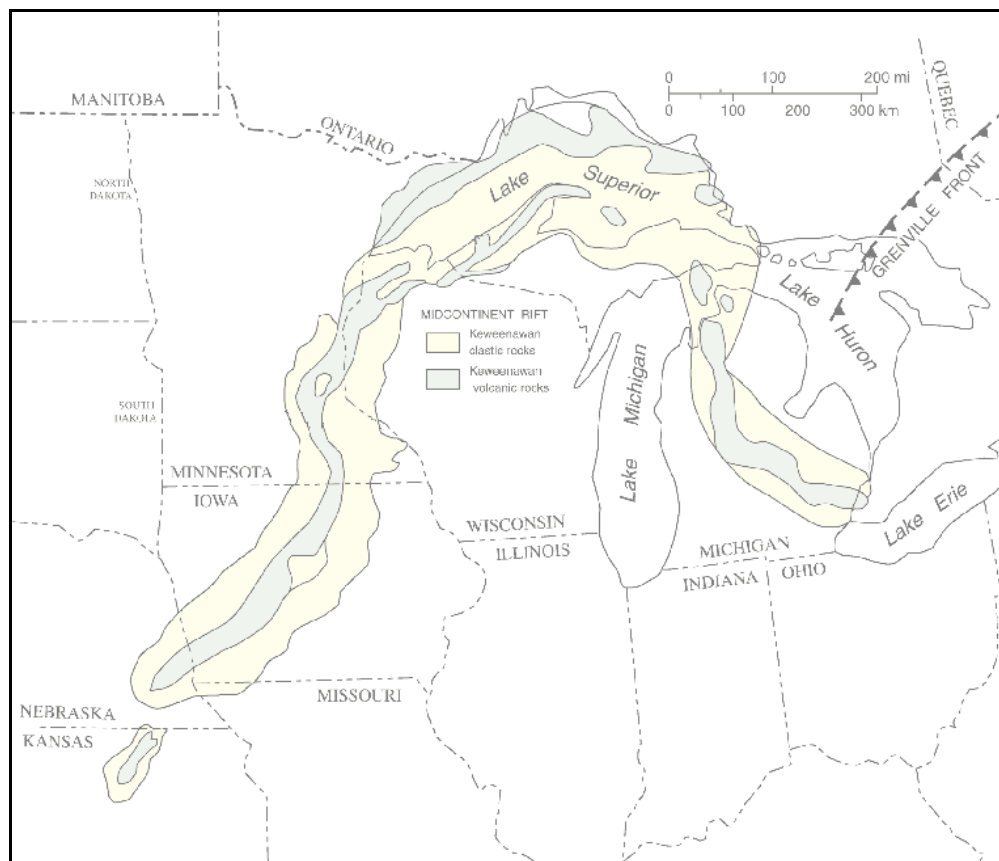


Figure 2: Regional extent of the Midcontinent Rift. (From Ojakangas et al., 2001)

During the 23 m.y. period of magmatic activity, the MRS evolved through several stages, evidence of which is preserved in the rocks of the Lake Superior

region. Based on geochronologic, geochemical, and isotopic data, workers have divided this period into four stages, termed the early, latent, main and late stages (Miller and Vervoort 1996, Nicholson et al., 1997, Vervoort et al., 2007). Figure 3 shows Miller and Vervoort's (1996) tectonomagmatic model for the evolution of the MCR and description of the MCR stages below are taken from their model.

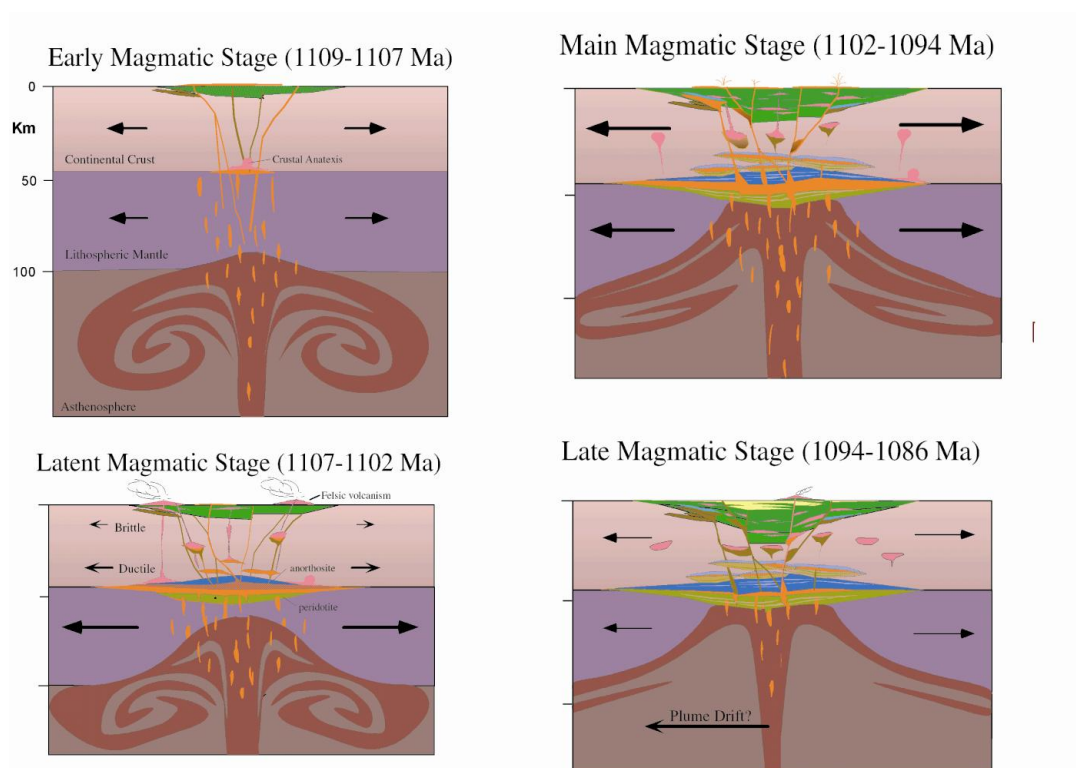


Figure 3: Tecto-magmatic evolution of the Midcontinent Rift (based on model by Miller and Vervoort (1996)).

The early magmatic stage (1109 to 1107 Ma) occurred during a period of reversed polarity and is characterized by initially primitive melts that transition into evolved and contaminated melts. The lowermost primitive lava flows formed from

plume-generated melts that did not interact with the cool, brittle lithosphere. These primitive magmas soon gave way to evolved and crustally contaminated compositions that are thought to indicate the initial stages of crustal underplating and lower crustal melting. Crustal anatexis of the lower crust is thought to have created a low-density barriers of felsic melts that impeded the rise of any mantle derived melts and triggered the growth of the mafic crustal underplate. A mafic crustal underplating is evident in gravity models over the rift (Trehu et al., 1991) and is thought to explain the hiatus in mafic magmatic activity in the upper crust between 1107 and 1102 Ma. This period is termed the latent magmatic stage.

By 1102 Ma, mafic melts began to emerge from lower crustal magma chambers, leading to a new period of magmatic activity, termed the main magmatic stage. This stage, which occurred during a period of normal polarity, is characterized by high eruption rates of evolved, but uncontaminated magmas. Crustal spreading and rift graben development continued as magmatic activity began to decrease, marking the late magmatic stage (1094 to 1086 Ma). Rocks formed during this stage include evolved volcanic rocks interbedded with clastic red-bed sediments.

In northeastern Minnesota, the major rock units comprising the MCR are the North Shore Volcanic Group (NSVG), the Beaver Bay Complex, and the Duluth Complex (Figure 1). The NSVG is a 7-10 km thick volcanic edifice comprised of compositions ranging from olivine tholeiites to rhyolites. This volcanic pile serves as the hanging wall to the intrusive complexes, and is slightly tilted southeast towards

the rift axis. The two intrusive complexes are distinguished by intrusion shape, degree of internal differentiation, age, and most significantly, level of emplacement within the NSVG. The Beaver Bay Complex is a group of mostly hypabyssal intrusions emplaced within the medial portion of the NSVG. These intrusions range in composition from mafic to felsic, but most are composed of noncumulate rocks. U-Pb age results indicate a general emplacement age of about 1096 Ma (Paces and Miller, 1993). In comparison, the Duluth Complex is comprised of larger composite intrusions that were multiply emplaced into the base of the NSVG. The DC also contains a broad range of rock types ranging from mafic to felsic, but cumulates predominate. U-Pb dating indicates early and main stage emplacement ages (1108 and 1099 Ma; Paces and Miller, 1993). The footwall of the Duluth Complex is comprised primarily of Archean greenstones and granites and Paleoproterozoic argillites, iron formation, and arenites (Figure 1).

The varied lithologies of the Duluth Complex are divided into four informal series, defined by their age/magnetic polarity, dominant lithologies, and internal structure (Figure 1). These series have been termed the felsic, early gabbro, anorthositic, and layered series (Phinney, 1972a; Miller et al., 2002). The felsic series is comprised of relatively small granitic to intermediate intrusions focused along the roof zone in the central and eastern portion of the complex. The early gabbro series contains layered gabbroic cumulates occurring in the eastern extent of the complex. Both the felsic and early gabbro series are reverse-polarity and formed during the

early magmatic stage (Fig. 4). U-Pb ages from the two series are indistinguishable around 1107Ma (Paces and Miller, 1993; Vervoort et al., 2007), but field relations indicate that the felsic series is older. The anorthositic and layered series, both of which formed during the main magmatic stage, comprise a majority of the volume of the Duluth Complex and will be the primary focus of this study.

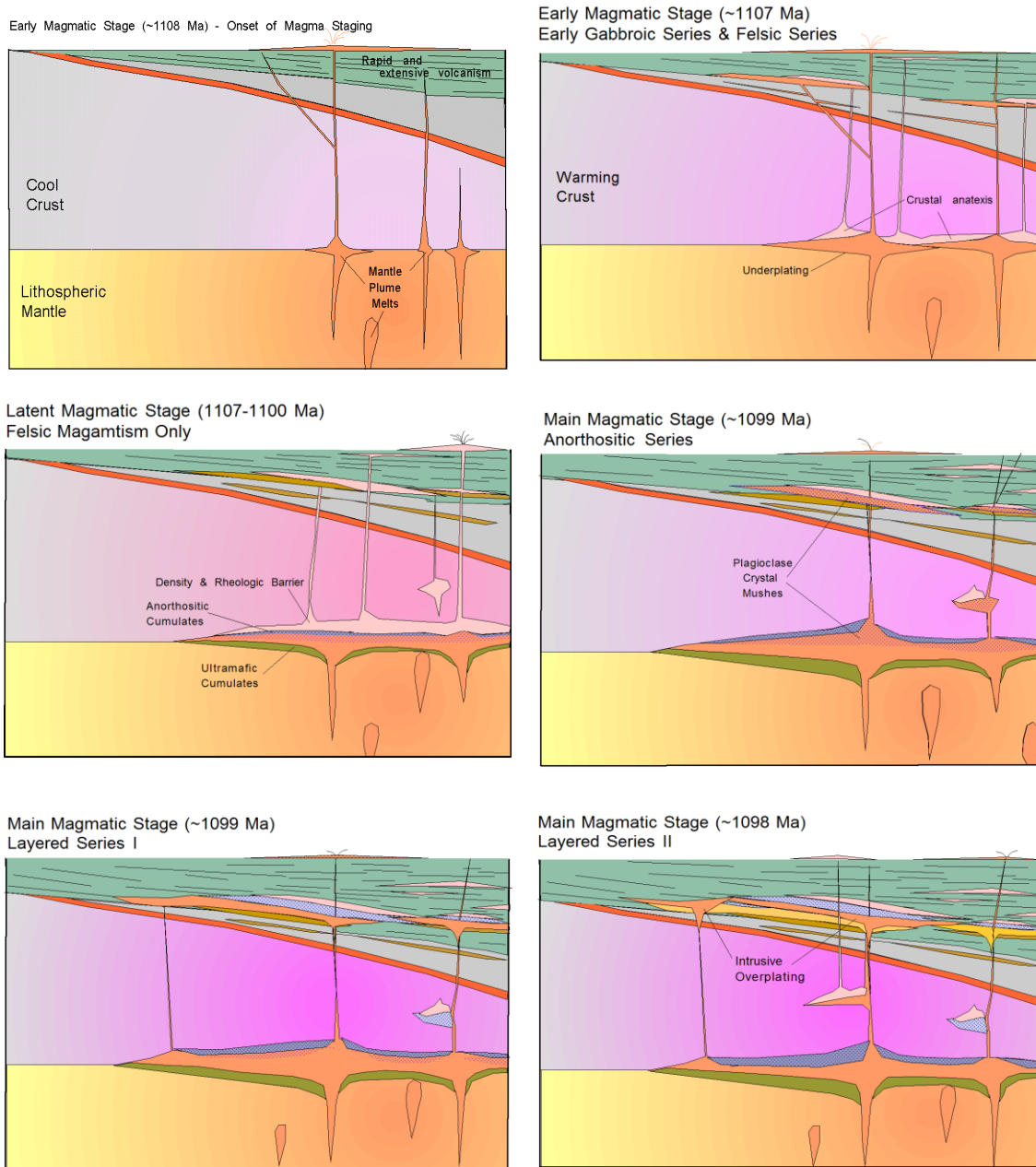


Figure 4: Tectono-magmatic evolution of the Midcontinent Rift System, illustrating rock types formed in the Lake Superior Region. From Miller and Vervoort (1996).

The Anorthositic Series is a suite of plagioclase-rich gabbroic rock types that occurs as a semi-continuous mass across the medial and upper extent of the complex usually just beneath felsic series intrusions or in direct contact with the base of the NSVG (Figure 1). Modal rock types comprising the Anorthositic Series include various types of plagioclase-rich gabbroic compositions such as anorthosite, troctolitic anorthosite, olivine gabbroic anorthosite, gabbroic anorthosite, oxide leucogabbro, olivine leucogabbro, and leucotroctolite. Miller and Weiblen (1990) interpreted these rocks to have been formed by multiple injections of plagioclase crystal mush derived from lower crustal magma chambers wherein plagioclase was buoyant (Fig. 4). The lines of evidence they cited for this interpretation include:

- Anorthositic Series rocks display generally well developed, but structurally complex plagioclase foliation.
- Various anorthositic lithologies are commonly observed to be in sharp, unchilled contact that locally show cross-cutting foliation.
- Most Anorthositic Series rocks have textures that would imply that they are plagioclase cumulates to plagioclase-olivine cumulates, yet Anorthositic Series sequences exhibit little to no evidence of in-situ differentiation.
- Plagioclase commonly displays zonation patterns wherein cumulus cores experience an episode of resorption followed by higher An content

overgrowths - a pattern that is consistent with decompression during crystallization.

- Anorthositic rock types rarely grade into normal gabbroic compositions which would be expected if they simply represented crystallization of somewhat plagioclase oversaturated (hyperfeldspathic) magmas.
- Anorthositic lithologies have generally evolved mineral compositions, which vary significantly in Mg/Fe ratio of mafic minerals, but little in plagioclase composition (avg. \sim An 60). This is taken as evidence that the mushes were derived from deeper differentiating systems where mafic minerals were fractionally crystallizing and plagioclase maintained equilibrium with its parent magma.

In contrast, layered series intrusions are discrete sheet-like to trough-shaped bodies that contain stratiform, differentiated sequences of rock types that may progress from melatroctolite/dunite to troctolite to olivine gabbro to ferrogabbro to intermediate rock types (Miller and Ripley, 1998; Miller and Severson, 2005). The layered series consists of at least 11 mafic layered intrusions emplaced below and into the Anorthositic Series (Figure 3). Layered series rocks typically display cumulate textures, local modal layering, and varying extents of cryptic layering. These features are consistent with layered series intrusions forming by in situ fractional crystallization driving magmatic differentiation with periodic recharge of more primitive magma. Each intrusion has its own unique igneous stratigraphy that can

primarily be attributed to different degrees of open vs. closed behavior. The Tuscarora Intrusion is thought to be one of the earlier intrusions of the layered series based on its lithologic similarity to the Partridge River and South Kawishiwi intrusions (Miller and Severson, 1992).

I.2 Previous Studies of the Tuscarora Intrusion

The gabbroic rocks of northeastern Minnesota were first identified as part of a regional federal geological survey of the upper Midwest in the mid-1800s (Owen, 1852). More detailed mapping of the area began in 1872 as part of the Minnesota geological and natural history survey commissioned by the state and headed up by N.H. Winchell. Although Winchell had, what would be by today's standards, some unconventional ideas about the origin of the gabbro (Miller, 2004), he and his colleagues created the first reconnaissance-scale (1:100,000) geologic maps of the Duluth of northeastern Minnesota (Winchell, 1900). These maps distinguished mafic and felsic intrusive rock types and established the basic outline of the Duluth Complex that still holds true today.

The next stage of geologic mapping in the northern part of the Duluth Complex was conducted by Frank Grout and coworkers from the University of Minnesota in the first half of the 20th century. Mapping along newly surveyed section lines, Grout distinguished the Mesoproterozoic rocks of northeastern Minnesota into six basic types: anorthosite, basalt, sandstone/conglomerate,

diabase/gabbro, granophyre (red rock) and felsite. His mapping in Cook County was summarized in MGS Bulletin 39 (Grout et al., 1959).

The Tuscarora Intrusion was first mapped in detail by a pair of projects in the early 1970s (Morey and Nathan, 1978; Morey et al., 1981). Both of these studies focused on the eastern extent of the intrusion and, due to the thick brush cover of the BWCAW, these surveys focused on shoreline mapping. The western extent of the intrusion, beyond the Gillis Lake quadrangle, has not been mapped in detail, although the aeromagnetic anomaly pattern associated with the Tuscarora can be traced for more than 30 kilometers of strike length (Miller et al., 2002).

As part of a Ph.D. study, Nathan (1969) conducted detailed mapping in the Hungry Jack Lake, South Lake, and Gunflint Lake quadrangles, which straddle the base of the Duluth Complex in the Gunflint Trail area. The main focus of Nathan's study was the delineation of the Poplar Lake Intrusion (formerly known as Nathan's Layered Series), which is now recognized as the major component of the early gabbro series. Nathan also recognized the presence of a younger intrusion in the western part of the Gunflint Lake quadrangle, which he mapped as unit R (Fig. 5) and later came to be recognized as the Tuscarora Intrusion. Unit R is described as a "heterogeneous, undivided assortment of intrusive rocks truncating the (Poplar Lake Intrusion) sheet-complex" containing medium grained olivine-augite-plagioclase cumulates (Nathan, 1969). Nathan's principal conclusions about the geology, igneous stratigraphy, and petrogenesis of the Poplar Lake intrusion was summarized in the

Minnesota Geological Survey's Centennial Volume by Phinney (1972b). Also, about a decade after Nathan's PhD study, his mapping was summarized in three 1:24,000-scale geologic maps published by the Minnesota Geological Survey (Hungry Jack Lake - Mathez, Nathan and Morey, 1977, South Lake - Nathan and Morey, 1977; and Gunflint Lake – Morey and Nathan, 1978).

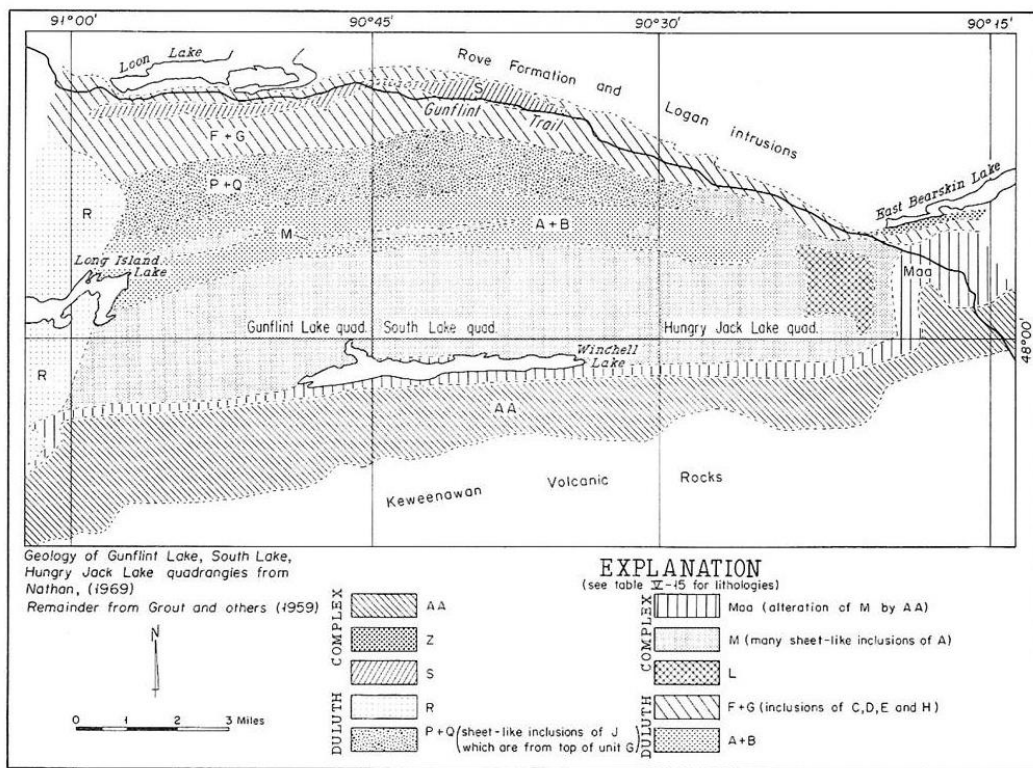
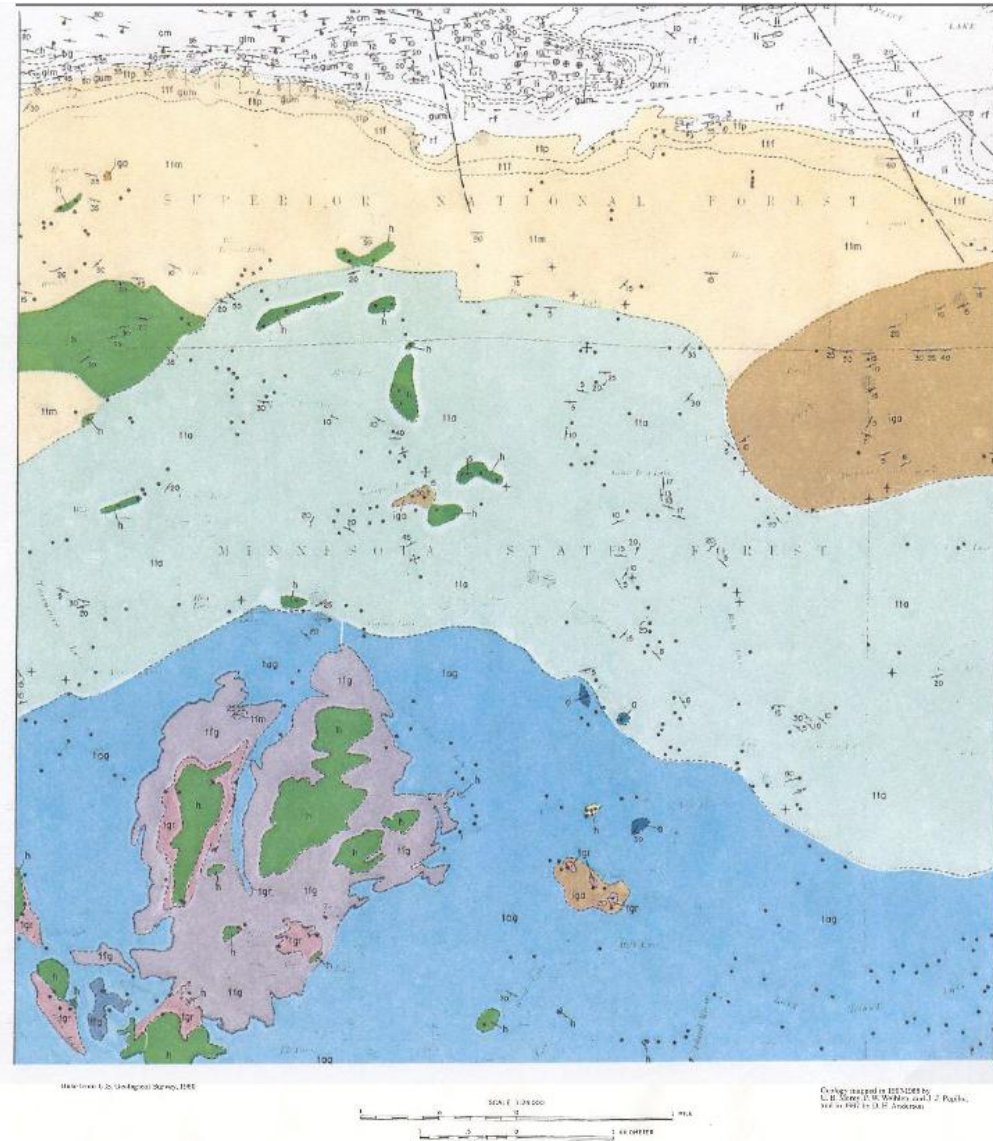


Figure 5 – Generalized geologic map of the northern prong of the Duluth Complex from Phinney (1972b, figure V-32) based on the mapping of Nathan (1969). Map Unit “R” later came to be recognized as the Tuscarora Intrusion with mapping in the adjacent Long Island Lake quadrangle (Morey et al., 1981).

In their geologic map of the Gunflint Lake quadrangle, Morey and Nathan (1978) describe different units than originally denoted by Nathan (1969). This change

was likely made from information gained by mapping by Wieblen and Papike in the adjacent Long Island Lake quadrangle (see below). The basal unit of the Tuscarora (unit ttf) is described as a thin horizon of well foliated, fine-grained ophitic troctolite, which grades upward to a medium-grained troctolite displaying similar textures. Above this, Morey and Nathan (1978) describe a unit of interlayered troctolite and anorthositic gabbro (unit tta) interlayered on the scale of centimeters up to a meter. Overlying this interlayered unit is a medium-grained anorthositic gabbro (unit tag), containing well developed but variable plagioclase foliations, similar to the Anorthositic Series.

In their geologic map of the Long Island Lake quadrangle, Morey, Weiblen, and Papike (1981) subdivided the Tuscarora Intrusion into three units, in a similar fashion to Morey and Nathan's (1978) work in the adjacent Gunflint Lake quadrangle (Figure 6). A basal unit of ophitic olivine gabbro to augite troctolite (unit ttm) is overlain by a fine-grained troctolite (unit ttf). These units are overlain by a 100 meter thick sequence of interlayered anorthositic gabbro and troctolite (unit tta). The authors describe this unit as interlayered on the scale of centimeters to several meters, with irregular, undulatory contacts. This interlayered unit transitions upwards into a massive anorthositic gabbro (unit tag), which has structural and lithologic characteristics similar to the Anorthositic Series.



GEOLOGIC MAP OF THE LONG ISLAND LAKE QUADRANGLE, COOK COUNTY, MINNESOTA

By
G. B. Morey, P. W. Weiblen, J. J. Papike, and D. H. Anderson
1981

TUSCARORA INTRUSION

- tip — troctolite, augite troctolite
- tif itm — interlayered anorthositic gabbro & troctolite
- tia — anorthositic gabbro
- tag — ferrogranodiorite
- tifg — granophyre

OTHER UNITS

- ga — Iron Lake gabbro
- h — mafic hornfels
- a — anorthosite
- pre-Keweenaw rocks

Figure 6: Partially colorized bedrock geologic map of the Long Island Lake quadrangle (Morey et al., 1981). Original Map is black and white.

The most recent study of the Tuscarora Intrusion was part of an MS thesis by Beitsch (1991) in the Gillis Lake quadrangle, which is adjacent to the west side of the Long Island quadrangle (Figure 6). While the main focus of Beitsch's thesis was a petrofabric study of the orientation of olivine in troctolitic rocks, he also conducted extensive shoreline mapping in the Gillis Lake quadrangle. During his field mapping, Beitsch divided the Duluth Complex of the Gillis Lake quadrangle into six packages based on cumulate mineralogy (Figure 7). The stratigraphically lowest unit, the Peter Lake unit, is described as a medium-grained troctolite containing cumulate plagioclase and olivine and is shown as continuous across the Gillis Lake quadrangle.

Stratigraphically above the Peter Lake unit, five units of varying cumulus textures and assemblages are found. The Owl Lake unit, a four-phase cumulate containing granular plagioclase, olivine, pyroxene, and iron oxides, is noted only in the eastern portion of the study area. The Virgin Lake unit, occurring as a lateral wedge in the western half of the Gillis quadrangle, is described as containing cumulus plagioclase and is characterized by large oikocrysts of olivine and clinopyroxene. In a similar fashion, the uppermost Tarry Lake unit contains plagioclase as its only cumulus phase, the difference being its abundance (>75%). Both the Tarry Lake and Owl Lake units contain inclusions of plagioclase-olivine cumulate rocks, which Beitsch proposes are inclusions of the underlying Peter Lake unit.

Mapping results from Morey et al. (1981) and Beitsch (1991) demonstrate a similar igneous stratigraphy in the Tuscarora Intrusion, although notable differences

do exist. Both describe a variety of cumulate textures found in troctolitic cumulates, all of which are overlain by plagioclase-rich lithologies. One striking difference is the presence of a four-phase cumulate described by Beitsch in the western half of the Gillis Lake quadrangle (his Owl Lake unit), which does not match up with any units in the Lake Island quadrangle as mapped. In addition, the curious interlayered troctolitic and anorthositic unit found by Morey et al. (unit tta, Figure 6) has no correlative unit(s) in Beitsch's map of the Gillis Lake quadrangle.

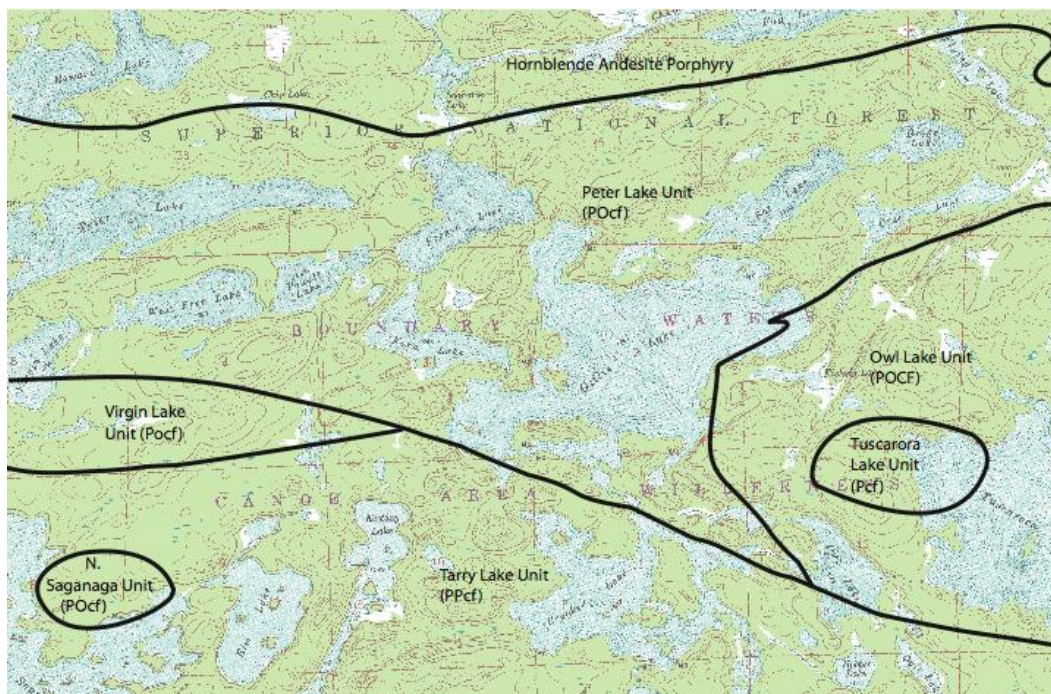


Figure 7: Distribution of map units identified by Beitsch (1991) in the Gillis Lake quadrangle. Dominant cumulate mineralogy of each unit is indicated by an abbreviated cumulate code (see Table 1)

I.3 Terminology and Nomenclature

The terminology used in this study to describe lithologic, textural, and structural attributes of rocks follow the definitions set out by the American Geological Institution's *Glossary of Geology* (Neuendorf et al., 2005). Furthermore, this study will follow the conventions for classifying mafic rocks recommended by Miller, Green, and Severson (2002) for the intrusive rocks of the Duluth Complex. Miller et al. (2002) suggest a modal rock classification that is more in line with natural modal populations of the essential mafic rock minerals (olivine, plagioclase, pyroxene, and Fe-Ti oxide) than is the case for other modal schemes (Phinney, 1972a; LeMaitre, 1989; Severson and Hauck, 1990). This scheme (Figure 8) is particularly useful in field identification of rocks of the Tuscarora Intrusion in that it is based on the relative ratios of the major mafic phases. A modal rock name was applied to outcrops during field mapping, and confirmed or corrected during later petrographic work.

In fully describing the rocks of this study, the texture of the essential minerals, especially pyroxene, is also emphasized. As recommended by Miller et al. (2002), the bulk texture of an intrusive mafic rock should be based on the texture of pyroxene (typically augite). Because the texture (and modal concentration) of pyroxene in a tholeiitic mafic cumulate rock is largely related to the degree to which the parent magma is saturated or undersaturated in pyroxene component, it serves as a general

indicator of the differentiated state of the magma at time of crystallization. The terms used to define the texture of pyroxene are as follows:

Ophitic- Multiple lath-shaped crystals of plagioclase totally enclosed in crystals of pyroxene.

Subophitic- Multiple lath-shaped crystals of plagioclase partially enclosed in crystals of pyroxene.

Intergranular- Generally equigranular euhedral to anhedral primary minerals, none enclosing the others.

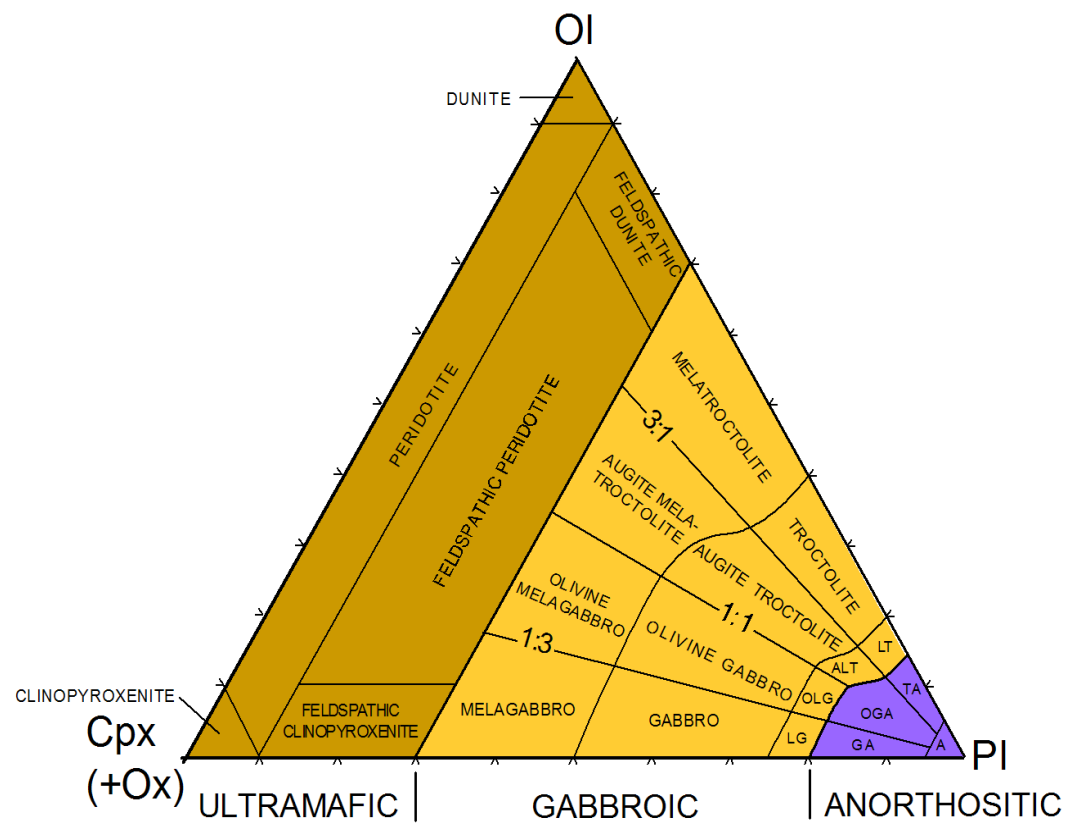


Figure 8: Modal rock classification scheme for mafic intrusive rocks used for this study (after Miller et al., 2002)

Ophitic textures within a mafic rock are indicative of a more primitive magma, in which pyroxene is not yet saturated. As the magma evolves and cools, the pyroxene component increases in the melt. Eventually, pyroxene and plagioclase will co-precipitate in the magma, resulting in formation of an intergranular texture.

In addition to modal and textural descriptions employed during field mapping, a “cumulate” code described by Miller et al.(2002) was employed as a short-hand way of describing the modal mineralogy and the texture of mafic cumulate rocks (Table

1). The code is assigned to rock types using the following criteria:

1. **Modal Mineralogy**- all phases that comprise greater than 2% of the rock are listed in decreasing order of abundance using abbreviations.
2. **Mineral Habit**- Capitalization is used to denote the texture of all minerals in rock. Granular (cumulus) minerals are denoted using capital letters, whereas subpoikilitic, poikilitic, or interstitial textured minerals (intercumulus) are in lowercase.

Table 1: Cumulate code used for this study (from Miller et al., 2002)

<u>Cumulus/Intercumulus Mineral Codes</u>			
PP*/Pp**/P	-plagioclase	F/f	-Fe/Ti oxide
O/o	-olivine	I/I	-inverted pigeonite
C/c	-clinopyroxene	b	-biotite
*designates anorthositic rocks (Plagioclase > 85%)			
**designates plagioclase rich (leuco-) rocks (Plagioclase 77-85%)			
<u>Cumulate code translation of common rock types in the Tuscarora</u>			
Ophitic augite troctolite		POcf	
Oxide troctolite		POFc	
Biotite-bearing augite troctolite		POcfb	
Troctolitic anorthosite		PPOcf	
Augite-bearing leucotroctolite		PpOcf	

II. Statement of Problem

Since Taylor (1964) first subdivided the main mafic component of the Duluth Complex in the Duluth area, into two suites – structurally complex anorthositic gabbros and well-differentiated layered gabbros – subsequent field and petrologic studies have confirmed this dichotomy throughout the Duluth Complex. These two suites became known as the Anorthositic Series and troctolitic (later, the layered) series, respectively (Phinney, 1972a; Weiblen and Morey, 1980; Miller et al., 2002). Moreover, Taylor's (1964) observations (earlier made by Grout, 1918) that anorthositic rocks commonly occur as inclusions in layered gabbros and that fine-grained “chilled” gabbros emanating from the layered gabbros were intrusive into coarse-grained Anorthositic Series rocks gave rise to the idea that there was a significant age gap between the two suites. Field studies in other areas of the Duluth Complex confirmed these relative age relationships noted at its type locality in Duluth. However, this well-accepted idea that the Anorthositic Series was significantly older than the layered series (Wieblen and Morey, 1980; Miller and Weiblen, 1990) was shown to be incorrect when U-Pb zircon dates revealed that the two series are essentially identical in age (1099 Ma) within the resolution of the dating (± 0.5 Ma) (Paces and Miller, 1993). The implication that the two series were emplaced within less than one million years of each other relative to the 23 Ma range of MCR magmatism compelled a major rethinking of the magmatic relationship between these two very distinctive series (Miller, 1992).

This similarity in age is puzzling not only because of the common observation of Anorthositic Series xenoliths in layered series intrusions, but also because of the very distinctive lithologic and structural characteristics of the two series. Seemingly more problematic is explaining the apparent “chill” of layered series gabbro intrusions along the contacts with rocks of the Anorthositic Series observed at Duluth by Grout (1918) and Taylor (1964). If this is a thermal chill zone, it implies that the Anorthositic Series had cooled significantly before the layered series was emplaced. However, Miller and Ripley (1998) noted that this “chill” is an evolved biotite-phyrlic ferrodiorite and could not be parental to the layered series. Instead, they suggested that this rock represents a decompression quench of a volatile-saturated magma that was tapped from the layered series after it was about 50% crystallized.

The discovery that the anorthositic and layered series are essentially contemporaneous in their age of emplacement led Paces and Miller (1993) to suggest a closer genetic link between the two series. Miller (1992) pointed out that evidence for a closer genetic relationship between the two series had been noted by previous workers who observed the many gradational to ambiguous relationships between the two series. However, these observations didn't match the prevailing paradigm of older Anorthositic Series and younger layered series and were largely ignored as inconsequential anomalies. Paces and Miller (1993) pointed specifically to the interlayered relationship reported by Morey et al. (1981) between troctolitic and

anorthositic rocks within the Tuscarora Intrusion as one of the best examples of this ambiguous age relationship and suggested that this system may offer an ideal opportunity to evaluate a possible genetic link. This suggestion drives the overall goal of this study.

Miller and Severson (2005) speculated that one way that the two series may share a common petrogenetic origin is by progressive flushing of suspended plagioclase from deep crustal mafic magma chambers (Figure 4). Under high pressures of the lower crust, plagioclase flotation and suspension in such chambers would result in early magma extractions carrying high crystal loads of buoyant plagioclase. Multiple emplacements of these crystal mushes into the lower sections of the volcanic rift fill, locally being trapped beneath felsic series granites, would give rise to the structurally complex, plagioclase-rich Anorthositic Series. As the deep chambers were flushed of their plagioclase suspension, later magmas would be crystal-poor basaltic liquids. These crystal-poor magmas underplated the low density Anorthositic Series rocks to form layered series intrusions. Miller and Severson (2005) also speculated that the more interlayered relationship of troctolitic and anorthositic phases of the Tuscarora reported by Morey et al. (1981) may record a more gradational transition from crystal mush magmatism of the Anorthositic Series to crystal-poor mafic magmas of the layered series.

The overall goal of this study is to better establish the petrologic relationships between the troctolitic and anorthositic rocks within the Tuscarora Intrusion. By

accomplishing this, the origin of two main series comprising the Duluth Complex will be better understood. The specific objectives of this study were as follows:

- 1) Document the field, petrographic, and geochemical relationships between troctolitic and anorthositic rocks within the Tuscarora Intrusion in the Gillis Lake quadrangle where Beitsch (1991) and, by extension, Morey et al. (1981) have noted an interlayered relationship.
- 2) Delineate from this information the boundaries and the igneous stratigraphy of the Tuscarora Intrusion and its relationship to anorthositic rock types and other igneous components encountered in the field area (e.g., volcanic hornfels inclusions, other intrusive bodies, etc.)
- 3) Estimate from mineralogic and lithochemical attributes, the parent magma composition for the Tuscarora Intrusion and anorthositic components.
- 4) Develop an emplacement and crystallization model that explains the temporal, spatial and magmatic relationships between the Tuscarora Intrusion and associated anorthositic rocks.

III. Methods of Investigation

In order to accomplish the goals and objectives set out in the previous section, several methods of investigation were undertaken to fully characterize this magmatic system. The methods employed include bedrock geologic mapping and sampling, petrographic studies, mineral chemical analyses, whole-rock geochemistry. A description of these procedures is provided below.

III.1 Geologic Mapping

Geologic field mapping was conducted during the summer of 2008. Three trips of ten days each were spent within the study area. The field area lies exclusively within the Boundary Waters Canoe Area Wilderness (BWCAW) and required a full day to transport gear and provisions into the study area via 7-8 portages. I was assisted by my advisor, Dr. Jim Miller, on the first outing, and by fellow geology students on subsequent trips. A base camp was established near the center of the study area, and canoes were used to travel between various map areas.

The nature of this study and focus on field mapping is very time-dependent, due to excellent bedrock exposure as a result of recent forest fires in the BWCAW. The Cavity Lake Fire of 2006 and Ham Lake Fire of 2007 both affected portions of the study area (Figure 9). Many of the areas encountered during field work were burned in a more erratic and incomplete fashion than expected, especially in the eastern portion of the map area. The eastern area, which was burned during the more recent Ham Lake fire and recent prescribed burns, had very patchy distribution

of burn areas, especially in the areas mapped as prescribed burns (Figure 9). The western half of the map had much better burn exposure due to having been burned during the extensive Cavity Lake fire of 2006. This provided excellent bedrock exposure and much easier access to inland areas that otherwise would have been impassible. While the fire was widespread, high ground was most thoroughly burned, whereas surrounding lowlands were often relatively unaffected.

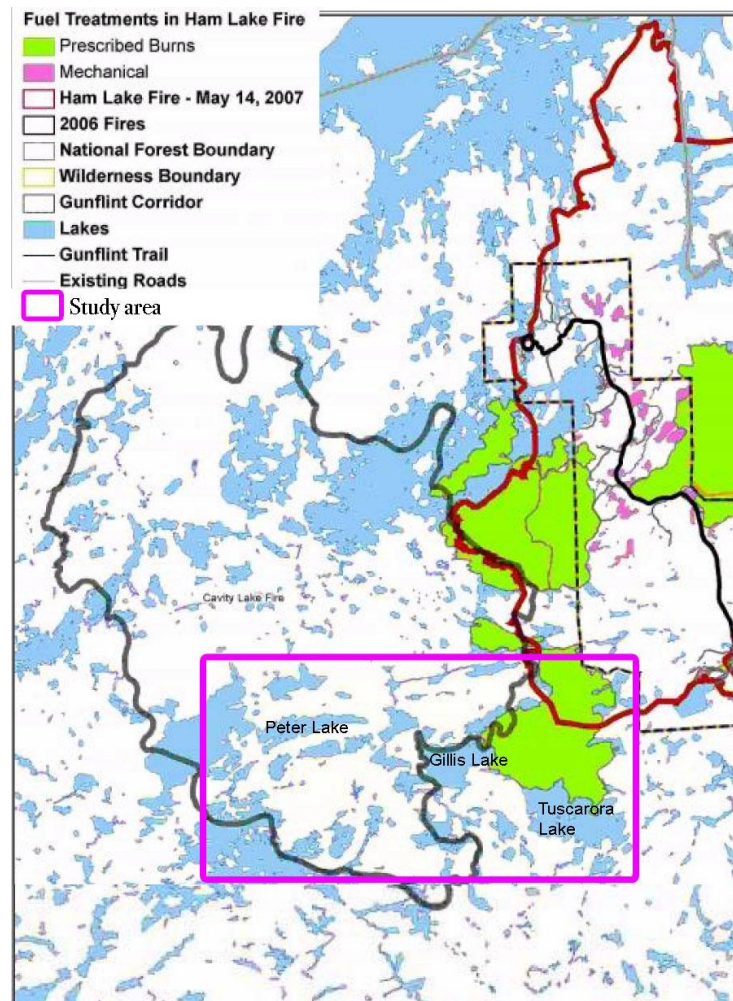


Figure 9: Map showing extent of recent wildfires and prescribed burns. Adapted from US Forest Service, 2008.

A total of 186 outcrops were visited over approximately thirty days of fieldwork. Outcrops were cataloged in order visited, starting with GC100 (Gillis Costello #). If there were numerous exposures within a small area, outcrops were subdivided using decimals- GC100.1, GC100.2, etc. Once a considerable distance was traveled or a significantly different lithology was encountered, a new station was established- GC101, GC102, etc. At each outcrop, detailed notes were taken describing the following criteria

- Location (UTM)
- Physical conditions, exposure type (fresh/weathered)
- Lithology (cumulate code, modal rock name)
- Pertinent structural information (most commonly plagioclase foliation, but also jointing, faulting, etc)
- Miscellaneous (weather, conditions of burn area, ticks, etc)
- Photo numbers and short description
- Description of any samples taken

The locations of outcrops, sample locations, and structural measurements were plotted on 1:12,000 topographic base maps with mylar overlays. Outcrops were sketched in colors according to their modal rock name. Orientations of plagioclase foliation, modal layering, contacts and other structural features were marked on the field map, as were traverse paths.

III.2 Sample Selection

A key component of summer fieldwork was selection of samples for later petrographic and geochemical analyses. The number of samples that were necessary

to collect was greatly reduced by having access to the sample and thin section suite that Sandy Beitsch had graciously provided from his MS thesis project (Beitsch, 1991). The main strategies for sampling were 1) to collect along a N-S traverse that would profile the igneous stratigraphy of the Tuscarora Intrusion, and 2) to collect across contacts between anorthositic and troctolitic rock types in order to better evaluate the mineralogical, textural, and geochemical changes between these adjacent rock types. A total of 109 hand samples were collected from the study area.

III.3 Petrographic Observations

Petrographic observations were conducted on thin sections from a total of 41 samples collected in this study and from Beitsch's (1991) thesis. Thin sections of samples collected for this study were prepared by Quality Thin Sections of Tucson, Arizona from rock billets cut at UMD. Of the samples collected for this study, 25 were polished for SEM work. Transmitted light petrography was conducted using Leica DM microscopes housed in the UMD Department of Geological Sciences' petrography lab.

Petrographic observations served to either confirm or correct rock descriptions made during fieldwork and to detect textures and minor phases not observable in hand sample. Specific attributes that were documented during the petrographic study include phase mineralogy, visual estimates of mineral modes, and significant textural information. During petrographic analysis, particular attention

was given to the degree of mineral alignment (primarily in plagioclase), on the approximate mineral modes, and on the habit of the primary and essential phases. Based on these observations, a “cumulate” code was produced, as discussed above (Table 1).

III.4 Mineral Chemistry

The mineral chemistry of 15 samples was analyzed using a JEOL JSM-6490LV scanning electron microscope (SEM) and Oxford Inca 250 energy dispersive x-ray spectrometer (EDS) at the University of Minnesota-Duluth. Polished thin sections were coated with a thin (~15 nm) carbon film to prevent sample charging. Analyses were conducted with a 20 kV accelerating voltage, 85 nA beam current, and 0.1 micron electron beam.

Only olivine and pyroxene were analyzed during this study. Plagioclase was not analysed because of difficulties in obtaining statistically accurate average compositions from complexly zoned minerals. Plagioclase compositional data were acquired as part of Beitsch’s (1991) thesis and will not be evaluated in this study. An average of ten spot analyses was acquired from each mafic phase in each section. If there was a wide variation observed during these measurements (more commonly in the pyroxenes), further analyses were collected to monitor the extent of variation which may reflect compositional zoning. Standardization of collected spectra was performed using a suite of Smithsonian standards acquired by the UMD SEM lab.

A total of 231 mineral analyses were acquired from the 15 samples mostly collected along a north-south transect through the field area. This data will be used primarily to evaluate evidence for magmatic differentiation and recharge within the Tuscarora Intrusion. Samples which straddle both sides of two troctolite – anorthosite contacts were also analyzed in order to compare their mineral chemical attributes.

III.5 Whole-Rock Geochemistry

Whole-rock geochemical data were obtained from ACME labs of Vancouver, British Columbia. Rock samples were submitted for crushing and pulverizing using mild steel. Analyses were completed from a 0.2 g sample by ICP-emission spectrometry following a metaborate/tetraborate fusion and dilute nitric digestion (2009 ACME brochure). In addition, base metals were examined from a 0.5 g split sample digested in Aqua Regia and analyzed by ICP mass spectrometry.

A total of twelve samples were selected from across the study area. Whole-rock compositions, especially incompatible trace element ratios, can be used to determine potential differences in parental magma composition(s) for the Tuscarora Intrusion rock types and thus to evaluate the petrogenetic relationship between anorthositic and troctolitic rocks.

IV. Results

IV.1 Field Data Compilation

Following conclusion of fieldwork, the field maps were scanned and the spatial information (outcrop, measurement and sample locations, traverses) were digitally transferred into ArcView 3.2. Attributes of outcrop lithologies, hand sample descriptions, and structural measurements were compiled into database files using the GeMS (Geologic Mapping System) interface with ArcView developed by the Minnesota Geologic Survey (Wahl et al., 2002).

Upon compilation of the field data, ArcView/GeMS was also used to construct linework (contacts and faults) and map units for the final geologic map (Plate 1). Each dataset (geologic units, lines, structural measurements, outcrops, topographic maps) was exported from ArcView as a unique layer at 1:12,000 as an EPS file. Certain datasets (structure and outcrop) contain data from both this study and Beitsch's (1991) MS thesis. Once exported from ArcView, these layers were imported into Adobe Illustrator and stacked to produce a comprehensive map of the study area. A map legend was produced to include a description of map units and any geologic symbols used in the geologic map.

During construction of the geologic map, results from other studies were incorporated. Preliminary mapping of the Tuscarora Intrusion (as well the genesis of this thesis project) occurred during a 2007 capstone mapping project for the Precambrian Research Center field camp (Jirsa et al 2007). Two groups of students

worked in the area of Gabimichigami Lake area over three days, dividing focus between the footwall metavolcanics and the basal contact of the Duluth Complex. A troctolitic dike into the underlying sediments was first discovered during this work. The footwall sedimentary rocks in the northern portion of the study area have been mapped by Mark Jirsa of the MGS as part of a STATEMAP grant to construct a geologic map of the area burned in the 2007 Cavity Lake fire (Jirsa and Starns 2008). Upon completion of this study, the geologic map interpretation of the Tuscarora Intrusion developed here will be merged with data from Jirsa's study to produce a comprehensive geologic map of the area.

The final map is presented in Plate 1 and the geologic interpretations portrayed will be discussed in Chapter V.

IV.2 Petrographic Descriptions

Petrographic observations were conducted on 41 samples from this study and 30 from Beitsch's (1991) MS thesis. Samples were assigned a modal rock name based on their modal mineralogy (Figure 10). The most common rock types identified were augite troctolite (eleven samples) and troctolite (eight samples). Of the 41 samples collected in this study, seven were identified as anorthositic, most commonly troctolitic anorthosite.

An aspect of the petrographic study to which particular attention was paid is the texture and mode of clinopyroxene (augite). As noted above, the texture and abundance of clinopyroxene in mafic cumulate rocks can be used as a general

indicator of the relative degree of differentiation of the magma at time of crystallization. More primitive melts that are undersaturated in augite will crystallize as ophitic to subophitic oikocrysts, indicating that it crystallized from the intercumulus liquid. The closer that magma is to augite saturation (the eutectic point, E, in Figure 11), the earlier it will crystallize as a postcumulus oikocrysts, and the more abundant it should be in the total mode of the rock. Of course, postcumulus compaction or melt migration can change the amount of intercumulus liquid ultimately trapped in the final cumulate, and thus the mode of postcumulus augite.

If the resident magma cools and differentiates to the point of augite saturation, this should result in its co-precipitation with olivine and plagioclase, and the development of an intergranular texture. Although not portrayed in the ternary phase diagram shown in Figure 11, Fe-Ti oxide also becomes a saturated cumulus phase at about the same temperature as augite in most Duluth Complex intrusions. (Miller and Ripley, 1996). Another sign of augite being cumulus is that it will occur with other cumulus phases in approximately cotectic/eutectic proportions.

Experimental data graphically shown in Figure 11 indicates that for a mafic magma multiply-saturated in olivine, plagioclase, and augite at low pressure, it should contain these phase in modal proportions of roughly 60:12:28 (McCallum and Raedeke, 1980). This modal proportion is plotted in Figure 10, as is the ideal cotectic proportions of a plagioclase-olivine cumulate (Pl:Ol~72:28). Note that modal compositions of all rocks investigated in this study plot between the ideal cotectic

troctolite and eutectic olivine gabbro compositions (points PO and PCO, respectively, Fig. 10).

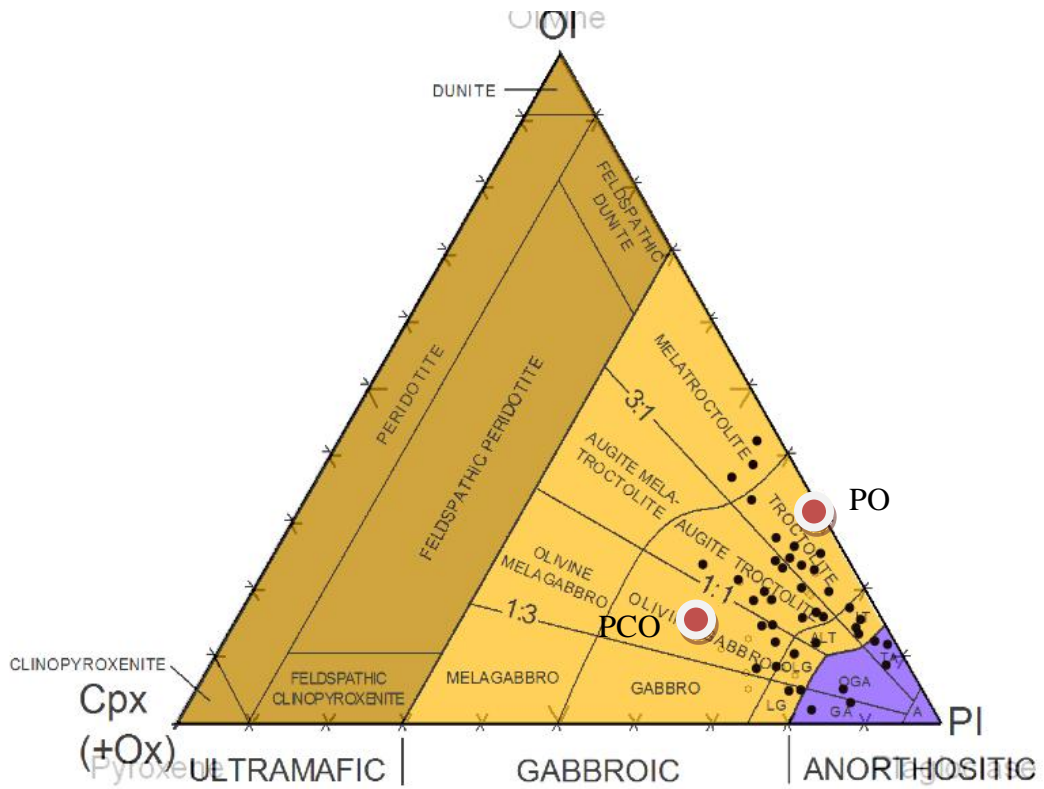


Figure 10: Modal mineralogy of samples collected during field work using the classification scheme of Miller et al. (2002). PCO and PO denote the eutectic and cotectic proportions of a mafic magma multiply saturated in plagioclase, augite, and olivine and plagioclase and olivine at 1 atm (McCallum and Raedke, 1980) as shown in Figure 11..

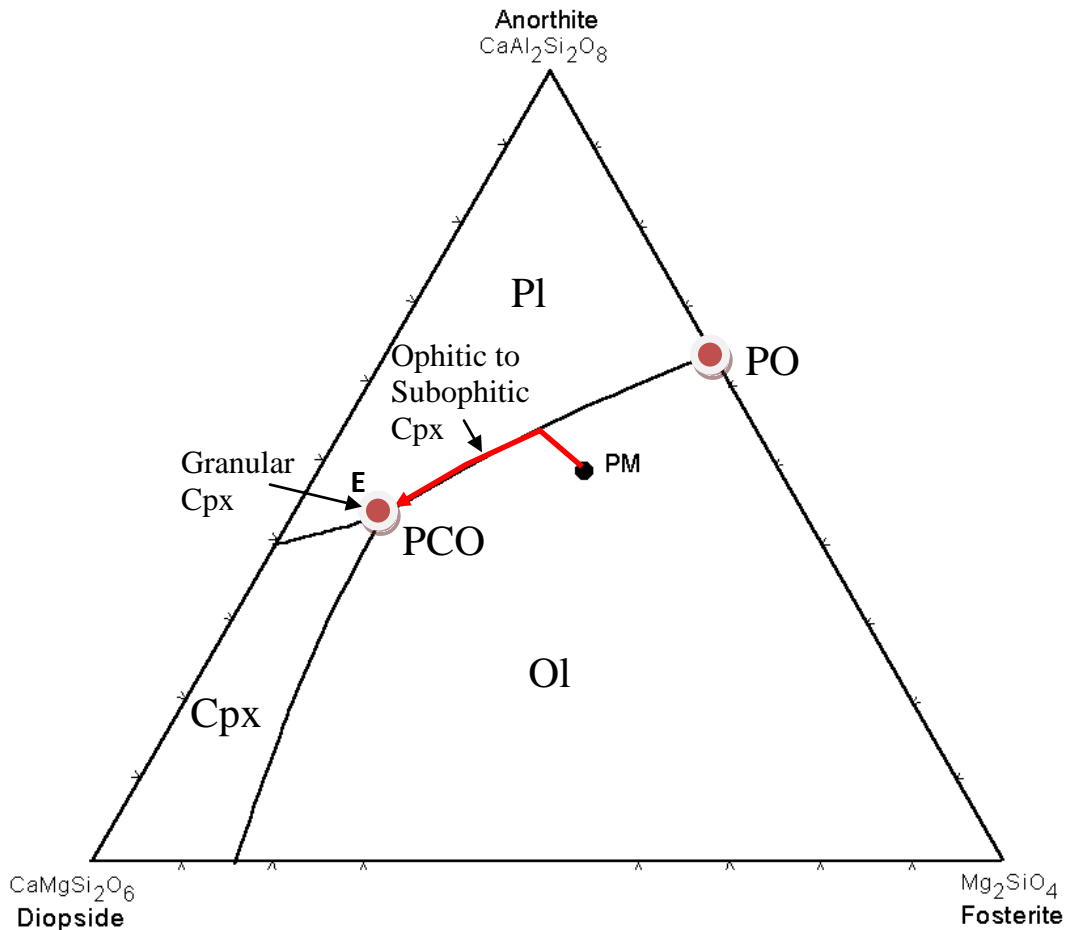


Figure 11. Anorthite-Diopside-Fosterite phase diagram at 1 atm (in mole %). PM indicates possible olivine tholeiitic parent magma of primitive MCR magmas (Miller and Severson, 2002). E is the eutectic point for a multiply saturated magma creating a PCO cumulate. PO show the mole % proportions of cumulus plagioclase and olivine of magmas on the Pl-Ol cotectic. Postcumulus clinopyroxene formed from such cotectic magmas will develop ophitic to subophitic texture. Clinopyroxene formed from eutectic magmas will develop granular textures. Phase relations taken from Winter, 2001.

IV.3 Mineral Chemistry

Both olivine (117 analyses) and pyroxene (115 analyses) were analyzed by EDS-SEM in 15 samples to monitor for evidence of cryptic variation throughout the stratigraphy of the Tuscarora Intrusion. Output data, reported as weight percent oxides, were converted to cation proportions based on 4 oxygen anions for olivine and 6 oxygens for pyroxene. The compositional components of Fo ($\text{Mg}/(\text{Mg}+\text{Fe})$) in olivine and En-Fs-Wo ($\text{Mg}/(\text{Mg}+\text{Fe}+\text{Ca})$, $\text{Fe}/(\text{Mg}+\text{Fe}+\text{Ca})$, and $\text{Ca}/(\text{Mg}+\text{Fe}+\text{Ca})$, respectively) and En' ($\text{Mg}/(\text{Mg}+\text{Fe})$) in pyroxene were calculated from the cation proportions. The ranges of Fo content in olivine and En' content in augite measured in this study as a function of modal rock type are shown in Figures 12 and 13, respectively.

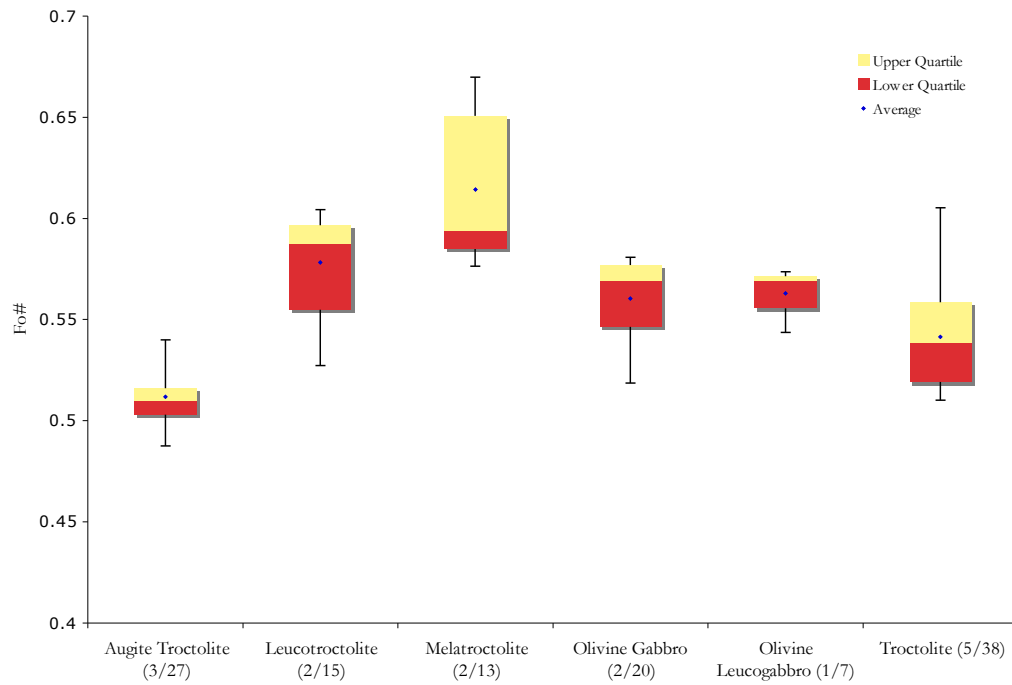


Figure 12. Box and whisker diagram illustrating the variation in Fo content ($\text{Mg}/(\text{Mg}+\text{Fe})$, cation %) of olivines for various modal rock types from study area (Fig. 10) excluding anorthositic rock types. Boxes represent medial 50% of data, lines illustrate range, and diamond represents the average composition. Number in parentheses represents number of samples analyzed/number of analyses performed.

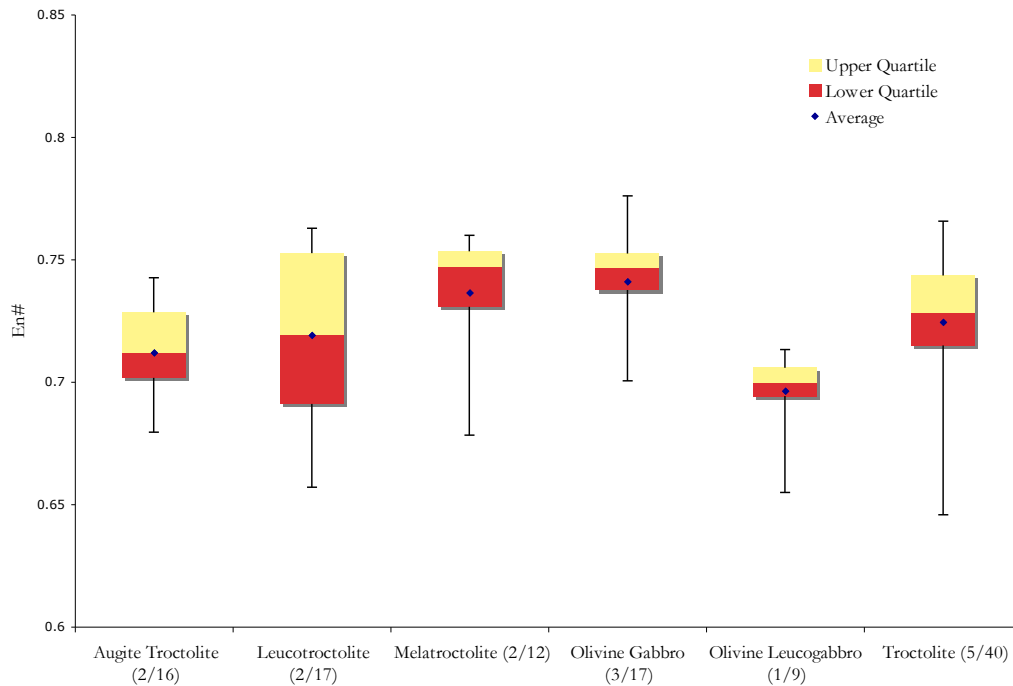


Figure 13. Box and whisker diagram illustrating the variation in En' content ($Mg/(Mg+Fe)$, cation %) of augite in various modal rock types occurring in the study area (Fig. 10), excluding anorthositic rock types. Number in parentheses represents number of samples analyzed/number of analyses performed.

A ternary diagram illustrating the En-Fs-Wo compositions of pyroxenes analyzed is shown in Figure 14. Petrographic observations revealed that augite consistently contains orthopyroxene exsolution lamellae. The high density of lamellae in many samples made it difficult to analyze only the augite host. Analyses of augites containing <38% Wo component are interpreted to contain some lamellae (Fig. 14).

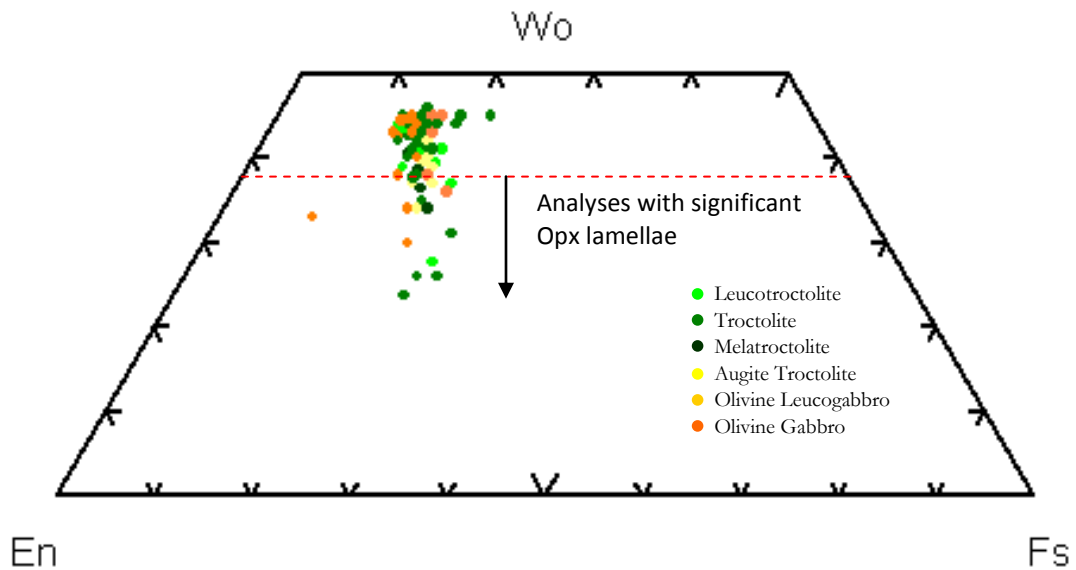


Figure 14 : Ternary diagram of En-Wo-Fs components in augite in samples from the study area distinguished by modal rock type. As discussed in the text, analyses with $Wo < 38\%$ are interpreted to include orthopyroxene exsolution lamellae.

IV.4 Whole-Rock Chemistry

The whole rock chemistry of the twelve samples analyzed for this study are plotted in Figures 15-17. Because the rock studied here are cumulates, the abundances of major elements are controlled by the modes of the primary phases. Since most trace elements are incompatible with cumulus mineral phases, their whole rock concentrations are largely a function of the amount and composition of intercumulus melt incorporated into a rock. Therefore, differences in trace element whole rock concentration may simply reflect variability in the cumulus-intercumulus ratio of a sample without any changes in the composition of the parental melt. To negate this effect, only ratios and relative abundances of incompatible trace elements

are used to evaluate the compositional attributes of the rocks and presumably their parental magmas.

The standard way to evaluate trace element compositions in cumulate rocks is to plot normalized variation diagrams (or spider diagrams). These diagrams use trace element concentrations that are normalized to a standard composition, such as chondrites, bulk earth, mantle, or MORB (Rollinson, 1993) and plot the normalized elements in order of increasing incompatibility to the left of the diagram. In this study, rare earth elements (REE) and trace-element variation diagrams were constructed using IgPet (1997). Figure 15 plots REE data collected for the various rock types analyzed for this study and normalized to chondrite (Sun and McDonough 1989). Figures 16 and 17 plot larger suites of incompatible trace elements from the analyzed samples normalized to chondrite (Thomson 1982) and to E-MORB (Sun and McDonough 1987), respectively.

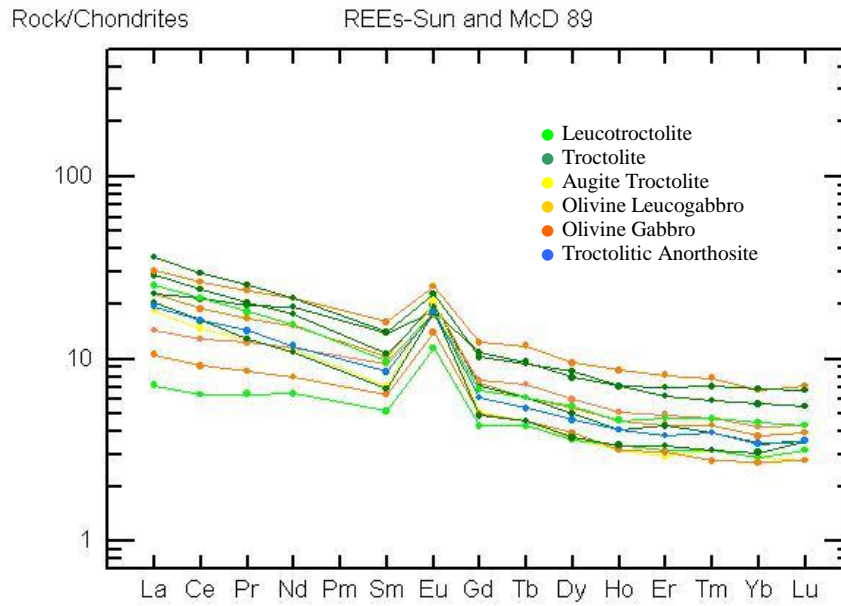


Figure 15: Rare earth element variation diagram for modal rock types analyzed in this study. REE data are normalized to chondrites reported by Sun and McDonough (1989)

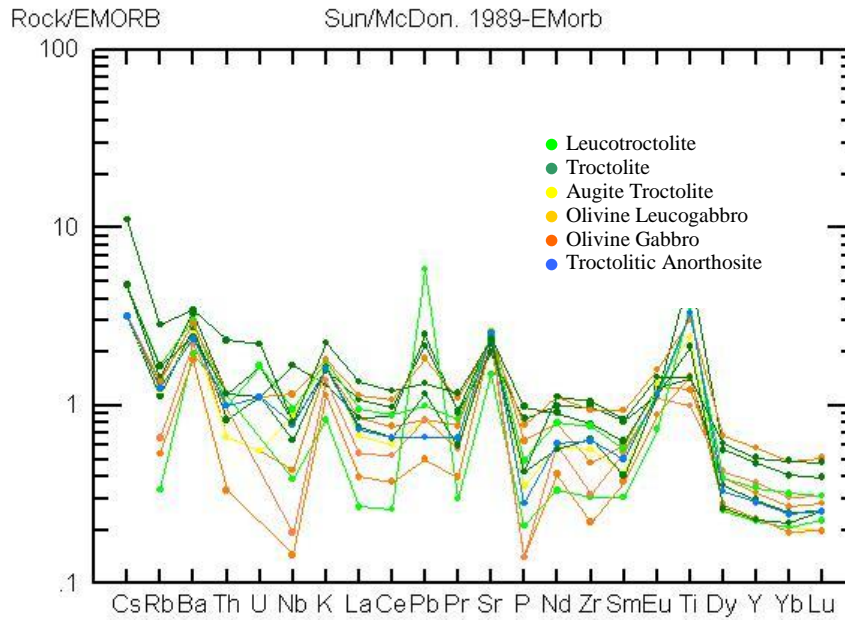


Figure 16: Spider diagram illustrating incompatible trace and minor element concentrations of various modal rock types normalized to E-MORB abundances (after Sun and McDonough, 1989)

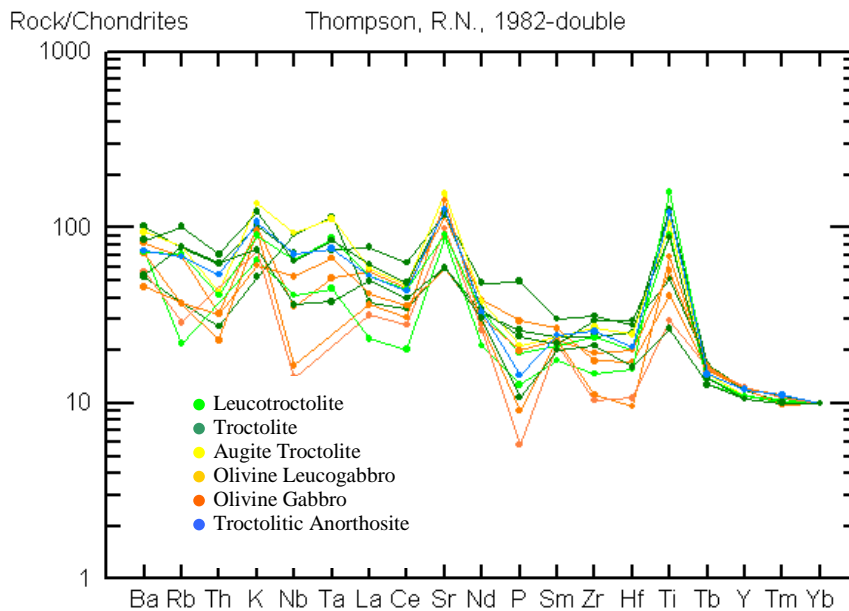


Figure 17: Spider diagram illustrating incompatible trace and minor element concentrations of various modal rock types normalized to chondrite abundances (after Thompson, 1982)

Table 2: Whole rock geochemical data for samples. Major oxides are in percentage, all others in ppm.

Element	GC-204	GC-205	GC-149	GC-153B	GC-154A	GC-186	GC-191	GC-193	GC-116	GC-118	GC-168	GC-215
SiO2	47.72	47.21	43.08	47.31	39.44	45.76	49.3	46.75	47.46	45.4	46.64	48.16
Al2O3	20.27	20.18	15.01	20.99	12.48	18.52	20.75	20.41	19.87	18.87	20.99	20.99
Fe2O3	11.72	11.94	16.39	11.26	25.49	13.14	7.74	11.26	10.29	14.85	10.43	10.48
MgO	5.54	6.65	7.63	4.79	10.59	7.89	5.36	5.6	4.28	6.72	5.28	5.4
CaO	9.5	8.65	9.21	9.45	6.89	9.92	11.92	8.55	11.1	8.43	9.54	9.19
Na2O	3.31	3.23	2.52	3.24	1.89	2.8	3.13	3.26	3.1	2.92	3.24	3.22
K2O	0.42	0.4	0.33	0.44	0.21	0.29	0.35	0.45	0.46	0.42	0.41	0.57
TiO2	1.23	1.42	5.68	2.43	3.66	1.48	1	3.26	3.06	2.15	3.34	1.45
P2O5	0.09	0.14	0.12	0.05	0.03	0.02	0.02	0.07	0.11	0.06	0.04	0.06
MnO	0.12	0.13	0.18	0.12	0.24	0.14	0.1	0.12	0.12	0.15	0.11	0.12
Cr2O3	0.041	0.011	0.012	0.026	0.106	0.146	0.037	0.038	0.032	0.038	0.053	0.037
Ni	116	159	122	105	212	202	129	122	70	166	117	147
Sc	12	7	33	12	22	19	24	12	27	12	11	11
Ba	164	188	156	145	112	103	126	172	166	139	135	196
Be	<1	<1	<1	<1	<1	<1	<1	<1	<1	<1	<1	<1
Co	48	57.1	68.9	45.6	108.1	65.9	34.2	48.5	35.6	61.2	48.7	43.9
Cs	0.2	0.3	0.2	0.2	<0.1	<0.1	<0.1	0.3	0.2	0.3	0.2	0.7
Ga	21.8	20.4	17.5	21.4	18.1	19.4	20.2	21.8	22.2	19.7	20.5	22.7
Hf	1	1.5	2.2	1.1	0.7	0.4	0.7	1.4	2.1	1.4	1.1	1.7
Nb	3.6	6.7	14	7.3	3.2	1.2	1.6	7.9	9.6	5.3	6.5	6.7
Rb	7	7.2	5.7	6.1	1.7	2.7	3.3	8.5	6.8	8.4	6.3	14.3
Sn	<1	<1	<1	<1	<1	<1	<1	<1	<1	<1	<1	1
Sr	397.2	376.2	307.8	410.6	232.2	353.9	382.6	374.5	361.2	344.9	395.9	366.9
Ta	0.3	0.4	1	0.5	0.2	<0.1	<0.1	0.6	0.7	0.4	0.4	0.4
Th	0.4	0.7	0.5	0.4	<0.2	0.2	<0.2	0.6	0.7	0.7	0.6	1.4
U	0.1	0.3	0.2	0.1	<0.1	<0.1	<0.1	0.3	0.2	0.2	0.2	0.4
V	209	91	364	174	942	338	132	175	249	253	220	150
W	<0.5	<0.5	<0.5	<0.5	<0.5	<0.5	<0.5	<0.5	<0.5	<0.5	<0.5	<0.5
Zr	34.7	57.4	72	41.3	22.3	16.1	23.1	56	68.9	47.7	46.2	76.6
Y	7.1	6.5	10.4	4.9	4.9	5.1	8.1	7.6	12.7	5	6.3	11.2
La	5.4	6.8	5.4	4.3	1.7	2.5	3.4	6	7.2	4.8	4.6	8.6
Ce	11.5	14.7	13.1	9	3.9	5.6	7.9	13.2	16.2	9.9	10	18.1
Pr	1.58	1.92	1.88	1.2	0.61	0.81	1.17	1.72	2.26	1.22	1.35	2.41
Nd	7.1	8.2	9	5.3	3	3.7	5.4	7.2	10.1	5.1	5.5	10.1
Sm	1.58	1.64	2.12	1.08	0.79	0.97	1.43	1.48	2.44	1.05	1.3	2.16
Eu	1.18	1.14	1.05	1.22	0.67	0.81	1	1.03	1.45	1.05	1.06	1.32
Gd	1.52	1.45	2.22	1.05	0.88	1.03	1.56	1.39	2.53	1	1.26	2.1
Tb	0.23	0.23	0.36	0.17	0.16	0.17	0.27	0.23	0.44	0.17	0.2	0.35
Dy	1.38	1.27	2	0.92	0.91	0.99	1.52	1.4	2.41	0.94	1.17	2.18
Ho	0.26	0.23	0.4	0.18	a	0.18	0.29	0.26	0.49	0.19	0.23	0.4
Er	0.72	0.71	1.03	0.48	0.52	0.51	0.82	0.78	1.35	0.55	0.63	1.16
Tm	0.11	0.1	0.15	0.08	0.08	0.07	0.12	0.12	0.2	0.08	0.1	0.18
Yb	0.64	0.59	0.96	0.49	0.49	0.46	0.72	0.76	1.15	0.52	0.58	1.16
Lu	0.1	0.09	0.14	0.07	0.08	0.07	0.11	0.11	0.18	0.09	0.09	0.17
Mo	1	0.7	1.6	2.3	0.7	0.3	1.6	0.7	1.3	1.9	0.6	1.3
Cu	103.1	101.3	486.6	158.7	211.9	174.4	66.2	42.5	206.1	300.8	40.1	109.4
Pb	0.5	1.3	1.5	0.5	3.5	0.3	0.5	0.6	1.1	0.7	0.4	0.8
Zn	52	60	51	46	148	55	29	37	28	83	41	44
Ni	86.5	135.7	78.9	85	176.2	162.2	89	78.6	42.1	147.6	89.6	113.1
As	<0.5	0.5	<0.5	<0.5	<0.5	<0.5	0.7	0.6	0.6	<0.5	<0.5	0.7
Cd	<0.1	<0.1	<0.1	<0.1	<0.1	<0.1	<0.1	<0.1	<0.1	<0.1	<0.1	<0.1
Sb	<0.1	<0.1	<0.1	<0.1	0.5	<0.1	<0.1	<0.1	<0.1	<0.1	<0.1	<0.1
Bi	<0.1	<0.1	<0.1	<0.1	<0.1	<0.1	<0.1	<0.1	<0.1	<0.1	<0.1	<0.1
Ag	<0.1	<0.1	0.2	<0.1	<0.1	<0.1	<0.1	<0.1	<0.1	<0.1	<0.1	<0.1
Au	<0.5	<0.5	0.9	<0.5	0.9	0.6	<0.5	<0.5	4.6	<0.5	<0.5	<0.5

V. Discussion

The Tuscarora Intrusion within the Gillis Lake 7.5' quadrangle has been studied through field mapping, petrographic observations, and geochemical analyses. The discussion to follow will focus on interpretations of the geology and petrology of the Tuscarora and related lithologies based on these data. First, the lithostratigraphic zones and units comprising the Tuscarora Intrusion in the study area will be defined and their lithologic, petrographic, and geochemical characteristics described. Next, the petrologic characteristic of the Tuscarora will be compared previous interpretations and to other layered series intrusions of the Duluth Complex. Thirdly, a possible parental magma to the Tuscarora Intrusion will be estimated from geochemical attributes. Finally, the petrogenetic relationship between the Tuscarora Intrusion and the Anorthositic Series will be discussed and a model for the emplacement of the two series will be proposed.

V.1 Geology of the Tuscarora Intrusion and Related Rocks in the Gillis Lake Quadrangle

Based on field, petrographic and geochemical attributes determined from this and previous studies, the Tuscarora Intrusion is defined to be a 2.5 km-thick, gently south-dipping mafic intrusion occurring along the northern margin of the Duluth Complex. It can be subdivided into two lithostratigraphic zones that are

distinguished on the basis of dominant lithologies, cumulate textures, and types of inclusions. These zones are hereafter referred to as the the Lower Zone (LZ) and the Upper Zone (UZ) (Figure 18 and Plate 1) and, as will be discussed below, are interpreted to represent successive episodes of magma emplacement.

In general, the Lower Zone is primarily composed of intermittently layered augite troctolite with a basal interval characterized by taxitic texture and with abundant footwall inclusions. A distinctive feature of the Lower Zone is that it contains numerous large basaltic hornfels blocks. In contrast, the Upper Zone is dominated by troctolite containing much less pyroxene than the LZ. A melatroctolite interval marks the base of the Upper Zone. Hornfels inclusions are conspicuously absent from the UZ. Instead, Anorthositic Series-type inclusions are ubiquitous and are concentrated in the roof zone of the Tuscarora Intrusion near the contact with the overlying Anorthositic Series. The field and petrographic attributes of the two major zones of the Tuscarora Intrusion are described in detail below, as are the characteristics of the bounding footwall rocks and the hanging wall rocks of the Anorthositic Series.

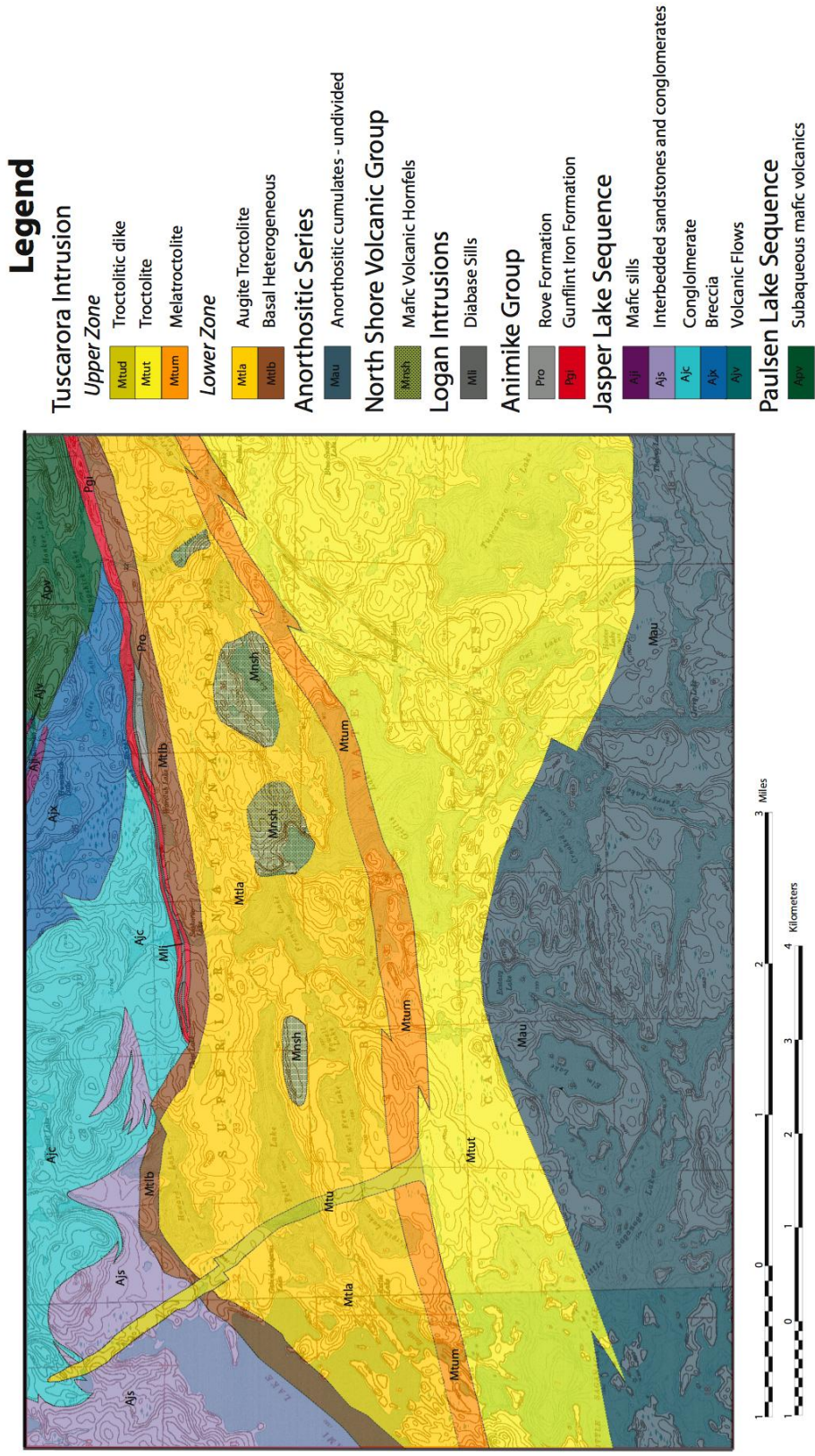


Figure 18: Generalized geology of the Tuscarora Intrusion in the Gillis Lake and Gabimichigami Lake 7.5' quadrangles. See Plate 1 for a 1:24,000 scale of this map.

V.1.A Footwall

The footwall of the Tuscarora Intrusion is composed of Archean metasedimentary and metavolcanic rocks, as well as Paleoproterozoic metasedimentary rocks. These lithologies have been mapped in detail by Jirsa and Starns (2008) as a major focus of their mapping in the Cavity Lake fire area and descriptions given here are taken largely from that study. The Archean rocks have been informally subdivided into the Jasper Lake and Paulsen Lake sequences, which are separated by a major regional unconformity. The Paulsen Lake sequence is the older sequence and contains mafic to ultramafic intrusive and volcanic lithologies with minor amounts of interbedded greywacke and slate. The Jasper Lake sequence, in comparison, is dominated by dacitic volcanic flows with overlying sandstone and conglomerates. Geochemical evidence suggests that magmas related to the nearby Saganaga Tonalite may be the source for Jasper Lake volcanism (Jirsa and Starns, 2008)

The Paleoproterozoic sedimentary units that unconformably overlie the Jasper and Paulsen Lake are the Gunflint Iron Formation and the Rove Formation. The Gunflint Iron Formation is composed of interlayered chert and silicate iron-formation. This unit is overlain by the Rove Formation, which is composed of interlayered slate, siltstone, and greywacke. Both of these units have very narrow

surficial exposure between Archean rocks and the base of the Tuscarora Intrusion (Figure 18, Plate 1).

Where encountered to the north of Flying Lake in this mapping study, the Gunflint Iron Formation is approximately 75 meters thick, and dips to the south at approximately 25°. The whole of the iron formation is observed to be magnetite-rich and thinly bedded. In addition, the unit displays a fine-grained, massive texture likely reflecting thermal metamorphism by the Duluth Complex. In one location (station #102), the iron formation is underlain by an approximately two-meter-thick interval of massive quartzite. This horizon is interpreted to be correlative with the Pokegama Quartzite, which underlies the Biwabik Iron Formation to the west.

Within the Gunflint Iron Formation, several mafic dikes were observed cutting across stratigraphy. These dikes are up to 10 meters across and are commonly characterized by a foliated plagioclase-porphyritic interior grading outwards to aphanitic margins. The concentration of plagioclase megacrysts in the core of the dike would seem to be indicative of flow differentiation during intrusion. Although these dikes were first thought to be offshoots of the Tuscarora Intrusion into footwall rocks, the largely aphanitic character is suggestive of a shallow depth of emplacement, and therefore the dikes are interpreted to be related to the Logan Sills, which have been documented in surrounding areas (Jones 1984). The contact between the Tuscarora and the Archean and Paleoproterozoic rocks was observed to

be irregular on a scale of 5 to 10 meters with apophyses of troctolite intruding into underlying units.

V.1.B Lower Zone of the Tuscarora Intrusion

The Lower Zone of the Tuscarora Intrusion can be subdivided into two lithostratigraphic units based on bulk texture, mineralogy, and inclusion types – the basal heterogeneous and augite troctolite units (Figure 18, Plate 1).

Basal Heterogeneous Unit - The lowermost basal heterogeneous unit (Mtlb, Figure 17) is generally composed of strongly taxitic-textured olivine gabbro to augite troctolite and is locally rich in footwall inclusions of underlying Paleoproterozoic and less common Archean lithologies. The largest of these observed in this study is a block of Gunflint Iron Formation exposed at the northern end of Flying Lake that is approximately 15 meters across. Although this iron-formation outcrops as an island and is not exposed in contact with the Tuscarora, it is identified as an inclusion by its steeply inclined bedding ($\sim 55^\circ$ relative to 25° in the GIF) and distance from the main exposure of iron formation.

In this study, the entire stratigraphic extent of the basal heterogeneous unit was observed in both the northeast (Howard Lake) and northwest (Flying Lake) parts of the map area, and was found to be lithologically and structurally similar in both areas. Therefore, the basal heterogeneous unit is inferred to be continuous to semicontinuous across the entire map area (Figure 18, Plate 1). Assuming a general dip of 35° to the south for the basal contact of the Tuscarora Intrusion based on

internal structures, the basal heterogeneous unit is estimated to have a stratigraphic thickness between 50 and 175 meters.

Directly at the contact, the Tuscarora is a fine- to medium-grained ophitic olivine gabbro. Across the full extent of the basal heterogeneous unit, however, it displays a classic taxitic texture, being mineralogically and texturally heterogeneous on an outcrop scale (Fig. 20). The modal mineralogic composition of the basal heterogeneous unit is very diverse and include olivine gabbro, olivine gabbro-norite, augite troctolite, troctolite, and leucocratic varieties. On average, basal unit rock types are more pyroxene-rich than lithologies in the overlying augite troctolite unit (Fig. 19). Textures range from ophitic to intergranular, and grain size ranges from fine-grained to coarse-grained, with local pegmatitic areas. While no modal layering was noted in the field investigation, plagioclase foliation was observed starting approximately 5 meters above the basal contact. The degree and orientation of this foliation was variable on an outcrop scale across the extent of the basal heterogeneous unit in the area. This structural variability is particularly obvious in the vicinity of footwall inclusions and within 5 meters of the basal contact.

Minor (<1%) amounts of interstitial sulfide (chalcopyrite and pyrrhotite) occur in this basal unit. This contrasts with the high concentrations of Cu-Ni sulfide that are characteristic of basal units in other layered intrusions of the Duluth Complex such as the Partridge River and South Kawishiwi intrusions (Hauck et al., 1997).

Petrographic investigation of four samples from the basal heterogeneous unit reveals that olivine is commonly subhedral to amoeboidal whereas pyroxene is ophitic, with oikocrysts measuring up to 3 centimeters across. Plagioclase exhibits euhedral to subhedral morphologies, and is moderately foliated. Inverted pigeonite is present in some thin sections, up to 8%. Opaque minerals (2-7%) are likely magnetite, given their subequant, subhedral morphologies. Orthopyroxene (2-3%) was found in many thin sections as a rim around olivine grains.

Augite Troctolite Unit - The basal heterogeneous unit grades into the augite troctolite unit (Mtl, Fig. 18, Plate 1) by a diminished variability in texture and loss of inclusions. In contrast to the taxitic texture of the basal heterogeneous unit, the augite troctolite unit is more consistent in texture and mineralogy. The dominant modal rock type within this unit is augite troctolite, with locally troctolitic, olivine gabbroic, and leucocratic mafic compositions (Fig. 19). The bulk rock texture is consistently medium- to medium coarse-grained, subophitic to ophitic, and moderately to well foliated (Figs. 20 & 21). In one outcrop (GC143) near a large basaltic hornfels inclusion, however, intergranular augite and oxide was noted. This texture may indicate more rapid cooling against the inclusion such that augite and oxide were locally brought into saturation in the adjacent magma along with olivine and plagioclase. Prominent modal layering is very common across the extent of the augite troctolite unit and tends to parallel well developed plagioclase foliation; both dip gently to the southeast (Plate 1).

Field observations and petrographic investigations of 11 sections from the augite troctolite unit reveal that olivine regularly occurs as anhedral to subhedral grains, but poikilitic texture was noted in a few outcrops and sections. Plagioclase is ubiquitous in all thin sections and is moderately foliated with a subhedral habit. Clinopyroxene consistently exhibits ophitic to subophitic texture (e.g., Figs. 21 and 22) across the unit with oikocrysts between 1 and 5 centimeters in diameter. Rounded magnetite grains are the dominant iron-oxide phase in this unit, although more elongate ilmenite grains also occur, often in association with biotite (up to 3%). Inverted pigeonite is present in some thin sections, up to 3%. Orthopyroxene (hypersthene) was commonly found as thin rims on olivine crystals. Both plagioclase symplectite (Pl + Opx) and olivine symplectite (Opx+Mt) textures were found in many of the thin sections (both up to 5%),

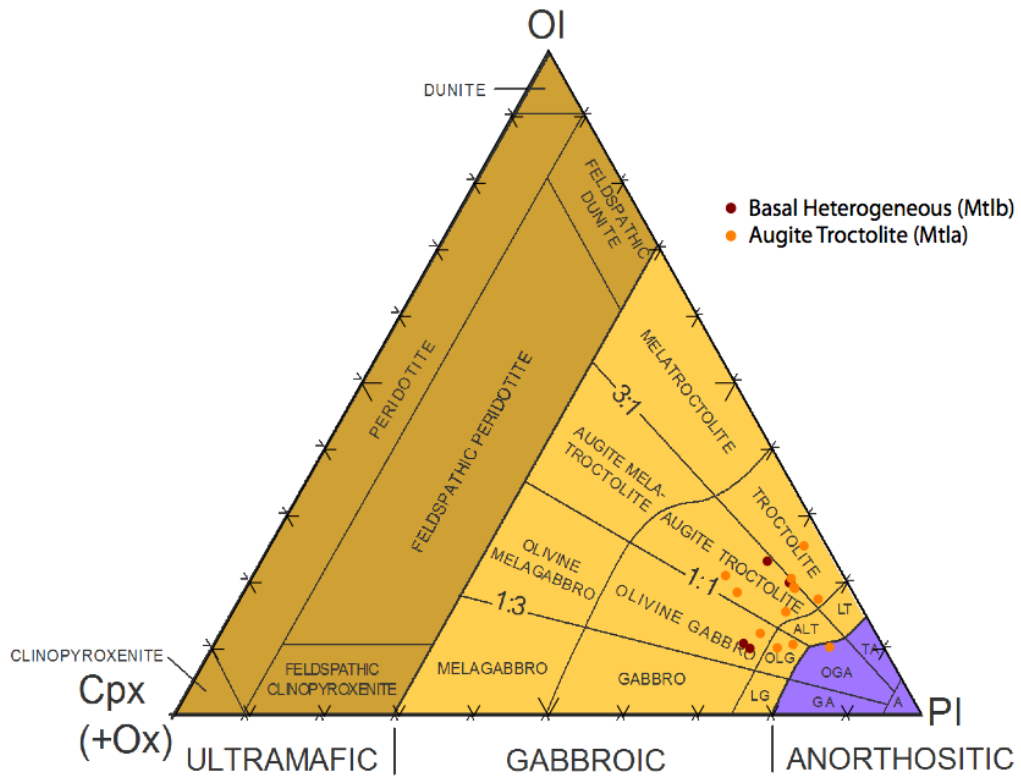


Figure 19: Modal mineralogy of samples from the Lower Zone of the Tuscarora Intrusion based on visual petrographic estimates. Modal classification scheme after Miller et al., 2002.



Figure 20: Taxitic texture typical of the basal heterogeneous unit (outcrop #108)



Figure 21: Typical texture and mineralogy of the augite troctolite unit (outcrop #136)

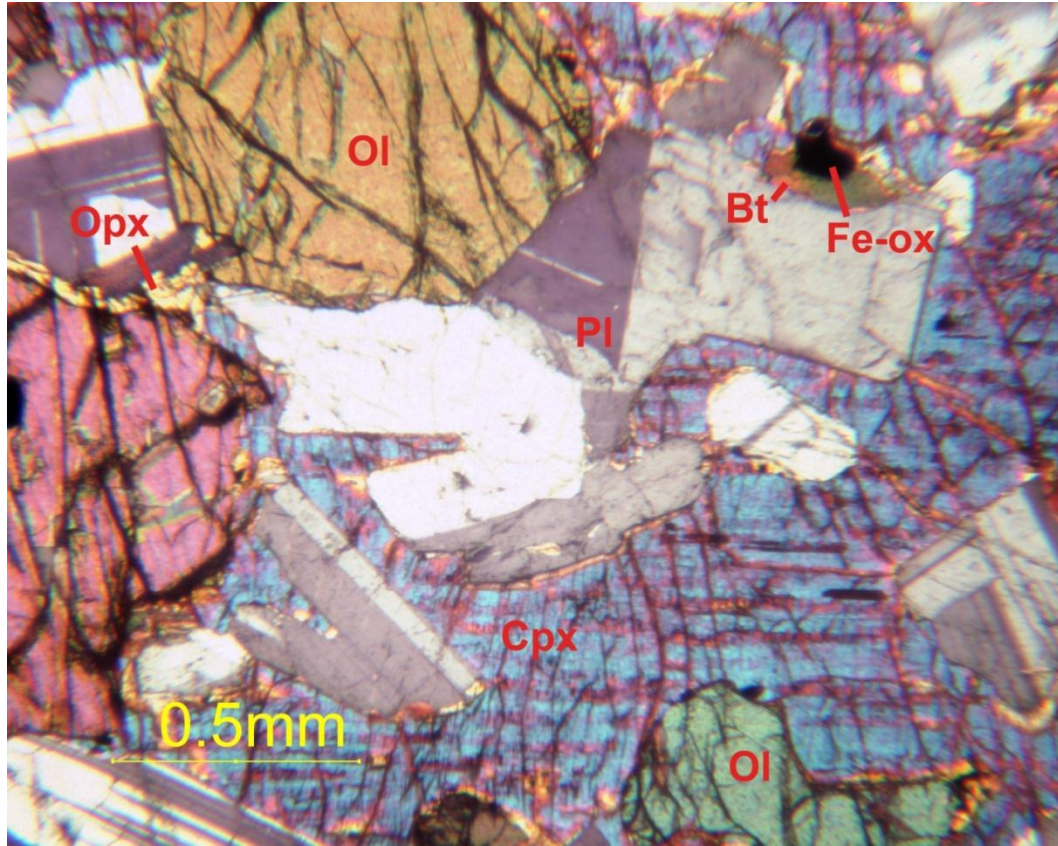


Figure 22: Cross-polarized photomicrograph of augite troctolite from Mtla unit. Contains subophitic clinopyroxene (Cpx), granular olivine (Ol) and plagioclase (Pl), orthopyroxene rims (Opx) on olivine, and Fe-oxide (FeOx) with biotite rim (Bio). Sample #134A.

Inclusions of the Lower Zone – The augite troctolite unit of the Tuscarora Intrusion is characterized by a great abundance of mafic hornfels inclusions, ranging in size from 15 cm up to several hundred meters (Fig. 23). The largest of these inclusions observed in the field area occurs northwest of Bat Lake and northwestern Gillis Lake (Fig. 18; Plate 1) and has map dimensions of approximately 500 by 750 meters. The mafic hornfels blocks are found dispersed evenly throughout the augite troctolite.

Interestingly, a high concentration of large blocks (up to 100 meters across) are located at approximately the same stratigraphic height in the upper section of the lower zone and occur along a trend parallel to the strike of modal layering. The surrounding augite troctolite within 10 centimeters of the sharp contacts with many of the larger inclusions is typically enriched in coarse-grained, subophitic to intergranular pyroxene and iron oxide. These oxide gabbroic halos are interpreted to indicate either contamination by volatiles driven off of the hornfels during thermal metamorphism or supercooling of the enclosing magma bringing augite and oxide into saturation.

The mineralogy of these hornfels inclusions is typically mafic, containing granoblastic-textured assemblages of pyroxene, plagioclase, olivine, oxide, and minor biotite. Several of these blocks exhibit moderate to strong plagioclase alignment. The orientation of this foliation is consistent within a single block, but variable among the different inclusions. This suggests that at least some of the foliation is a primary feature of the basalt, perhaps inherited from an original trachytic texture. The fine grain size, mafic mineralogy, and strong foliation of these blocks suggest they may represent thermally metamorphosed inclusions of basaltic lava flows derived from the basal section of the North Shore volcanics. This interpretation is supported by the occurrence of coarse knots of pyroxene (<2 cm) in some of the smaller inclusions, which have been interpreted elsewhere in the Duluth Complex to be metamorphosed amygdules (Patelke, 1996; Miller and Severson, 2002).

A majority of these inclusions are weakly magnetic, with a few (for example, those at GC191 and GC200) exhibiting notably stronger magnetism. The occurrence of primarily low-iron basaltic hornfels in the Tuscarora Intrusion is correlative with the predominance of primitive olivine tholeiitic basalts at the base the North Shore Volcanics further to the east (Grand Portage basalts of Green, 1972). The stronger magnetism found in GC191 and GC200 reflects a greater magnetite, and presumably, a greater iron content in these inclusions. These observations are consistent with the transition to more evolved basalt compositions observed in the NSVG (Hovland Lavas, Green, 1972).

Alternatively, some hornfels inclusions may have been derived from other nearby intrusive packages. During the emplacement of the Tuscarora Intrusion, fragments of the Poplar Lake Intrusion or Logan Sills could have been incorporated in rising melts and thermally metamorphosed. However, a majority of the Poplar Lake lithologies are too coarse grained to be analogous with the hornfels inclusions found in the Tuscarora. Further geochemical comparisons would be necessary to further constrain the source(s) of these mafic hornfels inclusions.

In addition to abundant mafic inclusions, several other lithologies occur as inclusions within the Lower Zone. Clasts of iron formation (up to 5 m across) are found concentrated within the basal heterogeneous unit, having been derived from Gunflint Iron-formation in the immediate footwall. At least one larger (~30 m diameter) metasedimentary inclusion is present within the augite troctolite, and is

found on the eastern shore of Flying Lake. This block includes both iron formation and metasedimentary rocks, probably of the Rove Formation.

Another curious inclusion of uncertain origin in the augite troctolite is an approximately 50 meter block composed of chert clasts within a fine-grained fragmental felsic matrix (Fig. 24). In their geologic map of the Cavity Lake fire area, Jirsa and Starns (2008) describe a unit of the Paulsen Lake sequence as a felsic tuff and chert. If that is the origin of this inclusion, the fact that this unit occurs at a considerable depth in the footwall would imply that basal contact of the Tuscarora cuts down through the stratigraphy of the footwall and that the inclusion was transported upward some distance within the rising melt. This seems possible given the low density of the felsic mass relative to the mafic melt.

The abundance and types of inclusions are very important in regards to characterizing the units of the Lower Zone of the Tuscarora Intrusion. The basal heterogeneous unit is dominated by sedimentary inclusions from the footwall to the intrusion; partial assimilation of these inclusions is thought to contribute to the heterogeneous texture and mineralogy of this unit. In contrast, the augite troctolite contains many inclusions of mafic hornfels, thought to be incorporated from the North Shore Volcanic Group. The abrupt disappearance of these blocks, along with a change in bulk texture and modal mineralogy, marks the transition to the Upper Zone of the intrusion.



Figure 23: Mafic hornfels inclusion found in the augite troctolite. The block disrupts local plagioclase foliation. Outcrop# 119.



Figure 24: Inclusion composed of cherty clasts within a felsic matrix found in the augite troctolite unit (M_{tla}). Outcrop #112.

V.1.C Upper Zone of the Tuscarora Intrusion

A sharp break in lithology, homogeneity, and abundance of inclusions marks the transition between the Lower Zone and Upper Zone of the Tuscarora Intrusion. The medium- to coarse-grained augite troctolite with abundant hornfels inclusions that characterizes the M_{tla} unit of the Lower Zone abruptly transitions upward to a homogeneous melatroctolite that itself grades upward to a normal troctolite. Because these two rock types can be traced across the field area, the Upper Zone (UZ) is subdivided into two main lithostratigraphic units – a thin lower melatroctolite unit and an upper troctolite (M_{tum} and M_{tut}, respectively; Figure 18, Plate 1). A third unit assigned to the Upper Zone is a troctolitic dike (M_{tud}, Figure 18, Plate 1) that

cross-cuts the lower zone. It is lithologically similar to the troctolite unit and appears to emanate from the upper zone, though geologic constraints are not well established.

Melatroctolite Unit - The lower interval of the Upper Zone is a medium fine- to medium-grained, well foliated, oxide-bearing melatroctolite. Field estimates suggest this unit contains up to 45% olivine. Many outcrops exhibit modal layering of olivine. This unit is relatively narrow, with a maximum thickness of 125 m. Its thin nature and olivine-rich mode likely accounts for its poor exposure. Olivine-rich troctolites elsewhere in the complex are notoriously poorly exposed due most likely to preferential weathering relative to normal troctolitic lithologies (e.g., Severson and Hauck, 1990; Miller and Severson, 2005).

Petrographic studies reveal a modal mineralogy that ranges from melatroctolite to oxide troctolite (Fig. 25). Olivine is typically subhedral granular and is locally significantly altered (up to 10%), most commonly to iddingsite and magnetite. Plagioclase is moderately altered to sericite and occurs as subhedral laths that are commonly aligned to a moderate to well developed foliation. Subophitic to ophitic augite was found in all thin sections, although in low modal amounts (<10%, commonly 3-5%). As in other units, orthopyroxene is present as peritectic rims on olivine grains. Some exposures contain up to 5% Cr-rich spinel phases.

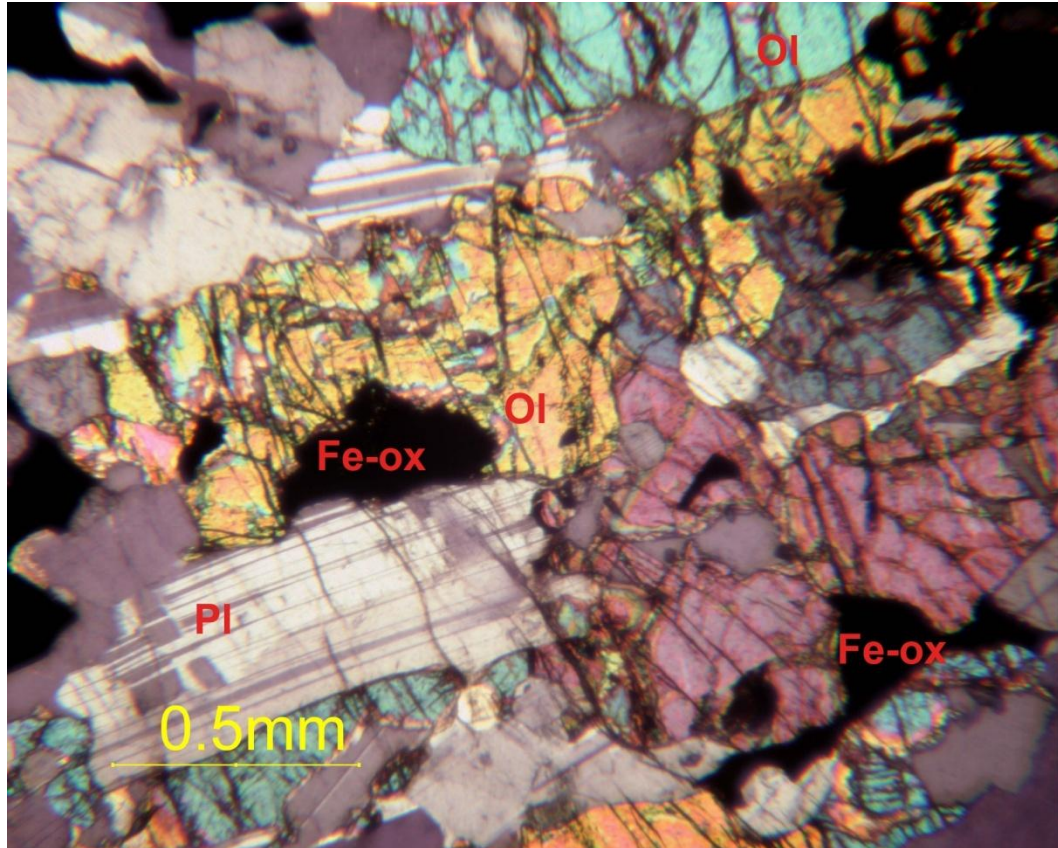


Figure 25: Photomicrograph of melatroctolite (sample #170; cross-polarized light)
Contains subhedral granular to subpoikilitic oxide (Fe-ox) that is spatially associated
with olivine (Ol). Some of the oxide may be Cr-spinel.

Troctolite Unit - The contact between the melatroctolite unit and the overlying troctolite unit is gradational over a 5- to 10-meter-thick interval and is characterized by a decrease in olivine content to below 25%. Overall, the troctolite unit has modal compositions ranging from troctolite to augite troctolite and more leucocratic compositions (Fig. 26). Clinopyroxene is present in low to moderate amounts (5-12%) and, like its occurrence in the lower zone, is consistently ophitic to subophitic.

Although the troctolite unit is remarkably homogeneous in texture and mineralogy on an outcrop scale, it has a ubiquitous internal structure that is defined by poorly to well developed foliation (Fig. 27) and well-developed, rhythmic modal layering. This layering contained multiple examples of cross-bedding, suggestive of channels cross-cutting one another during emplacement.

Petrographic observations of 13 samples from the troctolite unit reveal olivine to be most commonly subhedral granular (Fig. 28), with a poikilitic texture found in a few samples. The degree of iddingsitic alteration of olivine in the troctolite is much less than the underlying melatroctolite. Plagioclase symplectite (Opx + Ca-Pl) is very common across the unit, being found in nearly every section. Olivine symplectite (Opx+Mt) is also found in some samples. Although clinopyroxene is subophitic to ophitic across nearly all of the unit, two samples contained granular pyroxene. These two samples were taken adjacent to large hornfels inclusions, and may represent contamination through partial melting of the block or chill effects as noted around other inclusions. Orthopyroxene locally occurs as a reaction rims on olivine (<4%).

Iron oxides often displayed elongate forms, which implies that they are mostly ilmenite. Some rounded Ti-magnetite grains were also identified (<20% of all oxides).

A striking difference between the upper and lower zones is the absence of mafic hornfels in the Upper Zone. Instead, the UZ contains numerous inclusions of anorthositic lithologies, especially near the contact with the overlying Anorthositic Series (AS). These inclusions are most commonly poikilitic troctolitic anorthosite, but ranged from olivine gabbroic anorthosite to anorthosite. More details about the lithologic attributes of these inclusions and their contact relationships with the enclosing troctolite will be discussed in a later section.

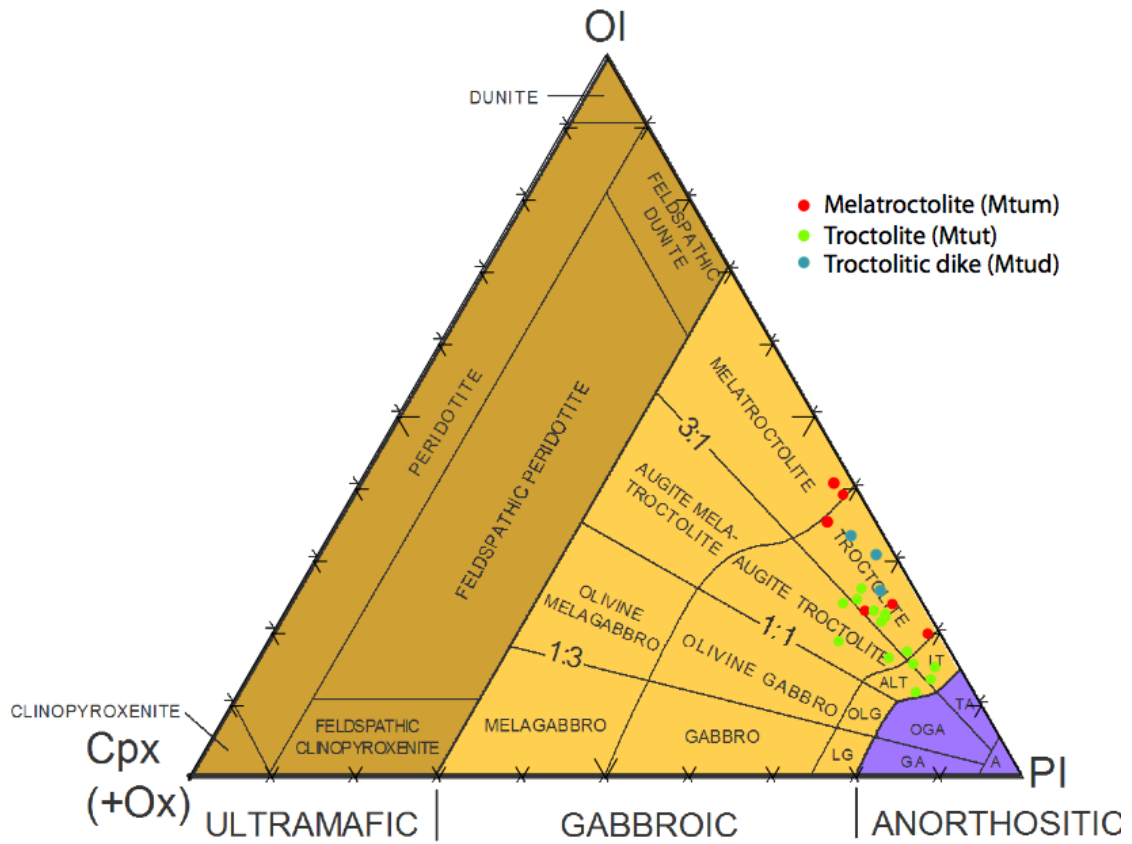


Figure 26: Modal mineralogy of samples from the Upper Zone of the Tuscarora Intrusion, based on visual petrographic estimates. Modal classification scheme after Miller et al. (2002).

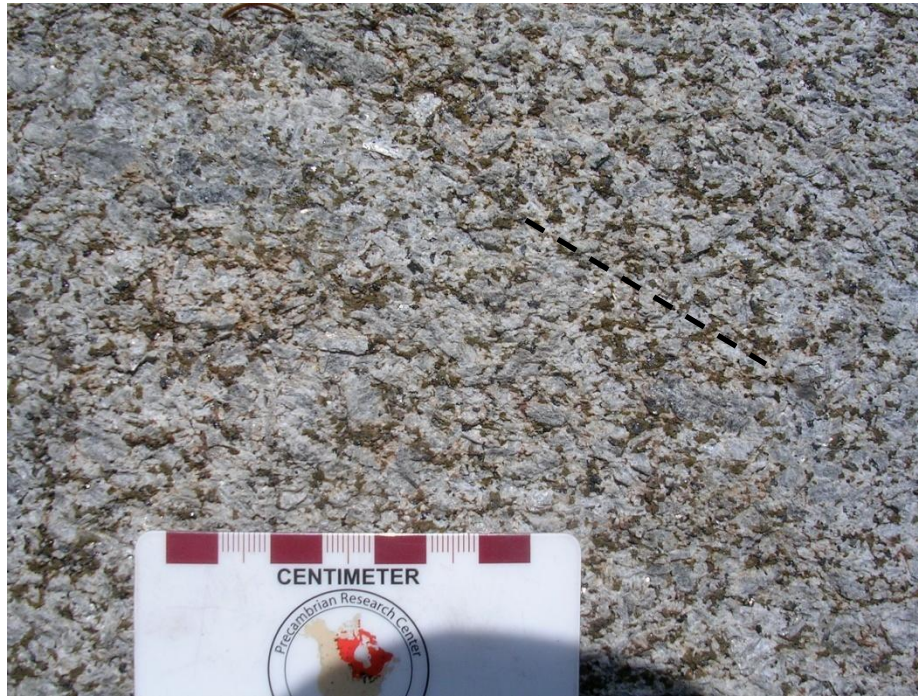


Figure 27: Typical texture of leucotroctolite found in the troctolite unit of the Upper Zone (unit Mtut). Orientation of moderate foliation denoted by black line (Outcrop #168)

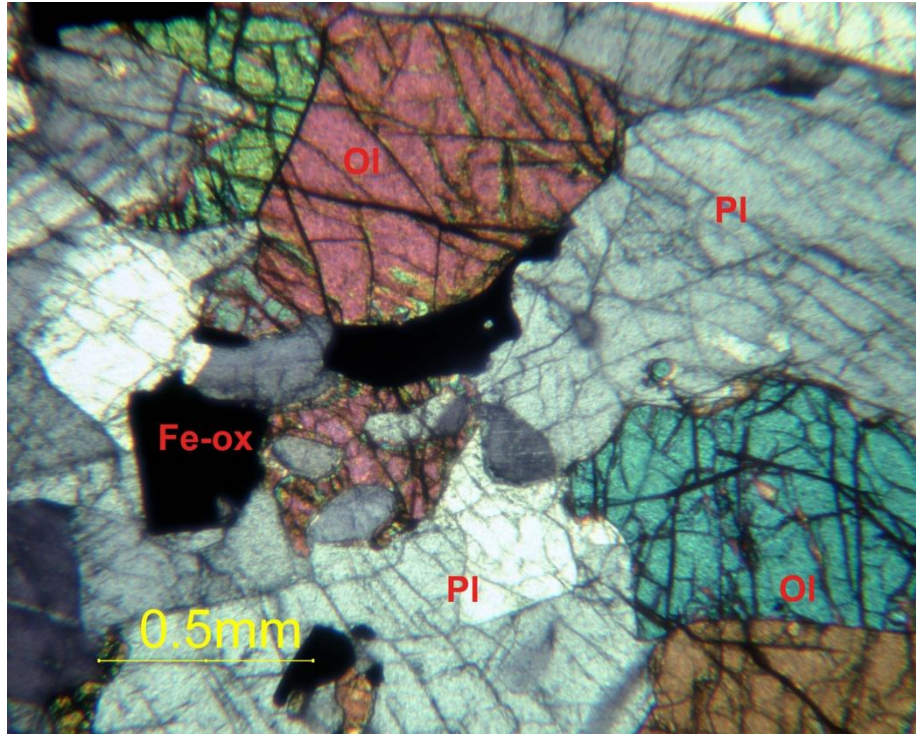


Figure 28: Photomicrograph of troctolite from the troctolite unit of Upper Zone (cross-polarized light). Olivine (Ol) and plagioclase (Pl) are granular, while augite displays subophitic texture (Sample #198).

Troctolite Dike - A troctolitic dike cutting the Lower Zone of the Tuscarora and the Archean footwall was discovered on the northeastern shore of Gabichigami Lake during mapping for the UMD Precambrian field camp (Jirsa et al., 2007). In this area, the dike (unit Mtud) is approximately 20 meters wide and trends north-northwest. The dike is a fine- to medium-grained troctolite with poikilitic olivine (up to 4 cm across) and weak modal layering present near the contacts with surrounding rocks. There is no evidence of chilling along the dike margins, Instead, plagioclase foliation and modal layering are oriented parallel to the contact and are associated with a change in mineralogy and texture. Anorthositic rock types locally occur as inclusions

ranging in size from 1 to 50 cm, most often concentrated in the center of the dike. The troctolitic dike intrudes through the augite troctolite (M₁la) and basal heterogeneous (M₁lb) units and into the footwall metasedimentary rocks. The dike was only mapped in the area surrounding Gabichigami Lake. Its extension to the south into the upper zone is largely speculative. However, its augite-poor composition and the occurrence of anorthositic inclusions in the dike is consistent with its being an offshoot of the upper zone troctolite (Figure 18, Plate 1). On the other hand, the common occurrence of poikilitic olivine is inconsistent with its being correlative with the Upper Zone since such textures are rarely observed in the UZ.

Anorthositic Inclusions of the Upper Zone

As mentioned above, both the abundance and lithologic types of inclusions vary widely over the extent of the Tuscarora. While the Lower Zone is characterized by an abundance of mafic hornfels inclusions as well as clasts of footwall material, the Upper Zone is dominated by anorthositic inclusions that are especially concentrated near the contact with the overlying Anorthositic Series. These blocks are interpreted to be inclusions based on the local disruption of plagioclase foliation in the surrounding troctolite around an included block: whereas the internal structure of the Upper Zone is typically well developed and uniform, mineral alignment is commonly disrupted locally around anorthositic blocks. The degree and breadth of this disruption is dependent upon the size of the included block.

The anorthositic inclusions of the Upper Zone (Fig. 29) are concentrated in the roof zone of the troctolite unit (Mtum) near the contact with the Anorthositic Series. The shapes of the anorthositic inclusions are typically equi-dimensional (<5 m in diameter) or elongate (up to 15 m) and subparallel to the internal structure of the host troctolite. Two particularly large (~25 m across) and equant inclusions of troctolitic anorthosite occur on the southern shore of Gillis Lake. These inclusions become more abundant with proximity to the contact with the Anorthositic Series. These inclusions hold up topographic highs presumably due to their plagioclase-rich lithologies being more resistant to weathering relative to the surrounding troctolites.

This phenomenon is commonly observed in other parts of the Duluth Complex (Miller, 2009, pers. comm.).

Petrographic observations of the anorthositic inclusions show them to have modal compositions that include troctolitic anorthosite, leucotroctolite, augite leucotroctolite, and olivine gabbroic anorthosite in decreasing order of abundance. Subhedral granular plagioclase composes of 80-95% of the inclusions.. Olivine most commonly occurs as 2-3 centimeter oikocrysts enclosing plagioclase, although in one sample, a low modal abundance of olivine has a medium fine-grained granular habit. Where present, clinopyroxene (<8%) and iron oxides (<3%) are poikilitic to subpoikilitic.

In addition to these troctolitic to gabbroic anorthosite inclusions, nearly pure anorthosite (>90% plagioclase) inclusions were found in several localities within the UZ. These inclusions are very distinct from the lithologies commonly found in the Anorthositic Series, which tends to contain only 75-90% plagioclase (Miller and Weiblen, 1990). Rather, they are more like the anorthosite inclusions found in the Beaver Bay Complex, which are thought to have been derived from the lower crust (Phinney et al., 1972; Miller and Chandler, 1997).

Throughout the Upper Zone, anorthositic inclusions are commonly mantled by a thin (up to 3 cm) rind of troctolite enriched in coarse pyroxene and iron oxides in a similar fashion to the hornfels inclusions as described above. Like the hornfels inclusions, this relationship might represent local contamination of the host troctolite

due to partial melting and/or the degassing of volatiles from the anorthositic block. Although the anorthositic inclusions are poor in hydrous phases, Anorthositic Series rocks typically display significant hydrothermal alteration (Miller and Weiblen, 1990). Though unlikely to undergo partial melting, devolatilization of altered anorthositic inclusion may account for the coarseness of the augite troctolitic rinds.

An alternative explanation may be that the gabbroic rind represents subtly more rapid cooling at the inclusion contact such that the liquidus temperatures of augite and oxide are reached more rapidly in the adjacent magma. If this were the case, it would imply that the anorthositic inclusions had cooled to a significant degree before being incorporated into the Upper Zone magmas of the Tuscarora Intrusion. Given the nearly identical ages of the Anorthositic Series and the Tuscarora Intrusion (Paces and Miller, 1993; Hoaglund, 2010), it seems unlikely that the Anorthositic Series could have cooled appreciably. Therefore, it seems more likely that devolatilization and slightly more rapid cooling are responsible for the development of these gabbroic rinds.



Figure 29: Small inclusion of troctolitic anorthosite within Mtut unit of the Upper Zone. Thin rim of coarse pyroxene and iron oxide is visible around block. Located on southwest corner of Gillis Lake.

V.1.D Anorthositic Series

The semicontinuous exposure of the anorthositic rock types in the southern third of the map area is interpreted to comprise the Anorthositic Series of the Duluth Complex (Figure 18, Plate 1). Outcrops in this area are composed of leucotroctolitic to leucogabbroic rocks that display complex internal structure and lithologic variations typical of the Anorthositic Series elsewhere in the Duluth Complex (Miller and Weiblen, 1990). The contact between troctolitic rocks of the Tuscarora Intrusion is gradational and irregular. The transition is marked by an increase in the concentration of anorthositic inclusions leading eventually to outcrops of

predominantly anorthositic rocks with local injections of troctolite. Identification of any exposure as part of the coherent Anorthositic Series rather than inclusions in Tuscarora came only after ensuring that the outcrop was not surrounded by the troctolitic lithologies of the Upper Zone. In this study, the Anorthositic Series was only mapped in detail where in close proximity to the Tuscarora.

The dominant rock types comprising the Anorthositic Series in the map area include troctolitic anorthosite, olivine gabbroic anorthosite, and olivine leucogabbro (Fig. 30). Lath-shaped plagioclase constitutes 75-90% of the anorthositic lithologies and typically is well foliated (Fig. 31). Orientations of the foliation are inconsistent across the study area, however, as found elsewhere in the Anorthositic Series (Miller and Weiblen, 1990). Olivine habit varies from granular to poikilitic (e.g., Fig. 32) and accounts for less than 15% of the total mode. Miller and Weiblen (1990) note that olivine oikocrysts up to 10 centimeters in diameter are common in the Anorthositic Series, and is informally referred to as “spotted anorthosite”. Pyroxene occurs as ophitic to subophitic oikocrysts throughout the area investigated and oxide typically occurs as subpoikilitic clots.

The Anorthositic Series in the map area is interpreted to serve as the hanging wall to the Tuscarora Intrusion. Based on the modal layering in the uppermost portion of the troctolite, the contact between the Tuscarora Intrusion and Anorthositic Series dips approximately 35° to the southeast.

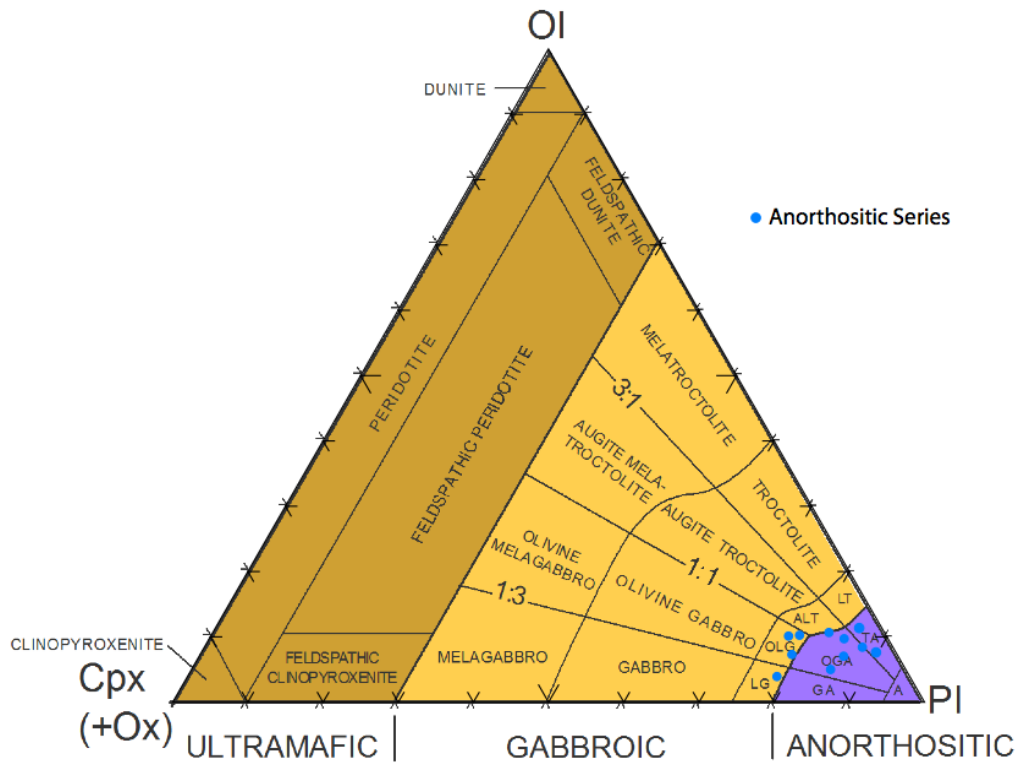


Figure 30: Modal mineralogy of select rocks of the Anorthositic Series within the Gillis Lake quadrangle.

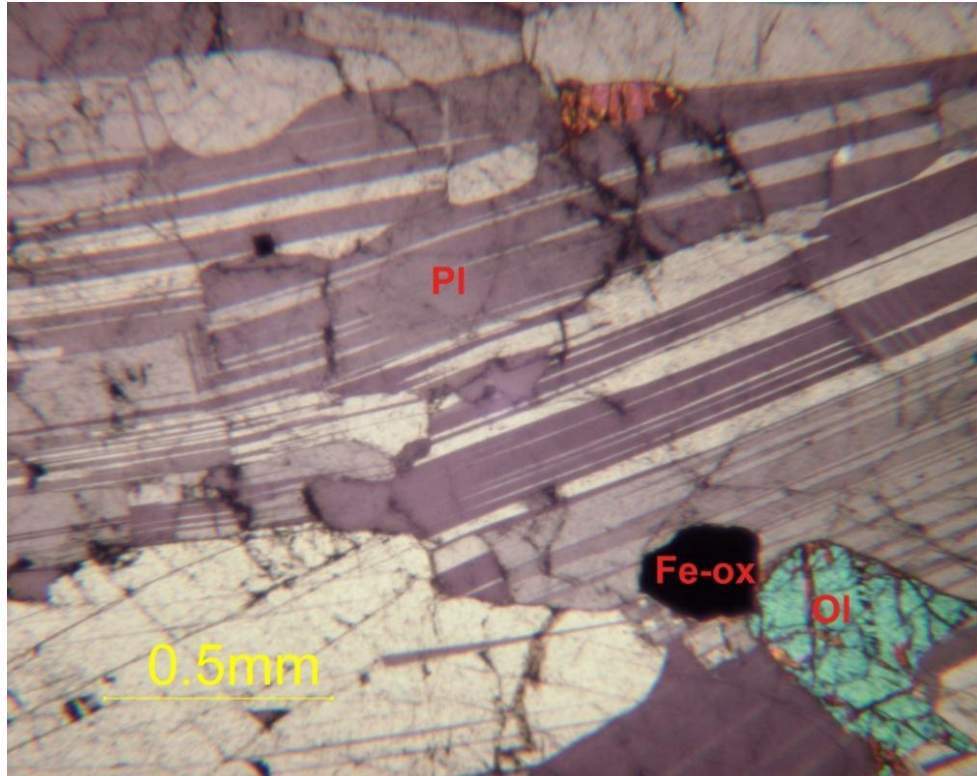


Figure 31: Photomicrograph displaying typical well-foliated texture of Anorthositic Series rocks. Sample #221.



Figure 32: Poikilitic troctolitic anorthosite (map unit Mau). Olivine oikocrysts average 1-1.5 cm in diameter. This texture is referred to as “spotted anorthosite”. Located on western shore of Gillis Lake (station #143).

V.1.F Structural Elements of the Tuscarora Intrusion

A variety of structural features have been observed in the study area that are interpreted to have formed either through magmatic processes during the emplacement of the Tuscarora Intrusion or through later tectonic activity. Within the Tuscarora, modal layering and plagioclase foliation are commonly well developed in all units with the exception of the basal heterogeneous portion of the Lower Zone (Plate 1). In the bulk of the intrusion, both modal layering and foliation generally dip

moderately to the east-southeast. Modal layering is locally well developed, especially within the augite troctolite (M_{tla}) and troctolite (M_{tut}) units, and in a few occurrences displays cross-bedding-like features suggestive of flow of convecting magma (e.g., Irvine et al., 1998). Both layering and foliation approximately parallel unit contacts within the Tuscarora, supporting the interpretation that these features formed through crystal flow and settling during crystallization.

Many large-scale faults have been inferred in the area, primarily through topographic expression and inferred offset of contacts. While some features cross-cut all units within the study area, others are restricted to the Archean footwall (Plate 1). This discrepancy allows a partial understanding of relative ages of these features. In general, the large-scale faults trend north-northeast and most show an apparent right lateral sense of offset. If the motion on these faults involved mostly vertical displacement, it implies east-side (rift-side) up displacement. This would not be expected from normal faulting related to the development of the Midcontinent Rift. It is more likely that these features formed well after the emplacement and crystallization of the Duluth Complex and the continued development of the rift and instead are related to the late compressional phase of the Midcontinent Rift resulting from far-field effects of the Grenville Orogeny to the east (Cannon et al., 1992).

V.2 Comparison to Previous Work

The interpretation of two distinct lithologic zones within the Tuscarora Intrusion is a significant new contribution to the understanding of the geology of the Tuscarora Intrusion. In this section, the findings and conclusions of this study will be compared with previous studies of the Tuscarora Intrusion, in particular with Weiblen and Papike's mapping of the Tuscarora Intrusion in the adjacent Long Island Lake quadrangle (Morey et al., 1981), and with Beitsch's (1991) mapping in the Gillis Lake quadrangle. In addition, the geology and petrology of the Tuscarora will be compared with other Layered Series intrusions of the Duluth Complex. From this discussion, it will become clear that, although the igneous stratigraphy of the Tuscarora Intrusion proposed here differs significantly from previous studies, this reinterpretation reveals that the Tuscarora has more in common with other Duluth Complex intrusions than previously appreciated.

V.2.A Comparison with Previous Mapping Studies of the Tuscarora Intrusion

During their mapping of the Tuscarora Intrusion within the adjacent Long Island Lake quadrangle, Weiblen and Papike (Morey et al., 1981) identified an augite troctolite interval overlain by a unit of interlayered troctolite and anorthosite (Fig. 6). They described the troctolite and anorthosite layers as "interlayered on the scale of centimeters to several meters, with irregular, undulatory contacts." (Morey et al., 1981). No field evidence for interlayering was found during the mapping conducted for this study. Numerous outcrops fitting descriptions of Weiblen and Papike were

found, with thin (up to 3 m wide) horizons of anorthositic rocks, most typically as poikilitic troctolitic anorthosite. However, detailed mapping of these exposures reveal the anorthositic rocks to be discrete inclusions within the troctolite. This interpretation is based on the following observations:

1. Local disruption and draping of plagioclase foliation within troctolite in areas surrounding anorthositic blocks.
2. Thin mantles of coarse pyroxene and iron oxide enveloping many anorthositic blocks, possibly representing subtle quenching of melt during incorporation of relatively cold inclusion block or devolatilation of the xenolith.
3. Internal structure of anorthosite is oblique to contacts with troctolite. This relationship suggests that the anorthosite had crystallized and developed a foliation prior to being incorporated into the troctolite.

Although more elongate blocks of anorthositic rocks are semi-conformable with modal layering and foliation of enclosing troctolites, the orientation of plagioclase foliation within most anorthositic blocks are typically at oblique angles to both the strike of the overall block and plagioclase foliation in the surrounding troctolite. This difference supports the interpretation that these anorthositic occurrences represent inclusions delaminated from the Anorthositic Series during emplacement of the Tuscarora Intrusion, rather than being conformable layers representative of alternating magmatic pulses of troctolitic and anorthositic magmas as implied by Morey et al. (1981).

A second striking difference between the geologic observations of this study and those of Weiblen and Papike in the Long Island Lake quadrangle is the distribution of mafic hornfels blocks within the Tuscarora Intrusion. Whereas this study shows hornfels blocks strongly concentrated in the lower portion of the intrusion, Morey et al. (1981) show hornfels blocks distributed equally throughout the whole of the troctolite (Fig. 7). However, the overall distribution of mafic hornfels is not readily apparent from the Long Island Lake map, since only the largest of these blocks are shown. Whether a greater abundance of small inclusions of mafic hornfels are present in the lower portion of the Tuscarora across the quadrangle is not apparent from the final geologic map of Morey et al. (1978).

Another major difference between the map interpretations is that no melatroctolitic unit is distinguished within the Long Island Lake quadrangle, nor are any olivine-rich lithologies described in the unit explanations. The melatroctolite unit is an obvious and important interval within the Gillis Lake quadrangle as it denotes the break between the Lower and Upper Zones. It also marks the upper stratigraphic limit to the significant occurrence of mafic hornfels inclusions within the intrusion. A possible explanation to account for the differences between the two adjacent quadrangles is variable thicknesses of the two zones, with the Upper Zone pinching out in the western portion of the Long Island Lake quadrangle. The area around Tuscarora Lake, which is critical to resolving this issue, was not mapped during this

study. Alternatively, the authors may have grouped any melatroctolitic occurrences with surrounding lithologies to comprise the whole of their troctolite unit.

Mapping by Beitsch (1991), as part of his Masters' thesis, identified five different units in the Gillis Lake quadrangle based on modal mineralogy and cumulate texture (Figure 6). Although the general mineralogical transitions upwards through the intrusion are similar, significant differences exist between Beitsch's units and those delineated in this study, most notably in terms of cumulate mineralogy. Beitsch's (1991) Peter Lake Unit (plagioclase cumulates) is generally correlative with the Lower Zone of this study, although this study interprets granular olivine to be a cumulus phase along with plagioclase throughout this unit. Beitsch (1991) shows the plagioclase-olivine cumulates of the Virgin Lake Unit as occurring only in the western portion of the study area; this seems to match up with the melatroctolite subzone (unit Mtum), which mapping for this study was able to trace across the field area. The Owl Lake Unit, which Beitsch (1991) describes as a four-phase cumulate, containing granular plagioclase, olivine, clinopyroxene, and iron oxide, was mapped in the eastern portion of the Gillis Lake quadrangle, between the eastern portion of Gillis Lake and western Tuscarora Lake. During this study, only one outcrop containing a four-phase cumulate was found. However, this occurs near the margin of a large anorthositic inclusion on the southeastern shore of Gillis Lake and is interpreted to have formed through contamination or thermal quenching. The

plagioclase-rich Tarry Lake Unit of Beitsch (1991) is correlative with what is interpreted as the Anorthositic Series (unit Mau) in this study.

A major conclusion of this study that contrasts with Beitsch's (1991) work is that the Upper Zone of the Tuscarora Intrusion contains abundant anorthositic inclusions concentrated near the contact with the Anorthositic Series. These inclusions are not described as part of Beitsch's work in the area. He describes many of his units as containing locally heterogeneous areas with an elevated modal percentage of plagioclase, but does not go as far to interpret these areas as inclusions within the troctolite.

V.2.B) Comparisons With Other Layered Intrusions of the Duluth Complex

Similarities between the geology of the Tuscarora Intrusion, as described here, and the basal Duluth Complex in the Lake One (Miller, 1986; 2009) and Ima Lake (Stifter et al., 2009) areas to the west suggest that the Tuscarora Intrusion may extend along the northern margin of the Duluth Complex. If this is the case, this intrusive body would have a strike length of approximately 100 to 150 kilometers, extending from the Snowbank Lake quadrangle to the Gunflint quadrangle, where Nathan (1969) mapped the Tuscarora as intrusive into the Poplar Lake Intrusion.

The igneous stratigraphy of the basal troctolitic rocks in the Gillis Lake quadrangle are similar to that observed in the Lake One and Ima Lake areas, where cyclic variations in modal mineralogy and texture are representative of an open-style

magma chamber. Notably, all three areas are almost exclusively composed of troctolitic (Pl+Ol) cumulates, with subunits characterized by variable amounts of intercumulus augite and Fe-Ti oxide. The lower units are typically an augite troctolite to olivine gabbro with a heterogeneous basal gabbroic unit that shows evidence of volatile and silica contamination, but are absent of any significant Cu-Ni mineralization. The lower units also contain a significant abundance of mafic hornfels inclusions. All three areas transition upward into a homogenous troctolite/leucotroctolite interval that commonly contain Anorthositic Series inclusions. These upper units are thought to represent one or more major new pulses of melt injected into Tuscarora system. While this study only found two macrocycles suggestive of significant episodes of magmatic recharge in the Gillis Lake quadrangle, Miller (1986) has interpreted the upper troctolites in the Lake One area to represent at least three cycles of recharge.

The monotonous troctolitic composition of the Tuscarora Intrusion and its western equivalents are similar to other layered intrusions even further to the west. Both the South Kawishiwi and Partridge River intrusions contain igneous stratigraphies (Severson and Hauck, 1990, Severson, 1994, Miller and Severson, 2002) similar to those recognized in the Tuscarora Intrusion from this study). These western intrusions are subdivided into at least six units that range from augite troctolite in their lower portions to troctolite/leucotroctolite in higher units. Commonly, the bases of individual units in the South Kawishiwi and the Partridge

River intrusions are marked by melatroctolite intervals (Severson and Hauck, 1990; Severson, 1994), as found for the Upper Zone of the Tuscarora Intrusion. These olivine-rich horizons are interpreted, both in this study and in previous work (Severson and Hauck, 1990; Miller and Severson, 2002), to mark the emplacement of recharging melts that were either slightly over-saturated in olivine and/or transporting olivine phenocrysts (e.g., Fig. 11).

Recent geochronologic studies (Hoagland, 2010) have shown the layered intrusions across the extent the northern and northwestern basal contact of the Duluth Complex to have nearly identical $^{207}\text{Pb}/^{206}\text{Pb}$ ages (Partridge River Intrusion - 1097.98 ± 0.37 Ma (Zr); Tuscarora Intrusion - 1098.8 ± 0.3 Ma (Bd)). These results, along with the similar igneous stratigraphies of these intrusions, suggest a widespread troctolite-producing magmatic event along a 100 km stretch of the basal contact of the Duluth Complex at 1098-99 Ma.

V.3 Parental Magma of the Tuscarora Intrusion

Having subdivided the Tuscarora Intrusion into two lithologic zones based primarily on modal mineralogy and inclusion types, this section will evaluate the mineral and whole rock geochemistry of the two zones in order to evaluate whether each zone crystallized from a common or distinct parental magma composition. Moreover, the cryptic variation within each zone will be evaluated to determine the extent to which each zone fractionally crystallized. Concluding that both the Upper

and Lower zones were likely created by a similar parent magma, the composition of that magma will be estimated based first on determining the mg# ($\text{MgO}/(\text{MgO}+\text{FeO})$) of magma in equilibrium with Upper Zone olivine, and then evaluating comagmatic NSVG lavas with similar mg#s as possible parent magma analogues.

V.3.A Evidence from Mineral Chemical Data

In order to determine the extent of parent magma compositions and the cryptic layering within the two zones of the Tuscarora Intrusion, a series of samples were collected on a N-S transect through the center of the mapping area. The stratigraphic heights of these samples were calculated using the surficial distance from the basal contact, along with the average dip of modal layering and/or mineral foliation surrounding the sample.

Mineral chemistry of olivines and clinopyroxene from samples along the stratigraphic profile were analyzed using energy dispersive spectrometry (EDS) on a JEOL scanning electron microscope (procedures described above). These analyses reveal cryptic variations in the mg# of olivine and pyroxene throughout both zones of the Tuscarora Intrusion (Fig. 33), which are generally consistent with fractional crystallization of two major magmatic cycles

Within the Lower Zone, the forsterite ($\text{Fo} = \text{Mg}/(\text{Mg}+\text{Fe})$; cation %) contents of olivine ranges from Fo_{58-56} in the basal zone to Fo_{58-49} in the augite troctolite (Fig. 33). In a similar fashion, the upper zone contains even higher Fo

contents in olivine from the lower melatroctolite (Fo_{58-67}) relative to the overlying troctolite (Fo_{51-58}). Although the spread of data is widely spaced, the generally decreasing Fo contents of olivine through each zone is consistent with fractional crystallization of two major impulses of moderately evolved tholeiitic magma into the Tuscarora Intrusion. The greater Fo content of olivine from the melatroctolite subunit of the upper zone compared with olivine from the basal heterogeneous unit may be interpreted to indicate that the upper zone formed from a more primitive magma. However, given that the melatroctolite unit is composed of adcumulates of olivine and plagioclase with only minor postcumulus augite and oxide, whereas the basal heterogeneous unit is composed of orthocumulates of ophitic olivine gabbro to augite troctolite, the lower Fo contents of olivine from the basal unit may be due to a trapped liquid shift (Barnes, 1986; Chalokwu and Grant, 1987). A greater amount of trapped liquid component in orthocumulate lower zone rocks may explain their more evolved compositions compared to upper zone rocks.

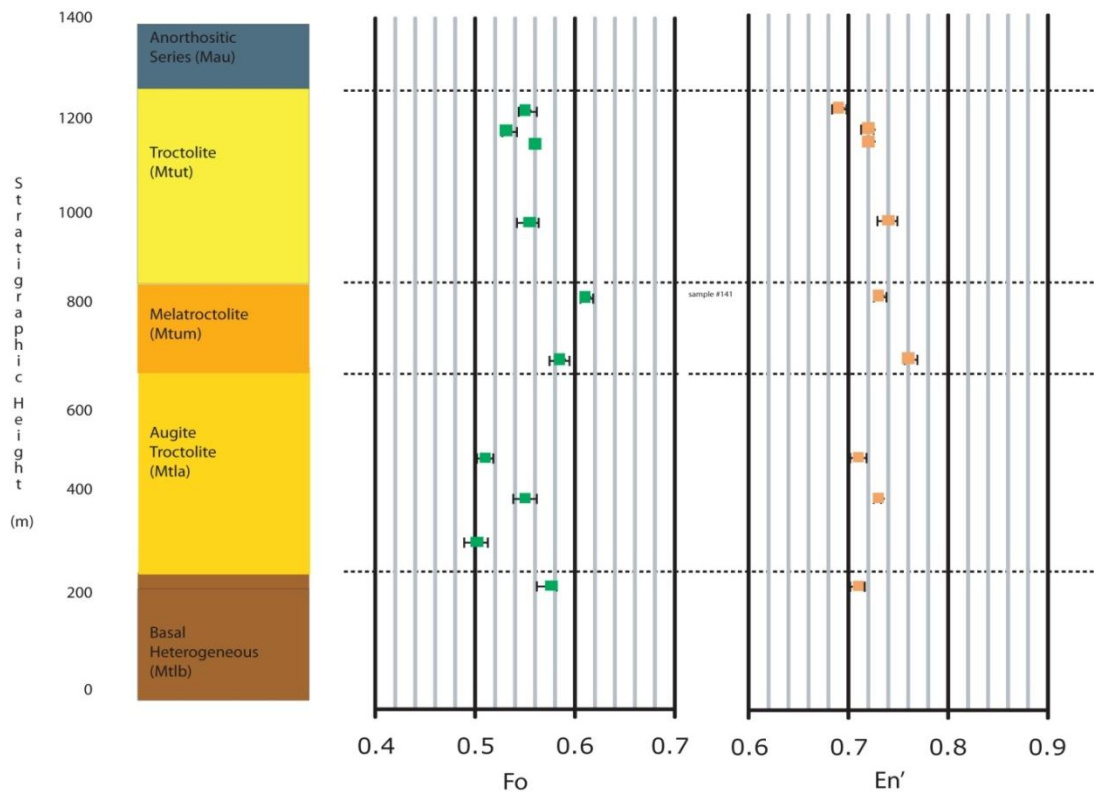


Figure 33: Cryptic variation of Fo content in olivine and En' content in augite through the stratigraphy of the Tuscarora Intrusion. Diamonds show average compositions; error bars show range of multiple analyses (8-10) per sample.

To test the idea that differences in Fo content between the upper and lower zones may be related to re-equilibration of cumulus olivine with a greater abundance of intercumulus liquid in the lower zone, the modal abundance of clinopyroxene is plotted against Fo content in Figure 34. Since pyroxene displays interstitial (subophitic to ophitic) textures throughout the intrusion, its mode can be used as a rough proxy for the volume of trapped liquid in each sample. In samples with a significant amount of intercumulus liquid component, the trapped liquid shift results from cumulus olivine re-equilibrating with the liquid (or the postcumulus olivine rims

crystallized from that liquid) and result in a lower average Fo content. Although not a strong correlation, the data plotted in Figure 34 does display a negative correlation, generally supporting the interpretation of a trapped liquid shift. In other words, it is plausible that the parental magma compositions for the two zones may have been similar and that the differences in olivine composition are due largely to different degrees of trapped liquid shift.

Additional evidence that the parental magmas for the two zones may have been similar is given by the similar average enstatite' (En') contents ($=\text{Mg}/(\text{Mg}+\text{Fe})$; cation %) of subophitic to ophitic (intercumulus) clinopyroxene across both zones of the Tuscarora Intrusion (Figure 33). Because all pyroxene crystallized from the intercumulus liquid, it should not show a trapped liquid shift caused by the reequilibration of cumulus cores and postcumulus rims, as experienced by olivine. Therefore, the similar En' contents of the two zones (save their basal units) supports the idea the parent magmas to the two zones had similar Fe/Mg ratios. Moreover, the generally decreasing En' contents upsection in the two zones are consistent with magmatic differentiation produced by bottom up fractional crystallization of each zone.

The significantly lower En' content of pyroxene in one sample from the basal heterogeneous unit (En₇₁) compared to basal melatroctolite unit of the upper zone (En₇₆₋₇₃) would seem to be inconsistent with similar magma compositions for each zone undergoing similar magmatic differentiation due to fractional crystallization.

The probable cause for this more evolved composition of the basal unit is assimilation and contamination by iron formation, basalt inclusions, and other Fe-rich lithologies that form the footwall and occur as inclusions throughout the basal heterogeneous unit. This Fe contamination may have also resulted in a more extreme trapped liquid shift of olivine composition in the basal unit.

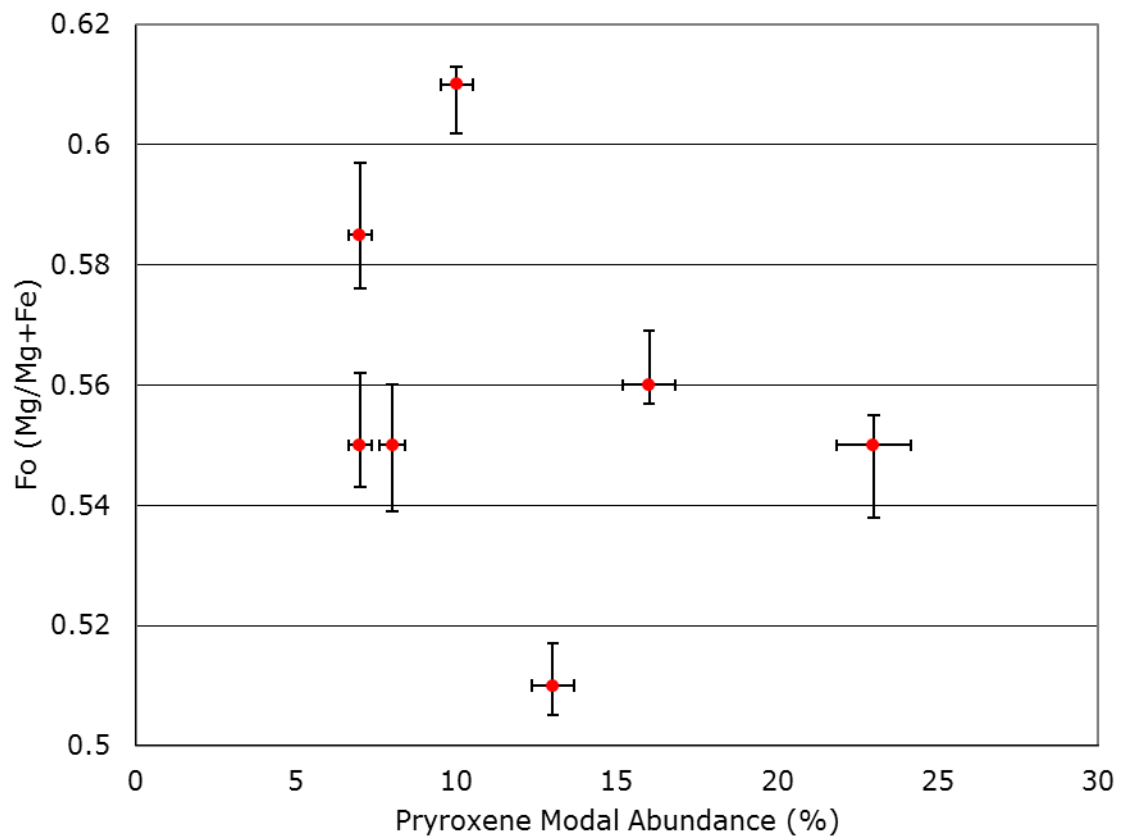


Figure 34: Fo content of olivines, as a function of pyroxene modal abundance (visual estimates). This negative correlation may suggest an ongoing trapped liquid shift during crystallization. Vertical error bars represent Fo range, and horizontal bars equal 5% to allow for estimation errors.

V.3.B) Evidence from Whole Rock Geochemistry

Whole-rock geochemistry was analyzed from samples of both zones within the Tuscarora. Interpretations of absolute trace element concentrations are precluded by the likelihood that all these cumulate rocks are composed of variable proportions of cumulus minerals and intercumulus liquid components of variably differentiated composition. According to classic cumulate theory (e.g., Wadsworth et al., 1961; Wager and Deer, 1967), incompatible elements will have negligible concentrations in cumulus minerals and instead will reside in the intercumulus melt, which eventually crystallizes to form the postcumulus mineral assemblage. Therefore, an orthocumulate with a large abundance of intercumulus melt component will possess a greater concentration of incompatible elements than an intercumulus melt-poor adcumulate. Without an independent way to determine the amount of trapped liquid component in a given sample, it is difficult to assess the degree to which the absolute abundance of incompatible elements in a cumulate rock reflects the amount of intercumulus liquid and the composition of that liquid. For this reason, the incompatible elements were plotted on rare earth element (REE) and multi-element variation (spider) diagrams (Figs. 35 and 37, respectively), where general patterns and trends of trace elements give a general indication of the parental magmas compositions.

Variation diagrams of REE data from the Upper and Lower Zones exhibit a slight enrichment of the light REE relative to generally flat heavy REE (Fig. 35). This pattern is common among mafic tholeiitic magmas worldwide (Rollinson, 1993). The most obvious feature of the REE plots is a sharp positive Eu anomaly found in both zones. This anomaly is no doubt due to the compatibility of Eu^{2+} substituting for Ca^{2+} in cumulus plagioclase, which is present in all samples. The abundance of plagioclase in these samples is evident when comparing these trends to the trend of partition coefficients of REE in plagioclase (Fig. 36).

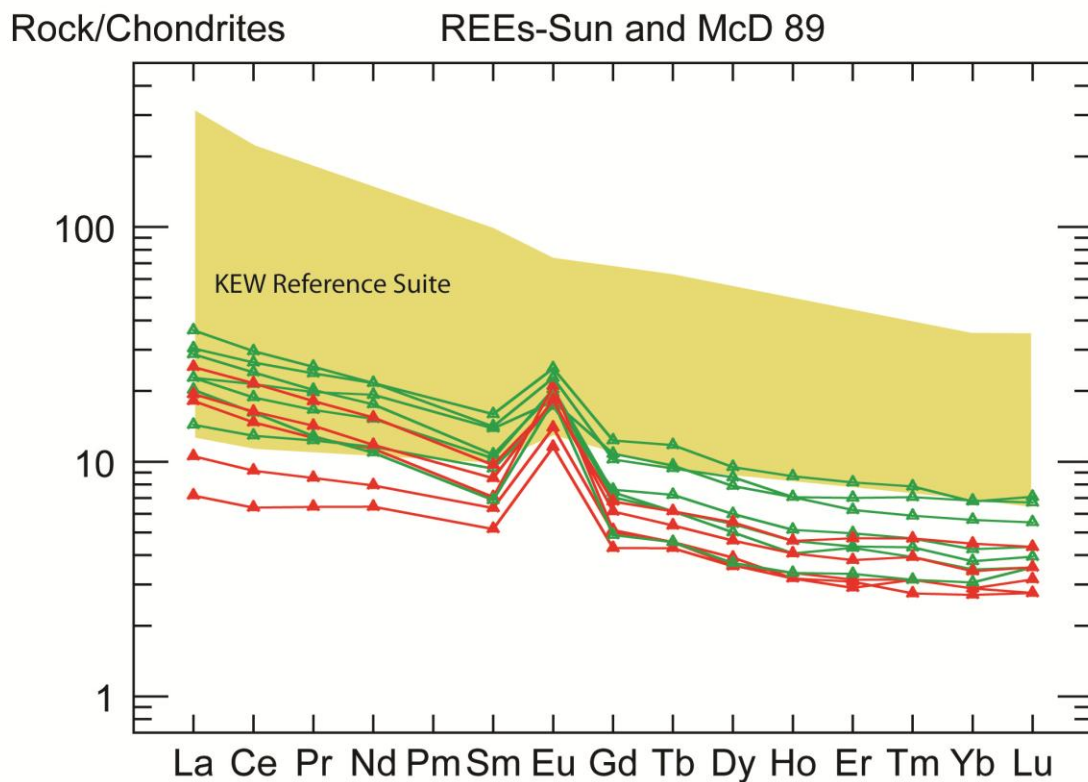


Figure 35: REE concentrations of the lower zone (green) and upper zone (red) samples, normalized to chondrite concentrations of Sun and McDonough (1989)

Relative to the moderate LREE enrichment found in many of the samples, three samples exhibit a flatter trend: two from the melatroctolite unit of the upper zone (samples #141 and #143), and one from the augite troctolite unit of the lower zone (sample #117). These flatter LREE patterns may be explained by the texture and mineralogy of these samples. All three contain abundant olivine (>20%), which prefer HREE over LREE in contrast to plagioclase, which prefers LREE (Fig. 36). In addition, the lower total REE abundance of these samples (particularly those from the melatroctolite) may be related to their being strongly adcumulate and thus contain less intercumulus liquid component. The similar pattern of the upper and lower zones reinforces the interpretation from the mineral chemical data that they formed from a similar parental magmas. The higher concentrations of total REE in the lower zone rocks likely indicates that they contain a higher proportion of intercumulus liquid component compared to their upper zone counterparts, as implied by the greater augite concentration in the lower zone .

These REE patterns are similar to the KEW reference suite of basalts from the North Shore Volcanic Group (BVSP, 1981) acquired by J.C. Green (range shown in Fig. 35). The troctolitic intrusive rocks of the Tuscarora contain much lower concentrations than the basaltic extrusive rocks of the NSVG, presumably due to the dilution effect caused by cumulus minerals. The resemblance between NSVG and Duluth Complex compositions in terms of REE patterns are consistent with both

igneous systems being derived from a similar mantle source, which Nicholson et al. (1997) have suggested was from an enriched mantle plume. In any case, this similarity suggests that the magma compositions represented by the Keweenaw reference suite data may be evaluated for specific compositions that may more directly correlate with the parental magma of the Tuscarora Intrusion. This possibility will be evaluated in the next section.

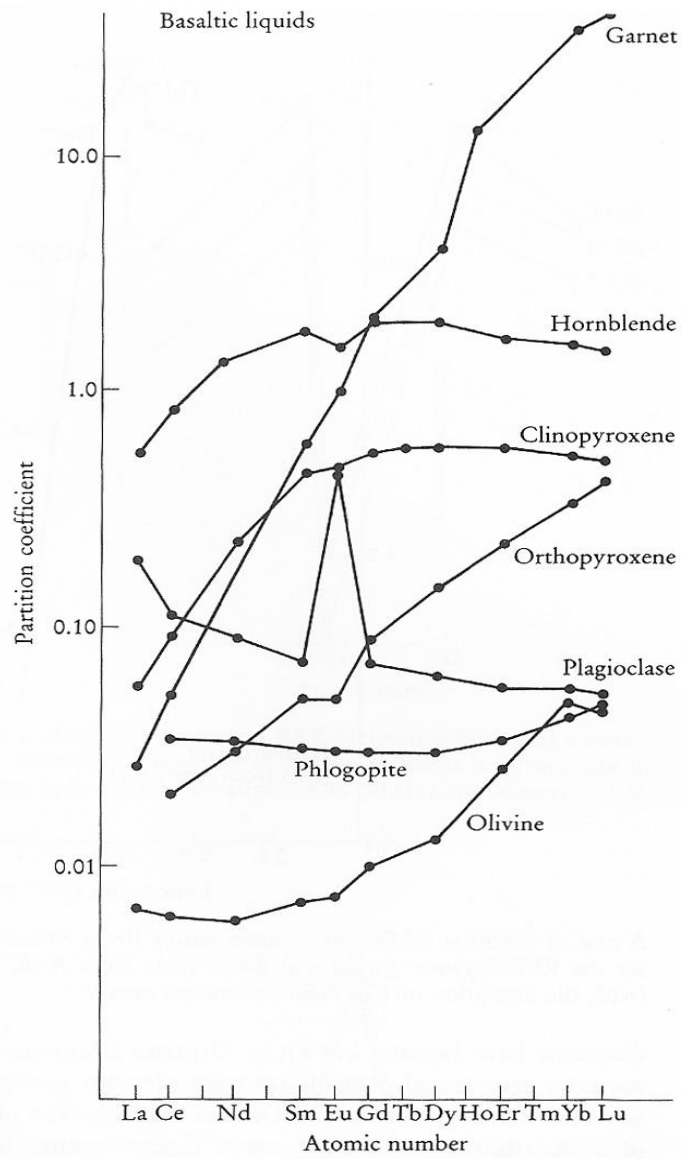


Figure 36: Partition coefficients of REEs between common minerals and mafic magmas. (Rollinson, 1993)

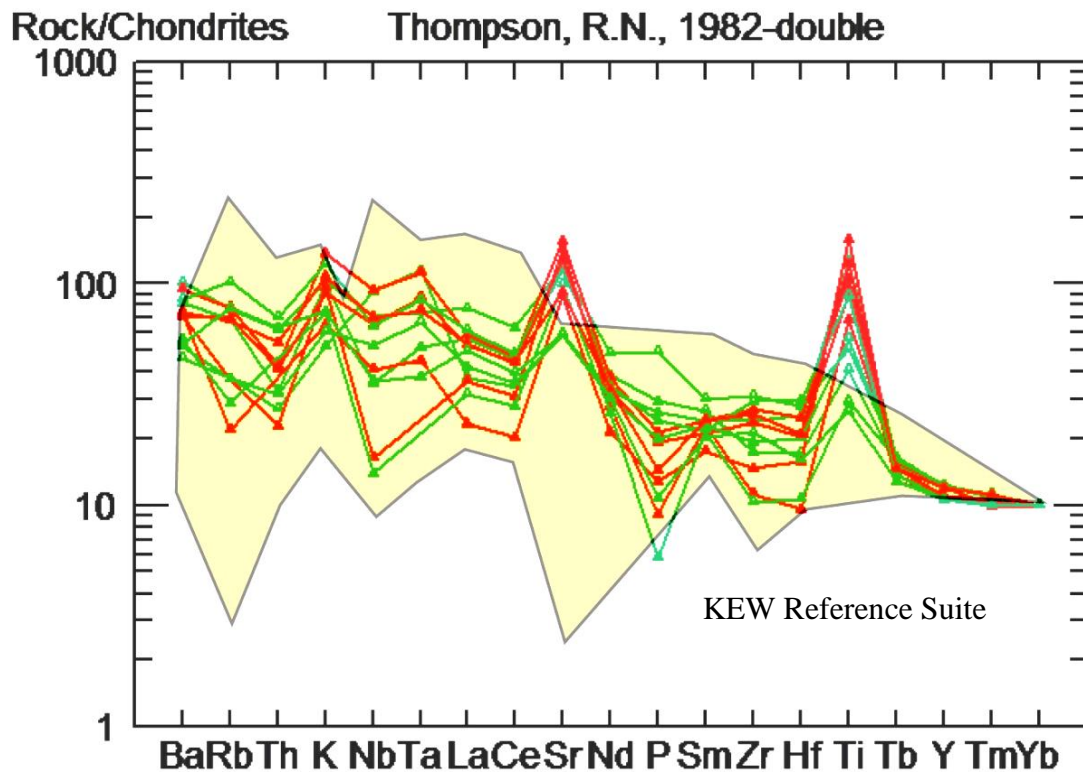


Figure 37: Trace element concentrations of samples from the Lower Zone (green) and the Upper Zone (red), along with range of compositions for NSVG reference suite. All samples are normalized to Yb (Thompson, 1982).

A similar set of subparallel patterns between upper and lower zone incompatible element compositions are observed in the spidergraph of incompatible trace elements plotted in Figure 37. While the concentration patterns are not uniformly co-parallel, an overall similarity of patterns is evident and suggests that both zones were formed from a similar parental magma. Several divergences from a co-parallel trends are seen in all samples, and are probably indicative of differences in

mineralogy. Strong peaks in both K and Sr are probably reflective of the high cumulus plagioclase content. In a similar fashion, the Ti peak common to all samples is likely a function of ilmenite and augite abundance, which is ubiquitous throughout the intrusion.

V.3.C Estimation of the Tuscarora Parent Magma Composition

Concluding that the Upper and Lower Zones of the Tuscarora Intrusion may have been generated by two major inputs of a common parental magma composition, the next step is to estimate that composition. Directly estimating the composition of the melt that formed the two zones of the Tuscarora Intrusion is difficult due to its cumulate nature and the lack of chilled margins. The varying proportions of cumulus and intercumulus material result in a range of whole-rock compositions, as discussed in the results section. One solution to this would be to subtract the cumulus mineral composition from the whole-rock geochemistry. Miller and Weiblen (1990) used this approach to estimate the parent magma compositions of Anorthositic Series rocks. Bedard (1994) developed a similar mass balance model for calculating the incompatible trace element composition of the trapped liquid in a cumulate by calculating out the composition of the cumulus minerals. However, the accuracy of these methods is very dependent on determining the exact modal percentages of cumulus phases. This is especially difficult to do because cumulus phases invariably have some portion that was crystallized as a postcumulus overgrowth rim on a

cumulus core. Although the preservation of zoning in plagioclase allows the discrimination of core from rim, it is difficult to accurately determine their relative proportions. For Fe-Mg silicates (i.e. olivine and pyroxene), any original core to rim zonation is destroyed by subsolidus re-equilibration under slow-cooling plutonic conditions.

Another common means for determining parental composition in igneous intrusions is seeking out the presence of a chilled margin or offshoot dike, which preserves the chemistry at the time of emplacement. Unfortunately, no such features have been found in and around the Tuscarora Intrusion during this study.

A third approach to estimating the parental magma compositions of cumulates is to apply an inverse method, whereby the compositions of cumulus phases are used to back calculate the major element composition of magma that would be in equilibrium with that phase using experimentally-determined partition coefficients. Such equilibrium parameters are not known for plagioclase and mafic magma, but partition coefficients of magnesium and iron in a melt-olivine system has been experimentally determined by Roeder and Emslie (1970). They found that the ratio of mole percent concentrations of FeO or MgO in olivine is related to the ratio in the silicate liquid by a simple equilibrium constant:

$$K_D = \frac{FeO^{ol}}{FeO^{liq}} \times \frac{MgO^{liq}}{MgO^{ol}} \quad \text{Equation 1}$$

For an olivine-mafic melt system, this value was found to equal 0.3 and to be independent of temperature.

The ideal sample to be used for this calculation is cumulus olivine which formed early (before significant fractional crystallization had taken place) and which had undergone little to no trapped liquid shift due to re-equilibration with the intercumulus melt. Sample #141 from the lower part of the troctolite unit of the Upper Zone is used here (Figure 32) as it is the most fosteritic of all analyses ($F_o=60.4$) and has undergone very little alteration. In addition, the sample exhibits an adcumulate texture, containing low amounts of intercumulus material, which minimizes the potential for trapped liquid shift.

The known parameters in Equation 1 are K_D and the mole percent concentrations of FeO and MgO in olivine, determined from mineral chemical data. Applying these data to the equation, the FeO/MgO ratio of the liquid can be calculated. However, a more useful parameter would be the mg# of the liquid. Equation 1 can be recast to calculate the mg# of the liquid as follows :

$$Mg\# = \frac{MgO}{MgO+FeO} \times 100 \quad \text{Definition of mg\#}$$

$$Mg\# \times (MgO + FeO) = 100 MgO \quad \text{Multiply both sides by (MgO+FeO)}$$

$$Mg\#MgO + Mg\#FeO = 100 MgO \quad \text{Distribute}$$

$$Mg\# + Mg\# \left(\frac{FeO}{MgO} \right) = 100 \quad \text{Multiply both sides by } 1 / MgO$$

$$Mg\# \left(\frac{FeO}{MgO} \right) = 100 - mg\#$$

Subtract mg# from both sides and multiply both sides by 1/mg#

$$\frac{FeO}{MgO} = \frac{100}{mg\#} - 1$$

Equation 2

Equation 2 can now be substituted for the FeO/MgO ratio of liquid in Equation 1.

$$K_D = \frac{FeO^{ol}}{FeO^{liq}} \times \frac{MgO^{liq}}{MgO^{ol}} = 0.3$$

Equation 1

$$0.3 = \frac{FeO^{ol}}{MgO} \times \frac{MgO^{liq}}{FeO}$$

rearrange for Fe/Mg ratios

$$\frac{FeO^{liq}}{MgO} = 3.333 \frac{FeO^{ol}}{MgO}$$

solve for Fe/Mg of liquid

$$\frac{100}{Mg\#^{liq}} - 1 = 3.333 \frac{FeO^{ol}}{MgO}$$

(FeO/MgO)^{liq}
mg# of liquid

substitute Equation 2 for
and rearrange to solve for

$$Mg\#^{liq} = \frac{100}{3.333 \frac{FeO^{ol}}{MgO} + 1}$$

Equation 3

Equation 3 can now be used to calculate the mg# in equilibrium with the Fo_{60.4} olivine in sample 141. The mole proportions of FeO and MgO in this olivine are 0.268 and 0.398 respectively, which yields an FeO/MgO ratio of 0.676. Applying this ratio to Equation 3 indicates that this olivine was in equilibrium with a magma of having an mg# of **30.74**. It is important to note that this value is a lower limit on the mg# of the Tuscarora parental melt, as the olivine used in this calculation occurs about 200 meters above the base of the Upper Zone and therefore may be somewhat

differentiated from the most primitive initial composition. In addition, the cumulus olivine in this sample may have undergone some degree of postcumulus re-equilibration.

Estimating other major and trace element components of the parental magma from the compositions of cumulus minerals by partition coefficients requires accurate analyses of mineral separates (e.g., Bedard, 2004), which has not been done here. Another way to get at a more complete parental composition is to search through the compositions of presumably comagmatic volcanic rocks and find those that show reasonable fits in mg# and trace element ratios. As discussed above, the North Shore Volcanic Group is interpreted to be the extrusive counterpart to magmatism that created the Duluth Complex (Green, 1982). A representative suite of 20 volcanic compositions from the NSVG was presented by J.C. Green as a Keweenawan reference suite (BVSP, 1981). These compositions will be evaluated to assess whether any would qualify as reasonable analogues to a Tuscarora parent magma.

In order to compare these compositions with the mg# calculated above, some additional considerations are necessary. Although mafic magma contains both ferric (+3) and ferrous (+2) iron, olivine only accepts the latter. Also, the ferric iron measured in the basalt lava probably does not represent the true concentration in the original magma since weathering and alteration have likely changed the oxidation state and thus the original $\text{Fe}^{+2}/\text{Fe}^{+3}$ ratios. Studies of fresh, unaltered MORB have determined that 85-90% of the total mole percentage of iron in basalt is as Fe^{+2} (e.g.,

Frey et al., 1974). Therefore, we will use 90% of the total iron concentration to be as the ferrous iron component in calculating the mg# of the basalts. In other words, the mg# of basalt analyses are calculated as follows:

First, the total weight percent iron is calculated as total ferrous iron by the formula:

$$FeO(t) = FeO + 0.8998Fe_2O_3$$

Then an idealized mg# is calculated by using only 90% of FeO(t) and converting weight percent to mole percent with the formula:

$$mg\# = \frac{\frac{MgO}{40.32}}{\frac{MgO}{40.32} + 0.9 \frac{FeO(t)}{71.85}} \times 100$$

In seeking out basaltic compositions from the NSVG reference suite that have an mg# of approximately 31 or slightly greater, four samples have mg#s in the range of 30 – 40. An mg# somewhat greater than 31 is acceptable, given that the actual ferrous/ferric ratio is unknown and that some degree of trapped liquid shift is likely to have occurred in even the most adcumulate of troctolitic samples. Samples KEW-10, KEW-14, KEW-17, and KEW-19 have mg#s of 34.7, 38.5, 30.7, and 38.6, respectively (Table 2) .

Table 3: Major and minor element compositions of NSVG Reference Suite samples (BVSP, 1981) having mg#s in the range of 30-40.

Weight %	KEW-10	KEW-14	KEW-17	KEW-19
SiO ₂	45.9	49.1	53.22	55.01
TiO ₂	4.92	3.19	2.05	1.65
Al ₂ O ₃	12.28	15.1	17.55	14.13
Fe ₂ O ₃	3.34	5.55	4.63	6.90
FeO	14.16	8.3	6.18	2.80
<i>FeO(t)</i>	<i>17.16</i>	<i>13.3</i>	<i>10.34</i>	<i>9.01</i>
MnO	0.22	0.18	0.13	0.11
MgO	4.63	4.24	2.33	2.88
CaO	7.29	6.17	4.79	5.62
Na ₂ O	3.52	4.06	5.35	3.79
K ₂ O	1.83	1.13	1.76	2.07
P ₂ O ₅	0.68	0.40	0.51	0.39
Cr ₂ O ₃	n.d	0.00	.002	.002
LOI	1.39	2.33	1.43	5.52
Total	99.8	99.3	99.5	100.0
mg#	34.7	38.5	30.7	38.6

These four samples are among the more evolved compositions in the NSVG reference suite. KEW-10 contains high amounts of incompatible elements, and is considered a mugearite as its primary feldspar is oligoclase (BVSP, 1981). KEW-17 and KEW-19 are in a group of basaltic andesites and are generally quartz-normative. KEW-14 is a transitional basalt (or Fe-basalt) and is the least evolved of the four compositions. While the equilibrium magma mg# calculated from the most primitive olivine (Fo_{60.4} olivine from mg#_{30.74} magma) is in the range of these samples, an additional test of the appropriateness of any of these basalts being possible analogues

of the Tuscarora parent magma is to calculate whether olivine and plagioclase are the main stable phases near the liquidus temperatures of these compositions.

To test the phase equilibrium of the four possible analogue samples, their compositions were applied to the PELLE software program, which is a version of the silicate liquid crystallization MELTS software program for the PC platform developed by Boudreau (1999). The calculations were run using several simplifying assumptions: QFM oxidation conditions, 1 Kbar pressure (~3 km depth), and equilibrium crystallization. In experimenting with the program, it became clear that the amount of water in the magma had a strong effect on phase stability, the liquidus temperature, and mineral compositions. Therefore, compositions were run under two conditions: dry and 1.5 wt.% H₂O. The liquidus temperatures, along with initially saturated phase and the next saturated phase (and its saturation temperature) are listed for each analogue sample in Table 3A for dry conditions, and Table 3B for hydrous conditions.

Except for KEW-10 under hydrous conditions, all magmas have both plagioclase and olivine early on the liquidus (Table 3). Hydrous conditions has the effect of lowering the liquidus temperature by as much as 100°C (KEW-17), promoting olivine over plagioclase as the initial liquidus phase (KEW-14 and KEW-19), and increasing the An content of plagioclase by 6-9%. With the cumulate stratigraphy of the Tuscarora Upper Zone being melatroctolite overlain by troctolite, this would suggest that results with olivine followed by plagioclase crystallization

would be more consistent with the observed mineral paragenesis. This would favor KEW-10(dry), KEW-14(hydrous), and KEW-19(hydrous). However, the ~40°C difference in liquidus temperature between olivine and plagioclase crystallization seems large, such that it should create significant layers of dunite rather than melatroctolite. In contrast, the liquidus temperatures of plagioclase and olivine in KEW-14(dry) and KEW-17(hydrous) are within 10°C of each other and should be considered as possibilities as well.

Table 4A: Liquidus temperatures and early saturated phases calculated with the PELE program for four NSVG reference suite samples assuming dry magma.

	KEW-10	KEW-14	KEW-17	KEW-19
Liquidus Temperature	1133°C	1145°C	1156°C	1133°C
Liquidus Phase	Olivine (Fo68)	Plagioclase (An53)	Plagioclase (An49)	Plagioclase (An52)
Second Phase	Plagioclase(An51) At 1108°C	Olivine (Fo70) At 1140°C	Olivine (Fo62) At 1112°C	Olivine (Fo66) At 1115°C

Table 4B: Liquidus temperatures and early saturated phases calculated with the PELE program for four NSVG reference suite samples assuming 1.5% H₂O in magma.

	KEW-10	KEW-14	KEW-17	KEW-19
Liquidus Temperature	1105°C	1113°C	1057°C	1079°C
Liquidus Phase	Olivine (Fo68)	Olivine (Fo71)	Plagioclase (An57)	Olivine (Fo68)
Second Phase	Ilmenite At 1083°C	Plagioclase (An64) At 1053°C	Olivine (Fo63) At 1051°C	Plagioclase (An61) At 1035°C

The calculated olivine compositions, which are unaffected by hydrous conditions (but do vary with oxidation state), are significantly more forsteritic than any found in the Tuscarora ($<F_{O60.4}$); the main exception being KEW-17. If these higher mg# liquids are parental to the Tuscarora Intrusion, it would require that the olivine analyzed had undergone a trapped liquid shift or had formed after some magmatic differentiation.

In contrast, the An content of plagioclase increases significantly under hydrous conditions. Plagioclase chemistry of the Tuscarora was studied by Beitsch (1991) using petrographic measurements on a universal stage and typically ranges from An₆₂-An₇₀. The plagioclase formed under hydrous conditions is more in line with these compositions.

A final test of the appropriateness of the four KEW reference compositions as analogues to the Tuscarora parent magma is to evaluate trace element ratios, in particular the REE patterns. Plotted in Figure 38 are the REE abundances for the four KEW samples along with the Tuscarora data and the range of the KEW reference suite. While all of these samples exhibit comparable trends with those seen in the Tuscarora, the best matches are KEW-10 and KEW-19 with their flat HREE patterns.

In conclusion, none of the four KEW compositions fits perfectly as an analogue for the parental melt to the Tuscarora Intrusion. Rather, some hybrid containing characteristics of each of these samples should be considered.

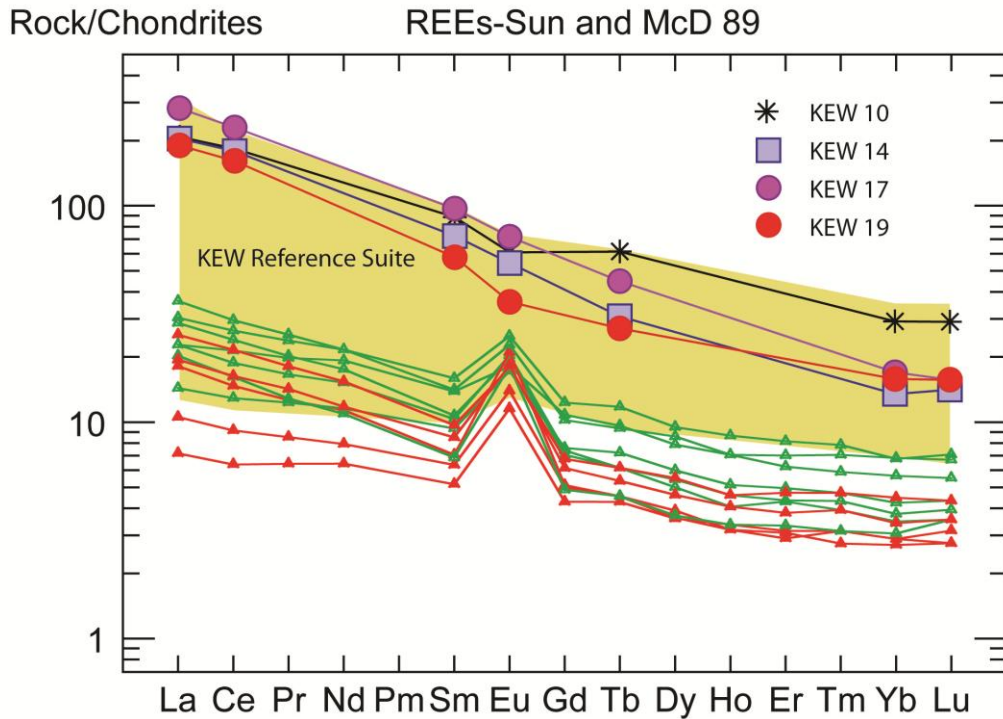


Figure 38: REE concentrations of the four NSVG compositions proposed as possible parent magma analogues for the Tuscarora Intrusion compared to the Tuscarora samples (Red- Upper Zone; Green- Lower Zone). Tan area shows the total range of KEW reference suite data (BVSP, 1981).

V.5 Emplacement Model for the Tuscarora Intrusion and Related Rocks

Field, petrographic, and geochemical results from this study are interpreted to indicate that the Tuscarora Intrusion is composed of two distinct emplacement episodes involving similarly evolved tholeiitic magma. Prior to the recent results of U-Pb zircon dating, two hypotheses had been considered for the formation of the two zones of the Tuscarora Intrusion. The first model, and the one proposed here, suggests that the whole of the Tuscarora Intrusion was emplaced in two major sequential pulses of magma during the main stage of MCR activity and shortly after the emplacement of the Anorthositic Series. A second hypothesis that was being considered early in this study proposed that the Lower Zone formed during the early magmatic stage, and represented a westward extension of the Poplar Lake Intrusion. This theory was based on the more gabbroic composition of the Lower Zone and the abundance of basaltic hornfels inclusions, which are not found in the Upper Zone. Although both these models initially seemed tenable based only on field and geochemical data, a recent U-Pb ($^{207}\text{Pb}/^{206}\text{Pb}$) date of 1098.81 ± 0.32 Ma (Hoaglund, 2010) places the Lower Zone into the main stage of MRS magmatism, effectively disproving the second working hypothesis.

The model proposed here (Figure 39) fits largely with the magmatic stages of the MCR (Fig. 3) and the Duluth Complex (Fig. 4) as a whole as described in the introduction. Early stage magmatism began with rapid eruption of primitive lavas through cold lithosphere. During the latter part of the early magmatic stage,

however, these plume-generated magmas began to pool in the lower crust, where they became contaminated, differentiated, and caused anatexis of the crust.

Anatectic felsic melts were evidently the first magma that ponded at the base of the volcanic pile to create the felsic series of the Duluth Complex. These felsic bodies served to trap evolved mafic magmas beneath them to create Early Gabbro Series intrusions such as the Poplar Lake Intrusion (Figure 39A).

During the latent magmatic stage, the lower crust was extensively underplated with mafic magmas that were prevented from erupting to the upper crusts by the rheologic and density barrier created by anatectic felsic melts (Figure 39B). During the development of this lower crustal magma system, buoyant plagioclase rose to form an anorthositic roof zone within these deep-seated magma chambers. As the lower crust was cleared of the anatectic melts, the density barrier was overcome and plagioclase crystal mushes were intruded into the base of the volcanic pile to form the Anorthositic Series (Figure 39C). In the Tuscarora area, the Anorthositic Series mushes were evidently emplaced some distance above the base of the volcanic pile, perhaps beneath granophyre bodies as occurred with the Early Gabbro series intrusions

As the lower crustal magma chambers continued to vent, the load of suspended plagioclase crystals was depleted and eventually gave rise to relatively crystal-free, evolved mafic magmas. By having staged and differentiated in the lower crust during the latent magmatic stage, these mafic magmas were relatively evolved

(though now uncontaminated). These first pulses of plagioclase crystal-poor magma were intruded below the Anorthositic Series intrusions and into the basal section of NSVG basalts to form the Lower Zone of the Tuscarora Intrusion (Figure 39D). As the magma was injected, it delaminated and incorporated many blocks of the intruded volcanics and pre-Keweenawan footwall rocks.. These inclusions were devolatilized and subjected to pyroxene hornfels-grade metamorphism during incorporation. The cold footwall, composed largely of iron formation and Archean metasedimentary rocks, cooled and contaminated the first emplacement of melt, which led to the formation of the basal heterogeneous unit. This initial emplacement of mafic magma served to pre-heat the country rocks and isolated the Archean and Paleoproterozoic footwall rocks from further interaction with successively overplated magmas emplaced during formation of the Lower Zone. These uncontaminated, higher level magmas crystallized to form the more homogenous augite troctolite to olivine gabbro orthocumulates of the augite troctolite unit of the Lower Zone. The Lower Zone formed through numerous pulses of melt, as evidenced by olivine-rich layers which result from the settling out of primocrysts following each injection.

After a hiatus of unknown duration, the next major magma emplacement event occurred between the basaltic hornfels-rich rocks of the Lower Zone and Anorthositic Series rocks and resulted in the formation of the Upper Zone. (Figure 39E) The presence of a melatroctolite marking the boundary between the lower and upper zone of the Tuscarora Intrusion suggests that the parent magma was carrying

an abundance of olivine phenocrysts or was oversaturated in the olivine components (e.g. Point PM, Fig. 11). This zone transition is also marked by a change in texture. Whereas the lower zone is often an orthocumulate containing significant intercumulus proportions of augite and oxides, the upper zone (especially the melatroctolite) is an adcumulate, with a higher proportion of primocrysts (primarily olivine in the melatroctolite, and olivine and plagioclase elsewhere). This transition in cumulate type may be the result of slow cooling of the Upper Zone due to preheating of the Lower Zone, which allowed time for expulsion of the intercumulus melt. The more gabbroic nature of the Lower Zone may indicate more contamination from basalt inclusions and older country rock. The strong leucocratic character of the Upper Zone may be due to the low amounts of interstitial pyroxene and oxides or may indicate that an extra amount of plagioclase either introduced as phenocrysts from the deep-seated magma source or incorporated as xenocrysts from the intruded Anorthositic Series.

The Upper Zone is much more homogenous than the Lower Zone and contains significantly less olivine-rich layers. This may indicate that the upper zone was emplaced through larger pulses of magma. Eventually the magma began to intrude into and delaminate the overlying Anorthositic Series, delaminating sheets into the melt as evidenced by the oblique plagioclase foliations and gabbroic haloes surrounding many of the anorthositic blocks.

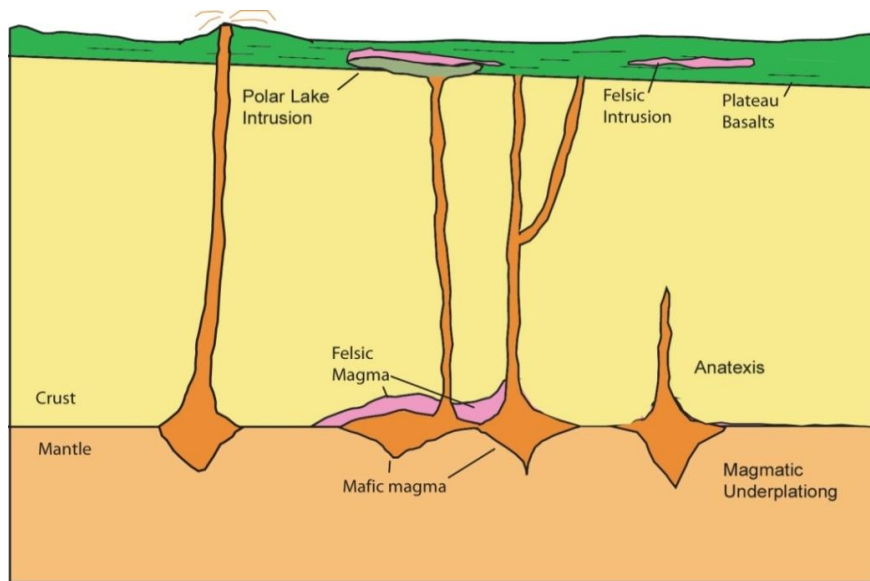


Figure 39A: During the early magmatic stage, extrusive volcanism dominated. Some intrusive activity also occurred, resulting in the formation of the Poplar Lake Intrusion to the east of the study area. Crustal melting during this time created a felsic density barrier, impeding further magmatism and leading to the latent magmatic stage.

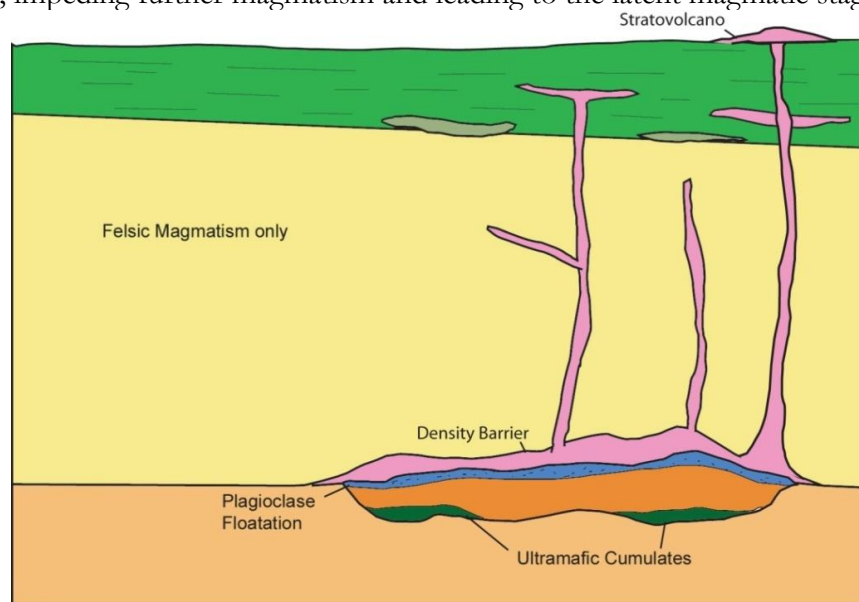


Figure 39B: During the latent magmatic stage, mafic melts were unable to rise due to a felsic cap acting as a rheological barrier. Fractional crystallization occurred in the deep magma chambers, resulting in the formation of an anorthositic roof zone due to the floatation plagioclase crystals under high pressures. Also crystallizing at this time were mafic minerals, which settled out to the bottom of the chamber to create ultramafic cumulates.

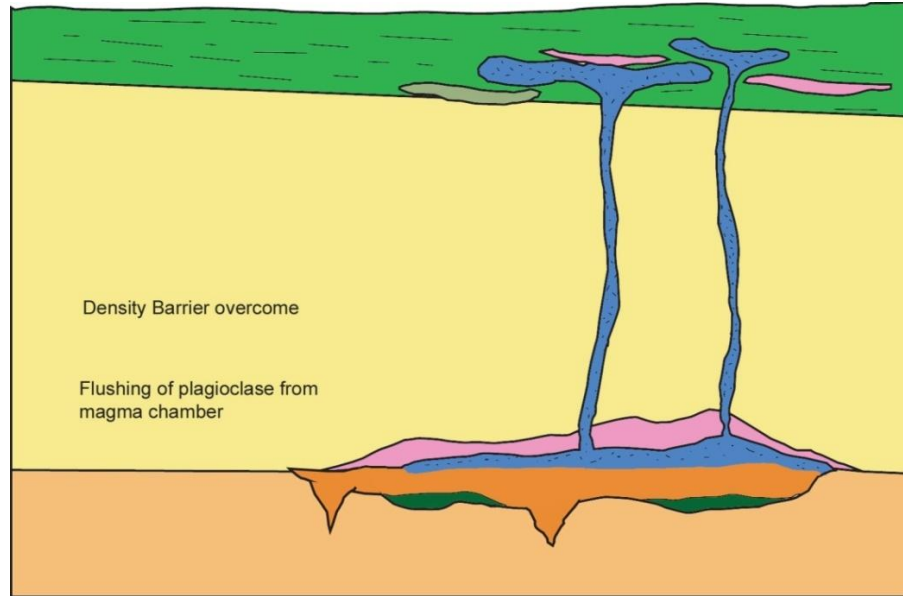


Figure 39C: In the early main stage, the density barrier was overcome allowing magmas to rise to the upper crust. The first pulses were heavily laden with suspended plagioclase crystals which were accumulating in the upper part of the magma chamber. These low density mushes became emplaced into the lower sections of the NSVG, but not at the basal unconformity.

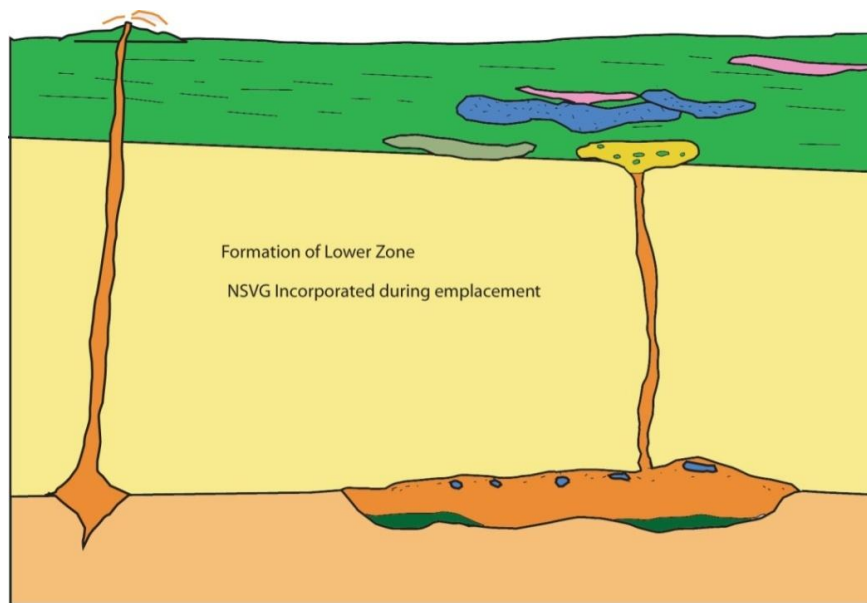


Figure 39D: Eventually the crystal load of the rising magma decreases, resulting in normal crystal-poor mafic magmas. This melt was emplaced into the base of the NSVG,

incorporating many blocks of basalt and some pre-rift inclusions during the process. This formed the Lower Zone of the Tuscarora Intrusion.

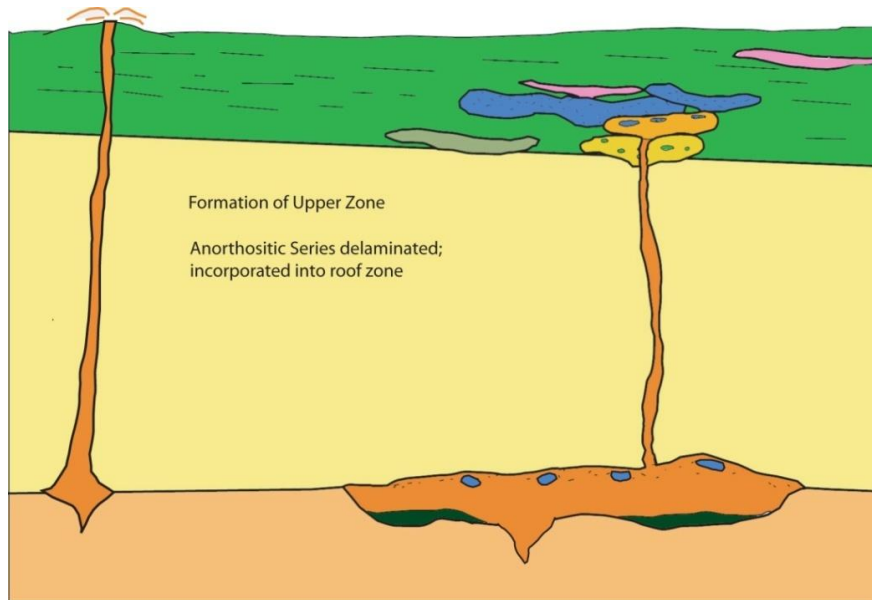


Figure 39E: A large pulse of olivine-saturated magma is emplaced between the Lower Zone and the Anorthositic Series to form the Upper Zone of the Tuscarora Intrusion. During the final stages of emplacement, the melt began to intrude into the Anorthositic Series, delaminating large sheets and incorporating them into the roof zone of the intrusion.

VI. Conclusions

The principal conclusions of this study are as follows:

1. The Tuscarora Intrusion is composed of at least two lithostratigraphic zones (the Lower Zone and the Upper Zone), which are interpreted to be representative of major episodes of magma emplacement. Comparisons to other intrusive suites suggest that the intrusions emplaced along the northern and northwestern margin of the Duluth Complex (Tuscarora, Lake One, South Kawishiwi) formed during a widespread troctolite-producing magmatic event along a 100 km stretch of the basal contact of the Duluth Complex.
2. Recently acquired geochronologic data implies that the Tuscarora Intrusion formed during the main stage of MRS magmatism. This indicates that the Tuscarora formed during the same magmatic event that produced other layered series intrusions, as well as the Anorthositic Series between 1099 and 1098 Ma. However, field relationships from this and previous studies show that the Anorthositic Series was emplaced and largely crystallized prior to the Layered Series.
3. The Anorthositic Series served as the hanging wall to the Tuscarora Intrusion, and was delaminated and incorporated as inclusions during emplacement of the mafic magmas that produced the Tuscarora Intrusion. These inclusions are often elongate slabs or blocks and are especially concentrated in the upper part of the Tuscarora.

4. The parental magma to the Tuscarora Intrusion was an evolved transitional basalt to basaltic andesite with a minimum mg# of 31.4.

VII. References

- Barnes, S.J., 1986, The effect of trapped liquid crystallization on cumulus mineral compositions in layered intrusions: *Contributions to Mineralogy and Petrology* 93:524–531
- Bedard, J.H., 1994, A procedure for calculating the equilibrium distribution of trace elements among the minerals of cumulate rocks, and the concentration of trace elements in the coexisting liquids: *Chemical Geology* 118:1 p143-153
- Beitsch, S., 1991, The geology of the Duluth Complex in the Gillis Lake Quadrangle Unpub. M.S. thesis, University of Minnesota, Minneapolis, 66p.
- Boudreau, A.E., 1999, PELE - A version of the MELTS software program for the PC platform: *Computers and Geosciences*, v. 25, pp. 21-203.
- Cannon, W.F., Green, A.G., Hutchinson, D.R., Lee, M.W., Milkereit, B., Behrendt, J.C., Halls, H.C.,
- Green, J.C., Dickas, A.B., Morey, G.B., Sutcliffe, R.H., and Spencer, C., 1989, The North American Midcontinent rift beneath Lake Superior from GLIMPCE seismic reflection profiling: *Tectonics*, v. 8, no. 2, p. 305-332.
- Cannon, W.F., and Hinze, W.J., 1992, Speculations on the origin of the North American Midcontinent Rift: *Tectonophysics*, 213: 49-55
- Chalokwu C.I., and Grant, N.K., 1990, Petrology of the partridge river intrusion, Duluth complex, Minnesota: 1. Relationships between mineral compositions, density and trapped liquid abundance: *Journal of Petrology* 31:265–293
- Frey FA, Bryan WB, Thompson G (1974) Atlantic Ocean floor: geochemistry and petrology of basalts from Legs 2 and 3 of the Deep-Sea Drilling Project. *J Geophys Res* 79:5507–5527
- Green, J.C., 1981, Pre-Tertiary continental flood basalts. P. 30-77 in *Basaltic Volcanism on the Terrestrial Planets*, Basaltic Volcanism Study Project, Pergamon Press, New York 1285 p.
- Green, J.C., 1982, Geology of Keweenawan extrusive rocks, in *Geology and Tectonics of the Lake Superior Basin - A Review*, R.J. Wold and W. Hinze, eds., *Geol. Soc. America Memoir* 156, p. 165-171
- Grout, F.F., 1918a, Internal structures of igneous rocks; their significance and origin; with special reference to the Duluth Gabbro: *Journal of Geology*, v. 26, p. 439-458.
- Grout, F.F., Sharp, R.P., and Schwartz, G.M., 1959, The geology of Cook County Minnesota: *Minnesota Geological Survey Bulletin* 39, 163 p., 16 pls.
- Hauck, S.A., Severson, M.J., Zanko, L.M., Barnes, S.J., Morton, P., Aliminas, H.V., Foord, E.E., and Dahlberg, E.H., 1997b, An overview of the geology and oxide, sulfide, and platinum group element mineralization along the western and northern contacts of

- the Duluth Complex, in Ojakangas, R.W., Dickas, A.B., and Green, J.C., eds., Middle Proterozoic to Cambrian rifting, central North America: Geological Society of America Special Paper 312, p. 137-185.
- Hoaglund, S, 2010, U-Pb zircon geochronology of the Duluth Complex and related hypabyssal intrusions: investigating the emplacement history of a large multiphase intrusive complex related to the 1.1 Ga Midcontinent Rift: : Unpublished M.S. thesis, University of Minnesota, Duluth
- IgPet. Somerset, NJ: Terra Softa.
- Irvine T.N., Andersen J.C.O., and Brooks C.K., 1998, Included blocks (and blocks within blocks) in the Skaergaard intrusion: Geologic relations and the origins of rhythmic modally graded layers: Geological Society of America Bulletin 110, p. 1398-1447
- Jirsa, M.A., and Starns, E.C., 2008, Preliminary bedrock geologic map of the 2006 Cavity Lake fire area, parts of the Ester Lake, Gillis Lake, Munker Island, and Ogishkemuncie Lake 7.5 minute quadrangles, northeastern Minnesota, 2008: Minnesota Geological Survey Open File Report 08-05. Scale 1:24,000.
- Jirsa., M., Starns, E.C., Costello, D., Gal, B., Hoaglund, S., and Putz, A., 2008, Student capstone map from the UMD Precambrian Research Center's field camp: Bedrock map of Gabichigami Lake and adjacent areas, Minnesota. 54th Annual Institute on Lake Superior Geology, Marquette, MI
- Jones, N.W., 1963, The relationships between the Duluth gabbro and the dikes and sills in the vicinity of Hovland, Minnesota: Minneapolis, University of Minnesota, M.S. thesis, 90 p.
- LeMaitre, R.W., 1989, A classification of igneous rocks and glossary of terms: Recommendations of the International Union of Geological Sciences Subcommittee on the Systematics of Igneous Rocks: Oxford, Blackwell Scientific, 193 p.
- Mathez, E.A., Nathan, H.D., and Morey, G.B., 1977, Geologic map of the Hungry Jack Lake quadrangle, Cook County, Minnesota: Minnesota Geological Survey Miscellaneous Map M-39, scale 1:24,000.
- McCallum, I.S., Raedeke (Swift), L. D., and Mathez, E.A., 1980, Investigations in the Stillwater Complex: Part I, Stratigraphy and structure of the Banded zone. *Am. J. Sci.* v. 280-A, pp. 59-87.
- Miller, J.D., Jr., 1992, The need for a new paradigm regarding the petrogenesis of the Duluth Complex. 38th Annual Institute on Lake Superior Geology, p. 65-67.
- Miller, J.D., Jr., 2009, Geology of the Lake One Troctolite by Canoe – Field Trip 6. 55th Annual Institute on Lake Superior Geology, Part 2 – Field Trip Guidebook, Ely, MN, p. 156-177.
- Miller, J.D., Jr., and Chandler, V.W., 1997, Geology, petrology, and tectonic significance of the Beaver Bay Complex, northeastern Minnesota. in Middle Proterozoic to Cambrian

- Rifting, Ojakangas, R.J., Dickas, A.B., Green, J.C. (editors), , Central North America: Boulder, Colorado, Geological Society of America Special Paper 312, p. 73-96.
- Miller, J.D. Jr., Green, J.C., Severson, M.J., Chandler, V.W., Hauck, S.A., Peterson, D.E., and Wahl, T.E., 2002, Geology and mineral potential of the Duluth Complex and related rocks of northeastern Minnesota. Minnesota Geological Survey Report of Investigations 58, 207p. w/ CD-ROM
- Miller, J.D., Jr., and Ripley, E.M., 1996, Layered intrusions of the Duluth Complex, Minnesota, USA, in Cawthorn, R.G., ed., Layered intrusions: Amsterdam, Elsevier Science, p.257-301.
- Miller, J.D., Jr., Severson, M.A. and Foose, M.P., 2005, Bedrock geology of the Babbitt Northeast quadrangle, St. Louis and Lake Counties, Minnesota. Minnesota Geological Survey Miscellaneous Map M-160, scale 1:24,000.
- Miller, J.D., Jr., and Vervoort, J.D., 1996, The latent magmatic stage of the Midcontinent rift: a period of magmatic underplating and melting of the lower crust: Institute on Lake Superior Geology, 42nd Annual Meeting, Cable, Wis., Proceedings, v. 42, Program and Abstracts, pt. 1, p. 33-35.
- Miller, J.D., Jr., and Weiblen, P.W., 1990, Anorthositic rocks of the Duluth Complex: Examples of rocks formed from plagioclase crystal mush: *Journal of Petrology*, v. 31, p. 295–339.
- Morey, G.B., and Nathan, H.D., 1977, Geologic map of the South Lake quadrangle, Cook County, Minnesota: Minnesota Geological Survey Miscellaneous Map M-38, scale 1:24,000.
- Morey, G.B., and Nathan, H.D., 1978, Geologic map of the Gunflint Lake quadrangle, Cook County, Minnesota: Minnesota Geological Survey Miscellaneous Map M-42, scale 1:24,000.
- Morey, G.B., Weiblen, P.W., Papike, J.J., and Anderson, D.H., 1981, Geologic map of the Long Island Lake quadrangle, Cook County, Minnesota: MN Geol. Surv. Misc. Map Series, M-46, scale 1:24,000
- Nathan, H.D., 1969, The geology of a part of the northeast segment of the Duluth Complex: Minneapolis, University of Minnesota, Ph.D. dissertation, 198 p.
- Neuendorf, J. P. Mehl Jr & J. A. Jackson (eds) 2005. *Glossary of Geology*, 5th ed. Berlin, Heidelberg, New York: Springer-Verlag.
- Nicholson, S.W., Shirey, S.B., Schulz, K.J., and Green, J.C., 1997, Rift-wide correlation of 1.1 Ga Midcontinent rift system basalts: Implications for multiple mantle sources during rift development, in Bornhorst, T.J., ed., *Petrology and metallogeny of intraplate mafic and ultramafic magmatism: Canadian Journal of Earth Sciences*, v. 34, no. 4, p. 504-520.
- Ojakangas, R.W., 1983, Tidal deposits in the early Proterozoic basin of the Lake Superior region the Palms and the Pokegama Formations: Evidence for subtidal shelf deposition

- of Superior type banded iron formation: Ed. L.G. Medaris, Jr., In Early Proterozoic Geology of the Great Lakes Region, Geol. Soc. America Memoir 160, p. 49 -66.
- Ojakangas, R.W., Morey, G.B., and Green, J.C., 2001, The Mesoproterozoic Midcontinent Rift System, Lake Superior Region, U.S.A.: *Sedimentary Geology*, v. 141-142, p. 421-442.
- Owen, D.D., 1852, Report of a geological survey of Wisconsin, Iowa, and Minnesota: Philadelphia, U.S. Department of the Treasury, 638 p.
- Paces, J.B., and Miller, J.D., Jr., 1993, Precise U-Pb ages of Duluth Complex and related mafic intrusions, northeastern Minnesota: New insights for physical, petrogenetic, paleomagnetic and tectono-magmatic processes associated with the 1.1 Ga Midcontinent Rift system. *Journal of Geophysical Research*, v. 98, no. B8, p. 13,997-14,013.
- Patelke, R.L., 1996, The Colvin Creek body, a metavolcanic and metasedimentary mafic inclusion in the Keweenawan Duluth Complex, northeastern Minnesota: Unpublished M.S. thesis, University of Minnesota, Duluth, 232 p.
- Phinney, W.C., 1972, Northwestern part of Duluth Complex, in Sims, P.K., and Morey, G.B., eds., *Geology of Minnesota: A centennial volume*: Minnesota Geological Survey, p. 335-345.
- Rollinson, Hugh R. 1993, *Using geochemical data : evaluation, presentation, interpretation*: J. Wiley & Sons, New York.
- Severson, M.J., 1994, Igneous stratigraphy of the South Kawishiwi intrusion, Duluth Complex, northeastern Minnesota: Natural Resources Research Institute, Technical Report NRRI/TR- 93/34, 210 p., 15 pls.
- Severson, M.J., and Hauck, S.A., 1990, Geology, geochemistry, and stratigraphy of a portion of the Partridge River intrusion: Natural Resources Research Institute, Technical Report NRRI/GMIN-TR-89-11, 236 p., 4 pls.
- Stifter, E., Wartmann, J., Carlson, A., Gibbons, J., Kane, K., Mason, T., Murphy, L., Peterson, D., and Hudak, G. 2009, Student capstone map from the UMD Precambrian Research Center's field camp: Bedrock map of Ima Lake and adjacent areas, Cook County, Minnesota. 55th Annual Institute on Lake Superior Geology, Ely, MN
- Sun, S.S. and McDonough, W. F. (1989) Chemical and Isotopic Systematics of oceanic basalts: implications for Mantle Composition and Processes. In A.D. Saunders and M.J. Norry (eds.) *Magmatism in the Ocean Basins*, Spec. Publ. Vol. Geol. Soc. Lond., No. 42, pp. 313-345.
- Taylor, R.B., 1964, Geology of the Duluth Gabbro Complex near Duluth, Minnesota: Minnesota Geological Survey Bulletin 44, 63 p., 1 pl.
- Thompson, RN, 1982, Magmatism of the British Tertiary province *Scottish Journal of Geology*, v. 18.4 p.9-107.

- Trehu, A., Morel-à-l'Huissier, P., Meye, R., Hajnal, Z., Karl, J., Mereu, R., Sexton, S., Shay, J., Jefferson, W.T., Chan, K., and Epili, D., 1991, Imaging the Midcontinent Rift beneath Lake Superior using large aperture seismic data: *Geophysical Research Letters*, v. 18, p. 625-628
- Vervoort, J.D., Wirth, K., Kennedy, B., Sandland, T. and Harpp, K.S., 2007, The magmatic evolution of the Midcontinent rift: New geochronologic and geochemical evidence from felsic magmatism. *Precambrian Research* v. 157, p. 235-268.
- Wadsworth, W.J., 1961, The layered ultrabasic rocks of south-west Rhum, Inner Hebrides. *Philosophical Transactions of the Royal Society*, B244, 21–64.
- Wager, L.R. and Brown, G.M., 1967, *Layered Igneous Rocks*: W.H. Freeman & Co.
- Wahl, T.E., Miller, J.D., Jr., Jirsa, M.A., Boerboom, T.J., Chandler, V.W., Runkel, A.C., Dahl, D., and Severson, M.J., 1997, Geologic Mapping System (GeMS): A digital approach to bedrock geologic mapping. 43rd Annual Institute on Lake Superior Geology, p. 59-60.
- Weiblen, P.W., and Morey, G.B., 1980, A summary of the stratigraphy, petrology, and structure of the Duluth Complex: *American Journal of Science*, v. 280-A, p. 88-133.
- White, D.A., 1954, The stratigraphy and structure of the Mesabi Range: *Minnesota Geological Survey Bulletin* 38, 92p.
- Winchell, N.H., 1900, The geology of Minnesota: *Geological and Natural History Survey of Minnesota, Final Report*, v. 5, 1025 p., 6 pls.